DEVELOPMENT OF BIODEGRADABLE IMPLANTS FOR EXTENDED DELIVERY OF PROTEINS

Inaugural-Dissertation
to obtain the academic degree
Doctor rerum naturalium (Dr. rer. nat.)

submitted to the Department of Biology, Chemistry and Pharmacy
of Freie Universität Berlin

by

LUISA FERNANDA DUQUE ZAPATA

From Bogotá, Colombia

2017

Die vorliegende Arbeit wurde von Januar 2014 bis Dezember 2016 unter der Leitung von Prof. Dr. Roland Bodmeier im Institut für Pharmazie angefertigt.

1. Gutachter: Prof. Dr. Roland Bodmeier
2. Gutachter: Prof. Dr. Philippe Maincent

Disputation am 28.03.2017

A mis padres y mi hermanito

Acknowledgements

In the first place, I would like to thank Professor Dr. Roland Bodmeier for giving me the opportunity to join his group. I am very thankful for his support and for allowing to get involved in different activities that helped me to gain valuable experience for my future career. Herzlichen Dank!

I also would like to thank Professor Dr. Philippe Maincent for co-evaluating my thesis. Merci beaucoup!
Special thanks also to Professor Dr. Charlotte Kloft, Professor Dr. Daniel Klinger and Dr. Andriy Dashevskiy for serving as members of my thesis committee.

I am deeply grateful to Dr. Martin Körber for the nice discussions, valuable scientific input and advices along my PhD (Herzlichen Dank!). I am also thankful to Kristin Folmert from the institute of Chemistry and Biochemistry of the FU-Berlin, for her kind assistance and help with the CD and fluorescence measurements (Vielen Dank!).

A big “thank you” to Dr. Rahul Sonawane (धन्यवाद), Marius Heck (Danke schön!) and Marco Bellini (grazie mille!) for proofreading parts of this thesis and for their assertive feedback and suggestions. My deepest gratitude to Daniel Sironi (Danke schön!), Miriam Colombo (grazie mille!), Raquel Fernando (muito obrigada!) and Amanda Campos Fortes (muito obrigada!) for being my second pair of hands during some time, a great help and nice company. You helped me to get many things done and to move forward with my PhD project, thank you!

To all the current and former group members thanks for their support, patience, unforgettable group activities and the friendly atmosphere that we have in our group. Specially to Miriam and Marina for their lovely friendship and endless support, and to Marco for being a very nice lab-mate and friend, and for creating an enjoyable environment in R322.

Many thanks to Mrs. Eva Ewest, Mr. Stefan Walter, Mr. Andreas Krause and Mrs. Gabriela Karsubke for their assistance, generous help and support with many matters around the lab and within the group. Thanks are also extended to Cremer Oleo GmbH, Gattefossé GmbH and Stroever GmbH & Co. KG for kindly providing some of the excipients used during my PhD project.

Un agradecimiento de todo corazón para mi familia por su infinito apoyo, amor y motivación para seguir adelante; gracias a ustedes he podido llegar a donde estoy y he logrado recorrer el mundo mientras aprendo un montón de cosas sobre ciencias farmacéuticas, pero especialmente de la vida. ¡Gracias totales!

Y por último gracias infinitas a Esteban, por estar conmigo, por su amor, su apoyo, sus consejos (científicos y de la vida), sus ideas, su paciencia y su manera de ser. Sin el nada de esto hubiera sido posible. ¡Mil y mil y mil gracias!

Table of contents

1. INTRODUCTION 1

1.1 General introduction 1

1.2 Protein conformation 3

1.3 Protein stability 4

1.3.1 Physical instability 5

1.3.2 Chemical instability 5

1.4 Characterization and stability evaluation of peptide- and protein-loaded formulations 7

1.5 Parenteral controlled release formulations for peptide and protein delivery 8

1.5.1 Micro- and nanoparticles 9

1.5.2 Solid implants 9

1.5.3 In situ forming implants 9

1.5.4 Liposomes 10

1.5.5 Pulsatile drug delivery systems 10

1.6 Solid implants as drug delivery systems for peptides and proteins 11

1.6.1 Evolution of solid implants as drug delivery systems 11

1.6.2 Production methods for solid implants 13

1.6.3 Materials used for preparation of protein- and peptide-loaded solid implants 19

1.6.4 Drug release mechanisms governing the release from solid implants 21

1.7 Research objectives 24

2. MATERIALS AND METHODS 25

2.1 Materials 25

2.1.1 Proteins 25

2.1.2 Biodegradable matrices 25

2.1.3 Co-excipients 25

2.1.4 Reagents and kits 25

2.2 Methods 26

2.2.1 Preparation of Implants 26

2.2.2 Determination of Implant Morphology by Optical Light Macroscope 27

2.2.3 Mechanical properties of implants 27

2.2.4 Differential scanning calorimetry (DSC) 28

2.2.5 X-ray diffraction (XRD) 28

2.2.6 Protein extraction from implants 28

2.2.7 Protein quantification and structural integrity of ovalbumin 29

2.2.8 Fourier transform infrared spectroscopy (FTIR) 29
2.2.9 Circular dichroism (CD) 29
2.2.10 Fluorescence spectroscopy 29
2.2.11 Ovalbumin release 30
2.2.12 Determination of lipid composition 30
2.2.13 Polymer molecular weight determination 31
2.2.14 Protein-polymer interaction 31

3. PART I: PLGA BASED IMPLANTS - RESULTS AND DISCUSSION 33
3.1 Introduction 33
3.2 Understanding the incomplete release of ovalbumin 36
3.2.1 Ovalbumin stability after extrusion 36
3.2.2 Release incompleteness of Ovalbumin 37
3.3 Improving release completeness of OVA from PLGA based implants 43
3.3.1 Creation of a viscous environment 43
3.3.2 Pore formers 45
3.3.3 pH-stabilizers 48
3.4 Use of shellac as novel co-excipient in OVA-loaded PLGA-based implants 53
3.4.1 Upscaling from the mini-ram extruder to a twin-screw extruder 53
3.4.2 Storage stability of the up-scaled formulation 56
3.4.3 Effect of terminal sterilization on PLGA: shellac-based implants 59
3.5 Conclusions 63

4. PART II: LIPID BASED IMPLANTS – RESULTS AND DISCUSSION 65
4.1 Introduction 65
4.2 Understanding the release from lipid-based implants 67
4.2.1 Characterization of the lipids used as biodegradable matrix 67
4.2.2 Implant characterization 74
4.2.3 OVA stability after extrusion 76
4.2.4 Dissolution behavior of OVA from lipid-based implants 77
4.2.5 Effect of protein loading on implant properties 78
4.2.6 Loading a smaller protein leads to longer release: the case of lysozyme 81
4.3 Exploring formulation approaches to modulate the release of OVA from lipid-based implants 84
4.3.1 Effect of co-excipients on dissolution kinetics 84
4.3.2 Effect of processes after extrusion on protein integrity and dissolution 89
4.3.3 Effect of terminal sterilization on lipid-based implants 95
4.4 Design of experiments to optimize the release of OVA from lipid-based implants 101

4.5 Conclusion 110

5. SUMMARY 113

6. ZUSAMMENFASSUNG 119

7. REFERENCES 127

8. PUBLICATIONS AND PRESENTATIONS RESULTING FROM THIS WORK 143

9. CURRICULUM VITAE 145

Abbreviations

CAN	Acetonitrile
ANS	1-anilino-8-naphthalene sulfonate
BSA	Bovine serum albumin
CD	Circular dichroism
Comp	Compritol® 888 ATO
Cp	Heat capacity
D114	Dynasan 114, glycerol trimiristate
D118	Dynasan 118, glycerol tristearate
DoE	Design of experiments
DP60	Dynasan P 60, Hydrogenated palm oil
DSC	Differential scanning calorimetry
DTT	Dithiothreitol
ESI/TOF-MS	Electrospray ionization/Time-of-flight mass spectrometry
FD	Freeze dried
FDA	Food and drug administration
FTIR	Fourier transform infrared spectroscopy
GnHCl	Guanidinium chloride
GPC	Gel permeation chromatography
HME	Hot-melt extrusion
HTS	High temperature during sterilization
Im	Intramuscular
Iv	Intravenous
kGy	KiloGrays of gamma irradiation (i.e. irradiation dose)
LTS	Low temperature during sterilization
LYS	Lysozyme
NMR	Nuclear magnetic resonance
OVA	Ovalbumin
PEG	Polyethylenglycol
pI	Isoelectric point
PLA	Poly(D,L-lactide acid)
PLGA	Poly(D,L-lactide-co-glycolide acid)
Prec	Precirol™ ATO5
PVP	Polyvinylpirrolidone
QbD	Quality by design

Sc	Subcutaneous
SD	Standard deviation
SDS	Sodium dodecyl sulfate
SEC	Size exclusion chromatography
Tg	Glass transition temperature
THF	Tetrahydrofuran
Tm	Melting temperature
XRD	X-ray diffraction

1. Introduction*

1.1 General introduction

During the last decades, the delivery of proteins and peptides have gained more attention thanks to their potential therapeutic use (i.e. highly potent and specific). However, due to their structural conformation, stability issues arise during formulation activities yielding to loss of biological effect and/or immunogenic body reactions. Moreover, since the oral route is not suitable for the delivery of these kind of macromolecules because they present poor membrane penetration and instability in the gastrointestinal tract, they are usually administered parenterally. Nonetheless, the rapid clearance after injection leads to frequent administration and, hence, poor patient compliance. To overcome this issue and to protect these labile compounds from harsh conditions after administration (e.g. low pH at gastrointestinal tract), various injectable extended release formulations have been developed over the pass years (Kleiner et al., 2014; Schwendeman et al., 2014; Teekamp et al., 2015).

These formulations are presented as different dosage forms like implants, microparticles, nanoparticles, and gels, where different carrier systems, both biodegradable and non-biodegradable ones, have shown suitability for the preparation and administration of such formulations. They include synthetic and natural occurring polymers, lipidic excipients, polysaccharides and polypeptides. Although these carrier systems could preserve the stability of the protein or peptide upon administration, the preparation techniques used to formulate these dosage forms can cause degradation and instability issues as well. Thus, not many products have found their way through regulatory approval for commercialization (see examples in Table 1), which is an indication of the many challenges that have not been overcome yet.

Continuous efforts are being made to develop and to optimize drug delivery systems for protein and peptide delivery, as can be seen by the numerous research on this field. However, different challenges and unmet needs remain, which should be addressed to

* Parts of this chapter were taken from L. Duque et al., 2015. Expert Opin. Drug Deliv. 12, 1–21. http://dx.doi.org/10.1517/17425247.2015.1003807

facilitate the introduction of novel peptide- and protein-loaded formulations into the market (Mitragotri et al., 2014).

Table 1 Examples of marketed protein- and peptide-loaded parenteral extended release products

Product (Company)	Protein or Peptide	Dosage form	Carrier
Bydureon (AstraZeneca)	Exenatide	Microspheres	PLGA
Decapeptyl (Ferring)	Triptorelin	Microspheres	PLGA
Eligard (Astellas Pharma)	Leuprolide	In situ forming implant	PLGA / N-Methylpyrrolidone
Enantone Depot (Takeda)	Leuprolide	Microcapsules	PLGA
Lupron Depot (Abbvie Endocrine)	Leuprolide	Microspheres	PLGA
Leuprone HEXAL* (Sandoz/Hexal)	Leuprolide	Solid implant	PLGA
Nutropin Depot* (Genentech Inc)	Human growth hormone	Microspheres	PLGA
Pamorelin LA (Ipsen Pharma)	Triptorelin	Microspheres	PLGA
Profact (Sanofi-Aventis/Apogepha)	Buserelin	Solid implant	PLGA
Sandostatin LAR (Novartis)	Octreotide	Microspheres	PLGA-glucose
Somatuline Depot (Ipsen Pharma)	Lanreotide	Microspheres	PLGA/PLA
Supprelin LA (Endo Pharmaceutical solutions)	Histrelin	Solid Implant	Polyhydroxyethylmethacrylate (pHEMA)
Trelstar Depot (Allergan)	Triptorelin	Microgranules	PLGA
Vantas (Endo Pharmaceutical solutions)	Histrelin	Solid implant	Polyhydroxyethylmethacrylate (pHEMA)
Viadur (Janssen Pharmaceutical)	Leuprolide	Solid implant	Titanium
Zoladex (AstraZeneca)	Goserelin	Solid Implant	PLGA/PLA

*withdrawn from the market

1.2 Protein conformation

Despite the enormous number of naturally occurring proteins, only 20 aminoacids are responsible for their composition. The unique structure of a protein is determined by the physicochemical properties of the aminoacids align within the structure. This generates changes in protein conformation (i.e. its tertiary and quaternary structure), stability and activity.

Protein structure can be described at four different levels:

- Primary structure, which refers to the linear arrangement of aminoacid residues along a polypeptide chain and to the location of covalent bonds, such as disulfide bonds, between chains or within a chain.
- Secondary structure that defines the folding of the polypeptide chains into regular, ordered structures like α-helices and β-sheets. It can also present areas with increased flexibility, normally referred as turns or loops.
- Tertiary structure is the three-dimensional arrangement of the protein, which is generated by the domains of the secondary structure and all the non-covalent interactions such as hydrogen bonds and hydrophobic, electrostatic, or van der Waals interactions that occur within the structure (Figure 1). Usually, the non-polar fraction of aminoacids is embedded within the interior of the protein structure thanks to the association of secondary structures. Some proteins consist of several polypeptide chains.
- Quaternary structure characterizes the non-covalent interactions that bind several polypeptide chains into a single protein molecule.

The retention of the tertiary structure is considered the primary requirement for the biological activity of protein molecules (Frokjaer and Otzen, 2005; Jorgensen et al., 2006). However, the biochemical and structural complexity of these molecules bring along a high sensitivity to the external environment and its changes, even at a marginal level. This is especially critical for formulations that are intended to deliver the protein in a controlled and extended manner. In this case instability factors might arise at any moment from formulation preparation till administration into the body (Capelle et al., 2007). And thus, additional care should be given.

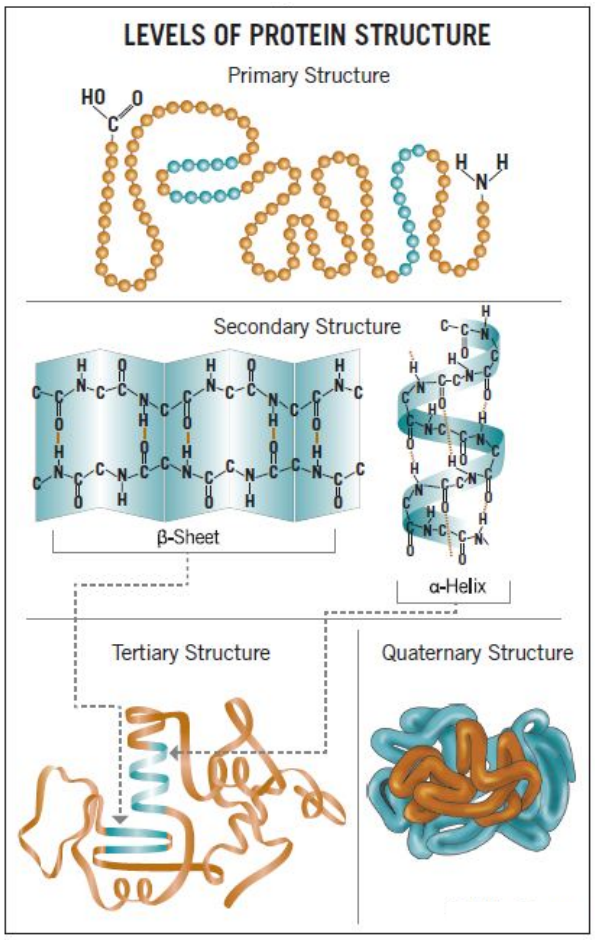

Figure 1 Levels of protein structure (Particle Sciences, 2009)

1.3 Protein stability

As mentioned before, one of the main concerns during the development of protein-loaded formulations is the preservation of the stability (i.e., structural integrity and activity, if applicable) of these compounds during manufacturing, after subsequent storage and during their release from the matrix in which they are embedded (Giteau et al., 2008; Houchin and Topp, 2008; Jorgensen et al., 2006). The induction of a specific degradation process may depend on the type of manufacturing process, specific manufacturing settings and/or chemical or physical interactions between the matrix (and/or its degradation products) and the protein. The biomacromolecules might lose their activity and conformation following different degradation pathways as described below: (Arbit et al., 2013; Banga, 2006; Houchin and Topp, 2008; Manning et al., 1989, 2010, Reubsaet et al., 1998a, 1998b; Wang, 1999).

1.3.1 Physical instability

1.3.1.1 Protein unfolding, denaturation:

Disruption of the tertiary structure and sometimes the secondary structure. Can be reversible except for most thermally induced denaturation processes where aggregation also takes place. Can be caused by changes in temperature, extreme pH values, presence of salts, guanidine, urea or organic solvents. And it results in changes in the spectroscopic and thermal properties, molecular shape and physical properties

1.3.1.2 Protein aggregation:

Intermolecular association by hydrophobic interactions of partially denatured protein chains or conformation intermediates. Can take place in the liquid or solid state of the peptide/protein. Can be caused by changes in temperature, changes in pH, presence and concentration of salts, presence of preservatives or surfactants, air-liquid and solid-liquid interfaces, which can be present in all stages of protein-therapeutics development. And results in the formation of insoluble aggregates, loss of activity and increase in immunogenicity.

1.3.1.3 Adsorption to surfaces:

Reorientation and rearrangement of proteins after adsorption to surfaces (plastics, glass, metal) or interfaces (air-liquid, liquid-liquid, ice-liquid). Subsequently, surface tension forces can induce aggregation. Susceptibility of protein to this phenomenon depends on its hydrophobicity and its structural stability. Cn be caused by agitation, presence of salts, freeze-thaw cycles and surface characteristics of the container in which the protein/peptide is stored. Results in aggregation, loss of activity and increase in immunogenicity.

1.3.2 Chemical instability

1.3.2.1 Deamidation:

Hydrolysis of asparagine (Asn) and glutamic acid (Gln) side chains to form a free carboxylic acid. C-terminal amides are also exposed to this reaction. It can happen at both acidic and basic pH. At acidic pH: direct hydrolysis of Asn; at neutral and basic pH: hydrolysis via a cyclic imide intermediate. Caused by temperature, ionic strength (buffer catalysis), steric hindrance due to secondary and tertiary structure and neighboring amino acids. Results in changes in hydrophobicity, polarity, mass and charge. In addition, the peptide/protein's bioactivity, half-life, aggregation and/or immunogenicity can also be affected.

1.3.2.2 Oxidation:

It is the oxidation of amino acid residues; histidine (His), methionine (Met), cysteine (Cys), tryptophan (Trp) and tyrosine (Tyr) by reactive oxygen species (ROS), molecular oxygen, metal catalysts and photooxidation. Caused by pH, buffer type, presence of ROS, molecular oxygen and redox active metals and the accessibility of the residues for these species. Exposure to light causes photooxidation. Results in oxidation products that are more hydrophilic and polar. Partial or complete loss of activity can also occur.

1.3.2.3 Hydrolysis:

It occurs at three sites: the peptide backbone at X-aspartic acid (Asp)-X at either C- or N-terminal bond (also known as proteolysis), peptide bond in hinge region of antibodies without Asp present, amino acid residues, i.e. Trp. It is caused by temperature, highly dependent on pH presenting a V-shaped pH-rate profile with minimums near pH 6 and sensitivity to buffer catalysis similar to deamidation. Results in changes of mass, size, charge, hydrophilicity and spectroscopic properties.

1.3.2.4 Disulfide bond breakage and scrambling:

Disulfide bond breakage is a reduction of Cys-Cys disulfide bond, and scrambling corresponds to incorrect disulfide bond formation after bond breakage. Disulfide bond reduction is catalyzed in neutral and acidic environment by thiols, e.g. mercaptoethanol. Results in disruption of tertiary and quaternary structure yielding to changes in shape, molecular weight, spectroscopic properties and loss of activity. Disulfide scrambling can also lead to aggregation.

1.3.2.5 β-elimination:

Deprotonation of hydrogen at the α-carbon in peptide backbone, followed by β-elimination at Cys, serine (Ser), threonine (Thr), phenylalanine (Phe) and lysine (Lys) residues. Caused by high temperature and basic pH (presence of OH^-). Metal ions catalyze this reaction. β-elimination of Cys residues leads to thiol formation and disulfide bond destruction and consequently additional disulfide bond breakage due to thiol groups. Disruption of tertiary and quaternary structure, aggregation, adsorption and precipitation can also occur, which all lead to loss of activity.

1.3.2.6 Racemization:

Deprotonation of hydrogen at the α-carbon in the peptide backbone, resulting in a carbanion intermediate, which upon ionization can result in the D-amino acid residue. All peptides except glycine (Gly), are susceptible to racemization. Racemization rate is fastest for Asn.

Caused by basic pH (presence of OH^-). Results in the formation of diastereomers with different physico-chemical properties (mainly hydrophobicity and polarity changes), leading to non-metabolizable structures and inaccessibility of peptide bonds for enzymes.

1.3.2.7 Maillard reaction/ Glycation:

It is linkage of sugar molecule to protein by the formation of a Schiff base after a reaction between basic amino acid residue (Lys, Arg) or N-terminus and carbonyl group of reducing sugar, which is the first step of a cascade of reactions eventually leading to the formation of cross-linked protein aggregates. Can occur in solid state and in protein solution. Susceptibility to glycation depends on microenvironment in the protein. The presence of phosphate, exposure to high temperatures or relative high humidity can catalyze the reaction. Results in brown color (in solid state), crosslinking of proteins, loss of activity, decrease in solubility, plasticization of material and reduction of pH due to formation of acidic by-products.

1.3.2.8 Acylation in the solid state (with PLGA):

Nucleophilic attack of peptide N-terminus or lysine side chain on ester bond/carboxylic acid group of PLGA, resulting in acylation of the peptide. Water potentiates reaction by increasing molecular mobility and promoting hydrolysis of polymer chains. Results in peptide/protein degradation and formation of impurities that may affect protein/peptide activity.

1.4 Characterization and stability evaluation of peptide- and protein-loaded formulations

The characterization of a protein drug is a complex undertaking, requiring the use of a wide range of methods to establish such properties of the drug substance as structural integrity, consistency, activity, purity, and safety (Table 2). The complexity of protein molecules means that there are many potential degradation pathways, each with its individual dependencies on such parameters as pH, ionic strength, and temperature. Each protein may represent a unique combination of such pathways and dependencies. It is therefore critical that a broad spectrum of methods be used to evaluate the effects of processing and storage to assure optimal maintenance of safety and efficacy of the drug (Chirino and Mire-Sluis, 2004; Harris et al., 2004).

Table 2. Common analytical methods for characterization of protein and peptide-containing formulations (Arbit et al., 2013; Banga, 2006; Teekamp et al., 2015)

Analytical method	Information retrieved
Reverse-phase high-performance liquid chromatography (RP-HPLC)	• Detection of degradation products
Mass spectrometry (MS) (usually after protein digestion/enzymatic cleavage)	• Primary structure and sequence: "Fingerprint"
Fluorescence spectroscopy	• Unfolding of proteins
Fourier transform infrared (FTIR) spectroscopy	• Changes in secondary structure and polypeptide backbone • Aspect of protein in solid state
Size exclusion chromatography (SEC)	• Concentration and apparent molecular weight • Protein aggregation: Covalently linked or stable non-covalently linked protein aggregates • Detection of low molecular weight degradation species
SDS polyacrylamide gel electrophoresis (SDS-PAGE)	• Approximate molecular weight • Aggregation (purity) • Cleavage products due to hydrolysis
Differential scanning calorimetry (DSC)	• Changes in protein conformation

1.5 Parenteral controlled release formulations for peptide and protein delivery

Several controlled release parenteral delivery systems have been investigated for the delivery of therapeutic peptides and proteins. These include microspheres, implants, liposomal delivery systems, nanoparticles, and pulsatile drug delivery systems. Nevertheless, design of long acting systems requires knowledge of the physicochemical properties of the system under development, the physicochemical properties of the drug being delivered, and the pharmacokinetic and pharmacodynamic properties of the drug. Additionally, body-response reactions should also be taken into consideration since the prolonged effect of the formulation might exert immunological responses that may impair the performance of the system (Andhariya and Burgess, 2016; Banga, 2006; Mitragotri et al., 2014; Tracy, 1998).

1.5.1 Micro- and nanoparticles

Microparticles are free-flowing powders, ideally less than about 125 µm in diameter, that can be suspended in suitable aqueous vehicles for injection with a conventional syringe using e.g. an 18- or 20-gauge needle. Nanoparticles are colloidal polymer particles with a size of less than about 0.1 µm. They can be used as carriers for active ingredients with the purpose of achieving drug-controlled release or drug-targeting.

The processes commonly used to make parenteral microspheres include emulsification-solvent evaporation, spray-drying, spray-freeze-drying, spray-congealing, solvent displacement, layer-by-layer methods, interfacial polymerization and super critical fluid technology (Teekamp et al., 2015; Vaishya et al., 2014).

1.5.2 Solid implants

Implants are often placed subcutaneously by a large-bore needle (14- to 16-gauge needle), pellet injectors, or minor surgery. If a non-biodegradable polymer is used, the implant will also need surgical removal at the end of the release period. A peptide or protein drug can be formulated into an implant by standard tableting or compression techniques. But generally extrusion processes (i.e. hot melt extrusion (HME)) are employed for the production of solid implants (Kleiner et al., 2014). A more detailed explanation of the different productions methods is given in section 1.6.2.

One of the most known examples for this kind of formulations, is Zoladex®. This is a depot formulation containing goserelin acetate, and LHRH agonist, which is used for the treatment of prostatic cancer, breast cancer and endometriosis. It is a poly(lactic-co-glycolic acid) (PLGA) based rod-shaped implant prepared by HME and formulated for hormone delivery for a period of 28 days and 12 weeks. This kind of formulations are supplied as ready-to-use products, without the need of reconstitution as in the case of micro- and nanoparticles. This has the benefit of a safer and easier administration by healthcare providers (Furp and Hutchinsonb, 1992).

1.5.3 In situ forming implants

To facilitate the administration of the formulation, in-situ forming implants have been developed for the release of macromolecules. Typically, injectable implants are liquids or syringeable semisolids that solidify in situ to form viscous gels. The gelling mechanism can be classified into three broad categories: (i) in situ precipitation, wherein the polymer is rendered insoluble under physiological conditions owing to a combination of physical forces, such as hydrogen bonding, hydrophobic interactions and ionic bonding between polymer chains. Precipitation of the polymer occurs due to phase separation, sol–gel transition at physiological temperatures or in response to a change in pH; (ii) in situ crosslinking, wherein

chemical crosslinking of polymer chains is initiated upon a change in temperature or ion concentration, as well as by photo-irradiation or in the presence of enzymes; and (iii) in situ solidifying systems, which are either hot melts that solidify on cooling to physiological temperatures or lyotropic liquid crystals, which self-assemble in aqueous solutions (Agarwal and Rupenthal, 2013).

1.5.4 Liposomes

Liposomes are microscopic vesicles composed of lipid membranes surrounding discrete aqueous compartments. These spherical structures can have diameters ranging from 80 nm to 100 µm (Grimaldi et al., 2016; Tan et al., 2010) they can be classified into small unilamellar vesicles/nanovesicles with a size of 200 nm; large unilamellar vesicles ranging in size from 200–1000 nm; giant unilamellar vesicles, which are bigger than 1000 nm; multilamellar vesicles consisting of several concentric bilayers; and multivesicular vesicles composed of several small vesicles entrapped into larger ones. Different ligands can be used to functionalize the surface of the vesicles leading to different physicochemical characteristics (Grimaldi et al., 2016)

Liposome preparation techniques may be divided into (i) bulk methods, where liposomes are obtained by transfer of phospholipids from an organic phase into an aqueous phase, and (ii) film methods, in which lipid films are first deposited on a substrate and subsequently hydrated to give liposomes (Allen and Cullis, 2013; Patil and Jadhav, 2014).

1.5.5 Pulsatile drug delivery systems

Pulsatile delivery systems should ideally function in an on–off manner in response to internal or external stimuli (Kikuchi and Okano, 2002; Yoshida et al., 1993). Externally regulated pulsatile delivery systems are considered as open-loop systems while the internal or self-regulated systems are considered closed-loop systems. The closed-loop systems are based on the homeostasis principle. Such systems have been developed for the delivery of e.g. insulin tied to the feedback of changing blood glucose levels (Banga, 2006). In open-loop systems, the release is controlled by a user-generated external signal (i.e. electric current, magnetic field, or ultrasound) or by the use of matrices sensitive to pH, temperature or electric fields (Banga, 2006; Yoshida et al., 1993).

Pumps can also be used as the controlling factors in a pulsatile release system. Here, the release of the drug is driven by a concentration gradient, generated by osmotic effects or mechanical action on the pump. Osmotic implant systems are a class of rate-controlling membrane (RCM) system. In these systems, the RCM controls the rate of water diffusion into the system, with the delivery of an equal volume of the drug solution or suspension from the system reservoir. These systems yield steady, zero-order delivery of drugs (Banga,

2006). Osmotic systems for human applications are based on a design with an outer cylinder of titanium (DUROS® implant) and a piston that separates the osmotic layer from the drug reservoir. Viadur™ is an adaptation of the DUROS® implant technology for the delivery of leuprolide acetate, a peptide LHRH agonist. The implant consists of a cylindrical titanium alloy reservoir capped at one end by a rate- controlling membrane and capped at the other end by a diffusion moderator. Within the diffusion moderator an orifice is located, through which the drug release occurs (Figure 2). The osmotic engine, containing sodium chloride, expands as the device is imbedded into water. Consequently, the pressure applied by the piston forces the drug formulation through the orifice. Leuprolide is delivered in a constant manner over 1 year. The external dimension of the implant is 4 mm in diameter and 45 mm in length (Wright et al., 2001)

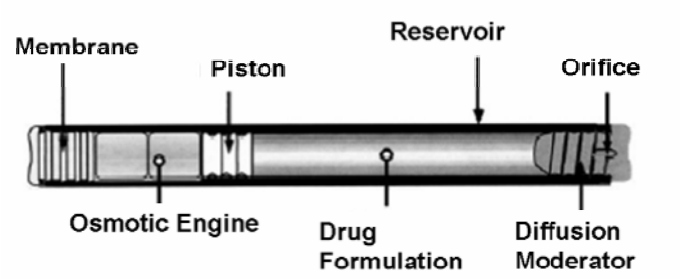

Figure 2 Cross-sectional diagram of the Duros® implant (Wright et al., 2001)

1.6 Solid implants as drug delivery systems for peptides and proteins

Solid implants are an interesting dosage form since high drug-loadings can be achieved leading to a more prolonged effect. Moreover, detrimental effects caused using solvents or presence of interfaces, characteristic of other methods to prepare other dosage forms, can be avoided, and thus, stability of the macromolecule can be preserved. Solid implants can be categorized as matrix- or reservoir-based systems, and depending on their geometry, matrix, drug loading, presence of excipients and production method different performance characteristics can be obtained (Bourges et al., 2006; Dash and Cudworth II, 1998).

1.6.1 Evolution of solid implants as drug delivery systems

The concept and research of implantable drug delivery systems started with Deansby and Parkes who described in 1938 the effect of subcutaneous implantation of compressed pellets of crystalline estrogen upon castrated male chickens. This was followed by the work of Folkman and Long in 1960s', who investigated the possibility of prolonged systemic drug administration with use of silicone rubber (Folkman and Long, 1964). Silicone rubber capsules containing a variety of different drugs were prepared and implanted into the cardiac muscle of dogs showing biocompatibility and achieving the controlled release of different

drugs. Since these early days, the research using implantable drug delivery systems has thrived with the use of different carriers, different classes of drugs, various implantation techniques and implantation sites (Del Valle et al., 2009; Hoffman, 2008; Kleiner et al., 2014; Langer, 1991; Langer and Folkman, 1976).

The research on this field has fluctuated over the time but has kept a steady interest during the last decades (Figure 3 and Figure 4). The emerging of newer formulation techniques and the challenge that solid implants present for implantation due to their size, might have impair the faster growth within this field. Nonetheless, the potential that solid-implants dosage forms have and the challenges that still need to be addressed, give big room to continue the research on this field.

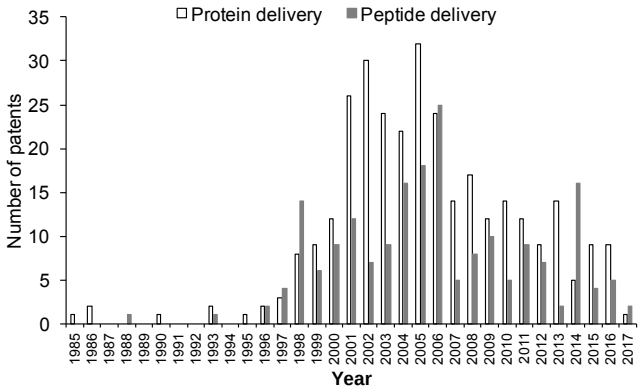

Figure 3 Number of patents related to solid implants for the delivery of peptides and proteins over the time (data retrieved from SciFinder up to 10.02.2017)

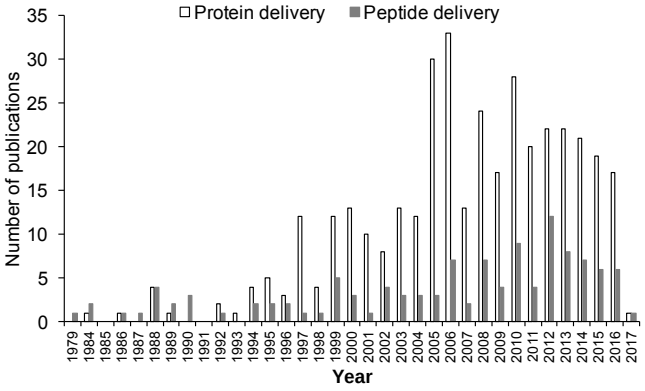

Figure 4 Number of research papers related to solid implants for the delivery of peptides and proteins over the time (data retrieved from SciFinder up to 10.02.2017)

1.6.2 Production techniques for solid implants

1.6.2.1 Compression

Compression is generally used for the production of lipidic implants (Guse et al., 2006b; Koennings et al., 2007; Kreye et al., 2011a; Mohl and Winter, 2004; Schwab et al., 2009) but has also been used for the preparation of polymeric devices (Ramchandani et al., 1997; Santoveña et al., 2006). Hydraulic presses equipped with special compaction tools are commonly employed at a lab scale. Usually, homogeneous powder blends are filled into these compaction tools, and force is applied for a certain time span. Different shapes can be obtained depending on the geometry of the compaction tools. However, their size and/or shape does not usually allow the implantation without a surgical procedure required. Nonetheless, this is a suitable technique for screening and preliminary evaluation purposes at the lab, as it has been exemplified in the studies mentioned before.

1.6.2.2 Melt compression/compression molding

Compression molding is one of the oldest techniques used for processing plastics that has been applied for preparation of implantable systems. One of the most remarkable examples is the Gliadel® wafer used for the treatment of brain cancer. It is a carmustine-loaded polyanhydride-based implant intended for the local delivery of the chemotherapeutic drug. The polymer matrix and the drug are dissolved in an organic solvent, spray-dried into microparticles and compressed molded in wafers with a diameter of 14 mm and 1 mm thickness. It requires the implantation by a surgical procedure, but due to its biodegradable character it is naturally eliminated and metabolized by the organism.

Typically, a metal mold is filled with the raw materials or blend (either pre-processed or not) and it is then heated, and pressure is applied until the powder has plasticized completely. The hot mold is finally cooled at a controlled rate, and the sintered implant is demolded (Kim et al., 2005). Compression molding has the benefit that shear-sensitive materials can be processed since there are no regions of very high stress, which can be advantageous for peptides and proteins. Furthermore, the shape of the implants is independent of the physicochemical properties of the materials used as matrices in contrast to other techniques where swelling of the implant can occur (i.e. melt extrusion). This enables better comparison of different formulations prepared with different materials (Witt et al., 2000).

1.6.2.3 injection molding

This manufacturing technique is also originated from the plastics industry. Normally, the materials are fed into a heated barrel, mixed, and forced into a mold cavity where it cools and hardens to the configuration of the cavity. The setup of the machine typically consists of

a hopper, an injection ram or a screw-type plunger, and a heating unit, which is comparable to hot melt extruders. The only difference is the final shaping of the implant formulation: hot melt extruders usually produced a rod-shaped implant, whereas injection molding allows the use of molds with multiple shapes and sizes (Zema et al., 2012).

Vapreotide-loaded biodegradable implants were prepared by both techniques, hot melt extrusion and injection molding, showing the suitability of both methods. However, the peptide purity was affected by the high shear forces and comparatively high process temperatures used during injection molding. Furthermore, an increase in the crystalline/amorphous ratio of the matrix was observed for the implants prepared by injection molding, which decreased the release rate of the peptide (Rothen-Weinhold et al., 1999b). Thus, extrusion techniques are still preferred as methods for implant preparation (Major and Mcconville, 2015).

1.6.2.4 Extrusion

Most polymeric implants are prepared by extrusion (Crowley et al., 2007; Repka et al., 2007). Generally, extrusion describes a process during which the raw material is forced through an orifice or a die. For that purpose, at least two main components are necessary: (1) a transport system that may impart a mixing function and (2) a die system, which forms the material. The pressure required for extrusion depends on the design of the die, on the extrusion rate, and particularly on the rheological characteristics of the formulation (Lang et al., 2014; Repka et al., 2007).

1.6.2.4.1 Hot melt extrusion (HME) – screw extrusion

Especially screw extruders are used for the manufacturing of granules or pellets that are further processed into capsules or tablets (Breitenbach, 2002; Crowley et al., 2007; Repka et al., 2007). Long-acting parenteral implants have also prepared with this technique yielding to cylindrical rods that can be administered by means of a hypodermic needle, as exemplified by the case of Zoladex® (Repka et al., 2008; Rothen-Weinhold et al., 1999b; Stanković et al., 2015a).

HME is a method that processes a raw material or blend into a product of uniform shape and density by forcing it through a die under controlled conditions such as temperature and pressure. Conventional extruders consist of two components: a transport system that may impart a mixing function and a die system that forms the material (Chokshi and Zia, 2004; Lang et al., 2014; Maniruzzaman et al., 2012; Singhal et al., 2011).

Screw extruders are characterized by at least one rotating screw inside a stationary cylindrical barrel (Figure 5). A die, that is connected to the end of the barrel, determines the shape of the extruded product. The heat required to melt the material inside the barrel is a

result of friction occurring as the screw(s) moves and the heat supplied externally (Breitenbach, 2002).

Three sections are usually found in the barrel: feed zone, transition zone, and metering zone. The starting material is fed from a hopper directly into the feed section, where the material is enabled to fall easily into the rotating screw. It is then conveyed along the barrel and reaches the transition zone where it is mixed, compressed, melted, and plasticized. The function of the metering zone to which the material is finally transported as a homogeneous melt is the reduction of the pulsating flow, thus ensuring a uniform delivery rate through the die (Breitenbach, 2002; Chokshi and Zia, 2004).

Twin-screw extruders consist of two agitator assemblies mounted on parallel shafts that might either rotate in the same or the opposite direction. Counter-rotating extruders have better mixing capabilities as their surfaces move towards each other, thereby squeezing the material through the gap between the two screws. This results in comparatively high shear forces, air entrapment, high pressures, low maximum screw speeds and poor output (Breitenbach, 2002; Crowley et al., 2007). Co-rotating extruders are generally of the intermeshing design which is known to be self-wiping. This ensures almost complete emptying of the barrel, hence minimizing product wastage on shutdown and lower screw and barrel deterioration (Breitenbach, 2002; Crowley et al., 2007; Stanković et al., 2015a). Furthermore, they can be operated at high screw speeds, achieving high outputs while maintaining good mixing and conveying characteristics (Crowley et al., 2007).

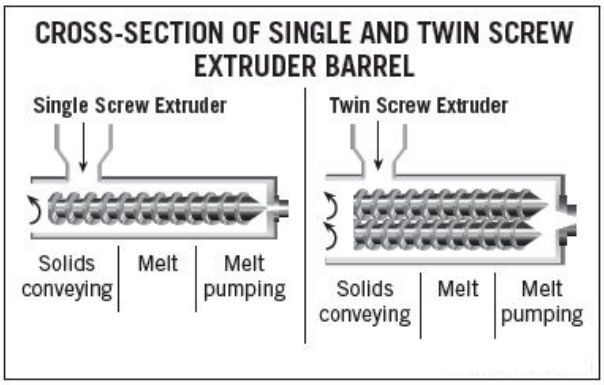

Figure 5 Schematic representation of a single-screw [left] and a twin-screw extruder [right] (Particle Sciences, 2011)

Preparation of protein-loaded solid implants using twin-screw extruders have shown to be a suitable technique. Although shear forces and the use of high temperatures characteristic of this process are detrimental for the protein, different studies have shown that stability of the protein can be preserved during implant preparation and protein release; in some cases, the inclusion of stabilizing excipients, like sugars or cyclodextrins, helped to maintain protein integrity. Both polymeric (Ghalanbor et al., 2010; Stanković et al., 2015b, 2014, 2013) and

lipidic (Even et al., 2014, 2015; Sax et al., 2012; Sax and Winter, 2012; Schulze and Winter, 2009) matrices have been investigated yielding to formulations that release the protein from a couple of days up to several months. Not only the composition of the matrix, but also the processing parameters and the protein properties are factors that influenced the performance of the formulations, as it has been exemplified by the different studies refereed above.

1.6.2.4.2 Ram extrusion

As depicted in Figure 6, the setup and operating principle of a ram extruder is quite simple: the barrel that is closed with a die at one side, is pre-filled with the raw material or blend. It is then mounted into the heating unit that enables a precise temperature control, and the piston moves downwards forcing the material through the die. The process is usually divided into different phases: the material inside the barrel is compressed to a plug (i.e. compression), to remove residual air, heat is applied to melt the material and allow its continuous movement through the barrel and die (steady state flow), and finally the material is pushed through the die with the movement of the piston controlled either by a constant piston speed or by a constant piston force (forced flow) (AGC Chemicals Europe, 2002).

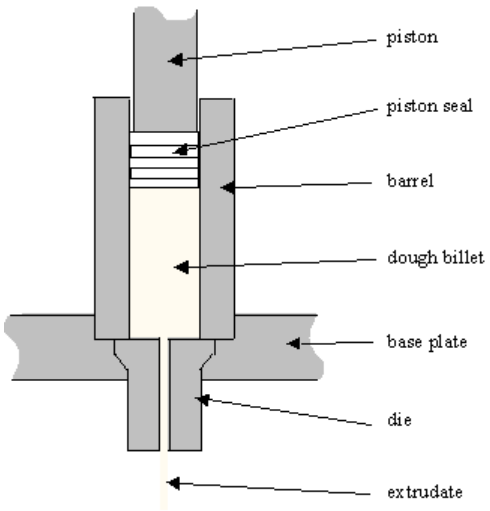

Figure 6 Schematic representation of a ram extruder (Cheyne, 2016)

In general, ram extrusion differs to HME in some characteristics: the process cannot be run continuously and so the batch size is limited by the barrel's capacity, the system does not provide mixing function, so the raw materials have to be pre-blended, and the melting capacity might be limited (depending on the sophistication of the system), which may cause poor temperature uniformity in the extrudate (Crowley et al., 2007). Nonetheless, examples of peptide- (Rothen-Weinhold et al., 1999b, 1997) and protein-loaded (Ghalanbor et al.,

2013, 2012) implants have shown the suitability of this preparation technique, specially at a small scale where screening activities are being performed.

1.6.2.5 Solvent casting

Although solvent casting has the disadvantage of involving large amounts of organic solvents, it has been used for the lab- scale manufacturing of PLGA-based implants (Frank et al., 2005; Santoveña et al., 2006; Vesna Milacic and Schwendeman, 2014; Wang et al., 2010; Zhu and Schwendeman, 2000). The polymer is typically dissolved in an appropriate solvent such as dichloromethane or acetone, followed by the addition of the drug and homogenization of this blend. Afterwards, it is poured into three-dimensional molds or cast onto glass plates, where the solvent is allowed to evaporate (it may last several weeks depending on the solvent and polymer used, and the mold geometry (Wang et al., 2010).
Protein encapsulation can be achieved by either suspending the solid particles or by emulsifying the aqueous protein in the organic polymer solution and subsequent solvent casting (Vesna Milacic and Schwendeman, 2014; Zhu and Schwendeman, 2000). Alternatively, the protein solution itself can be solvent casted by pouring the aqueous protein solution into molds and, after drying, the formed pellet is wetted with the organic polymer solution (Dorta et al., 2002; Santoveña et al., 2006).

Table 3 compares the different methods described above by summarizing the advantages and disadvantages of each of them. As mentioned before, extrusion and compression techniques are the most common for the preparation of protein- and peptide-loaded solid implants. Extrusion is usually preferred because it is closer to an industrial process that can be easily scale-up, it is continuous and have the possibility to be adjusted to the manufacturing conditions required to produce parenterals. Although few solid-implants products are in the market, they remain as an attractive dosage form (Kleiner et al., 2014). Comprehensive knowledge to address the challenges that the different preparation methods bring along, and additional efforts to preserve the macromolecule stability are necessary to achieve a more successful number of peptide- and protein-implant formulations on the market.

Table 3 Advantages and disadvantages of the preparation methods for solid implants

Manufacturing process	Advantages	Disadvantages
Compression	Does not involve the use of heat Different geometries possible Small batch size (optimal for screening)	Segregation could occur due to differences in flow properties Is not a continuous process (variability within implant)
Melt compression / Compression molding	Shape of implants remained unchanged independently of the matrix used and its physicochemical properties Smoother implant surface than in compression Small batch size (optimal for screening) Denser matrix: slower release	Heat that can cause denaturation and polymorphic changes Denser matrix: incomplete release Is not a continuous process (variability within implant)
Injection molding	Different geometries possible Small batch size (optimal for screening)	Heat that can cause denaturation and polymorphic changes High shear forces Carrier suitable for melt processing Is not a continuous process (variability within implant)
Ram extrusion	Homogenous drug distribution Simpler set-up than HME Various process parameters can be adjusted and controlled	Heat that can cause denaturation and polymorphic changes Carrier suitable for melt processing No continuous process Mixing is not possible
Screw extrusion (HME)	Continuous process Mixing is possible Different feeding zones and temperature ranges could be adjusted along the barrel Various process parameters can be adjusted and controlled	Heat that can cause denaturation and polymorphic changes Carrier suitable for melt processing Shear forces Shape of implant depends on carrier used (i.e. swelling) Drug-matrix interactions caused by heat and shear forces
Solvent casting	Small batch size (optimal for screening) Different geometries possible	Use of solvents Creation of interfaces Long drying times

1.6.3 Materials used for preparation of protein- and peptide-loaded solid implants

Implantable drug delivery systems include non-degradable and degradable systems, where usually the key parameters of the formulation are given by the type of matrix (usually polymeric materials) and its interaction with the encapsulated drug. These components usually serve to control the drug delivery (i.e. rate and place), but may also have additional functions, such as structural support and improvement of biocompatibility or stability (Kleiner et al., 2014).

1.6.3.1 Non-biodegradable materials

Non-degradable matrix system and reservoir systems are the two most common forms. In polymeric matrix system (i.e. monolithic system) the drug is dispersed, homogeneously, inside the matrix material. Slow diffusion of the drug through the polymeric matrix material or a membrane (as in the case of Viadur®, which is made of titanium with an osmotic system to control the release, see Figure 2) provides sustained release of the drug from the delivery system. The reservoir-type system, on the other hand, consists of a compact drug core surrounded by a permeable non-degradable membrane whose thickness and permeability properties can control the diffusion of the drug into the body (Ranade, 1990).

Non-degradable polymers include hydrophilic polymers such as polyacrylamide or hydrophobic polymers such as ethylene vinyl acetate (EVAc) copolymer and silicone elastomers. These matrices can release macromolecules for more than 100 days. The release rate can be adjusted by the addition of a hydrophilic pore-building excipients and the adjustment of the total matrix loading, among other parameters (Banga, 2006). Peptides and proteins investigated for their release behavior from silicone elastomers include the dipeptide Gly-Tyr, insulin, BSA, chymotrypsin, and pepsin (Carelli et al., 1989; Hoth and Merkle, 1991)

Hydroxyapatite is another biocompatible material that has been used as microcarrier for controlled release of proteins (IJntema et al., 1994). EVAc polymer is one of the more commonly used non-degradable polymers as it is biocompatible and offers control of the release rates of embedded polypeptides. The incorporation of a powdered polypeptide into EVAc polymer matrix creates a series of interconnecting channels. Water can diffuse into the matrix from these channels to dissolve the polypeptide, which is then released through the porous matrix. Because release occurs only when pores are interconnected, there is a minimum loading dose that should be used to enable the release (percolation threshold); this also depends on the size of the encapsulated compound (Banga and Chien, 1988; Cohen et al., 1984; Heller, 1993; Rhine et al., 1980). Polymethylmethacrylate (PMMA) and polydimethylsiloxane have also being used for implant preparation, especially in the treatment of osteomyelitis (Dash and Cudworth II, 1998). However, up to now, these

materials has been reported suitable for small molecules and not for the delivery of proteins or peptides.

1.6.3.2 Biodegradable materials

For the controlled delivery of peptides and proteins, the most studied systems are based on lactide/glycolide copolymers, poly(caprolactone), poly(ortho esters), and polyanhydrides (Heller, 1993; Stanković et al., 2015a). In the last years, lipid materials have also been explored as carriers for the delivery of proteins from solid implants (Kreye et al., 2008; Sax et al., 2012; Sax and Winter, 2012; Schulze and Winter, 2009).

In addition, cellulose derivatives, starch, chitosan and xanthan gum are additional suitable candidates for solid implant preparation. However, their degradation rate is difficult to predict since it occurs enzymatically. Moreover, they could trigger immune responses due to their inherent biological activity. Therefore, their use has not been widespread (Stanković et al., 2015a).

PLGA is a linear polyester that hydrolyzes by an acid- or base-catalyzed reaction to form the natural metabolites, glycolic and lactic acids. Thus, these polymers are biocompatible, biodegradable, and considered safe and have been used as bioerodible sutures and in many of the commercialized products (Table 1). The mole ratio of lactide to glycolide in the PLGA polymer can be changed; increasing the amount of glycolide in the polymer increases its rate of biodegradation. For polymers with the same lactide: glycolide ratio, the polymers with the lowest molecular mass degrade most rapidly. However, the lactide: glycolide ratio has more influence on the rate of polymer degradation than the polymer molecular weight (Ramchandani et al., 1997; Vey et al., 2008).

The lactide/glycolide copolymers undergo a hydrolysis process that occurs throughout the bulk of the material. In contrast, poly(ortho esters) and polyanhydrides undergo a hydrolysis process that is largely confined to the surface of the polymer (Banga, 2006). In the case of PLGA polymers, the permeability changes with time as the polymer undergoes bulk erosion, thus rendering the drug release rate unpredictable to some extent. In the case of the poly(ortho esters) and polyanhydrides this is avoided as they undergo only surface erosion and can provide precise release rates (Heller, 1993; Heller et al., 2002; Heller and Barr, 2004; Lopac et al., 2009; von Burkersroda et al., 2002). Multiblock co-polymers composed of poly(ethylene glycol) and poly(ε-caprolactone) have also shown suitability for protein-loaded implant preparation, with an extended release and preservation of protein stability (Stanković et al., 2015b, 2014, 2013).

A fibrin matrix has also been shown to be a biodegradable and biocompatible matrix that can be used as a surgically implantable or injectable delivery device (Kumar et al., 2004; Taylor and Sakiyama-Elbert, 2006). Bioerodible non-cross-linked poly(methyl methacrylate-co-

methacrylic acid) beads have also been used to achieve synchronization of swelling and dissolution fronts of the spherical bead for the release of a GH-releasing peptide (Lee, 1993).

Since some years, lipidic matrices are being explored as alternatives to the polymeric materials for implant preparation. As they do not degrade generating acidic species that impair protein integrity, they have been able to preserve the stability of the protein for long term (Even et al., 2015; Mohl and Winter, 2006; Sax et al., 2012; Schulze and Winter, 2009; Vogelhuber et al., 2003b). Nonetheless, the challenge with these materials remains in their polymorphic changes that can occur upon processing and over the time, changing the performance of the initial formulation.

1.6.4 Drug release mechanisms governing the release from solid implants

1.6.4.1 Release from non-degradable matrices

First reports of controlled release systems for proteins showed the sustained release of various proteins and peptides from cross-linked poly(acrylamide) and poly(vinylpyrrolidone) gels (Davis, 1974), and from poly-(2-hydroxyethylmethacrylate) and EVA devices (Langer and Folkman, 1976). Detailed mechanistic studies on these systems revealed that protein release occurs via diffusion through a complex porous pathway within the inert matrix (Langer and Moses, 1991). First, water penetrates the system and dissolves the incorporated macromolecule as well as hydrophilic excipients leading to the creation of the porous microstructure. The subsequent leaching out of the protein and the excipients alters the matrix morphology, creating pores and channels randomly distributed through the matrix, which enables the diffusion of the protein into the bulk fluid. Due to the randomness of the particle position, the created pores are not straight but very sinuous, and can be described with the tortuosity factor (Bawa et al., 1985; Cohen et al., 1984). The tortuosity directly relates to the effective distance the protein needs to transfer for diffusing out of the matrix: an increasing tortuosity is associated with an increase in the diffusion pathways and with a retardation of the release (Pitt, 1990). Therefore, the effective diffusivity, that characterizes the drug mobility within the matrix – is of magnitudes smaller than in aqueous media. Typically, for matrices comprising spherical particles rather low tortuosities between 1.5 and 3 are assumed (Schwartz et al., 1968). Besides to the tortuosity, the connection of the pores through narrow channels also contributes to the retardation of the protein release (i.e. the protein molecule needs certain time until it finds its way from one pore to another) (Cohen et al., 1984).

The pore morphology and thus the in-vitro release kinetics are influenced by the used manufacturing technique, the initial drug loading and the particle size of the drug powder. As

the protein is dispersed randomly within the matrix, the chance for two particles to encounter each other is very rare, when protein loadings are low. A certain amount of drug particles is then surrounded entirely by the matrix material and due to its impermeability for macromolecules, the protein cannot be released. Only at higher drug loadings the particles get in touch and upon dissolution a fully interconnected pore network is created, which ensures a complete protein liberation (Kleiner et al., 2014). Generally, protein release is reported to occur faster when larger drug particles are incorporated. Moreover, the diameter of the created pores as well as the overall porosity increases with increasing particle size (Bawa et al., 1985; Cohen et al., 1984).

1.6.4.2 Release from degradable matrices

An analogy to protein release from non- degradable polymeric matrices could be assumed for lipidic matrices since no erosion or swelling was revealed during in-vitro incubation implants based on various triglycerides (Guse et al., 2006c; Vogelhuber et al., 2003a).

For a degradable polymer matrix, the protein release is governed by several mechanisms: (i) diffusion through a water-filled pore network, (ii) degradation of the polymer, and/or (iii) swelling of the system. The real conditions are often a combination of all three processes (Gombotz and Pettit, 1995; Langer and Moses, 1991; Pitt, 1990). For example, protein release from PLGA-based systems is initially controlled by desorption of the protein from the surface. This phase is followed by the diffusion of protein through water filled pores, which in turn might be influenced by swelling. Finally, the polymer starts to degrade and a combination of diffusion and erosion phenomena governs drug release (Gombotz and Pettit, 1995; Sinha and Trehan, 2003). As a result, a multiphasic release profile is often observed: after a burst release of surface located and poorly encapsulated protein, a phase of lower release rates controlled by diffusion follows, and finally an increased diffusion rate, corresponding to the polymer cleavage (i.e. polymer erosion), mark the third release stage (Gombotz and Pettit, 1995).

The physical state of the polymer can also change during in-vitro release making this release process more complex and sometimes unpredictable. For instance, hydration of PLGA matrices during in-vitro release lowered the glass transition temperature, which accelerated polymer degradation and release rates (Park, 1995). Furthermore, osmotic effects as well as ionic and covalent interactions between polymer and protein chains also play a role in the mechanism behind the protein release properties (Bodmer et al., 1992; Ghalanbor et al., 2012; Park et al., 1998).

Moreover, the impact of protein stability on the in-vitro release kinetics from both, degradable and non-degradable delivery devices, seems to be of importance. Several authors attributed a high burst followed by a non-release phase to protein aggregation within

the device. As described above, protein aggregation may be induced during both, implant manufacturing and release (see 1.3.1.2). Because of their large size higher-order aggregates cannot diffuse through the restricted diameter of the pore network and hence are trapped within the matrix (Ghalanbor et al., 2012; Giteau et al., 2008).

1.7 Research objectives

The purpose of this work was to produce and characterize biodegradable implants prepared by hot-melt extrusion for the sustained parenteral delivery of proteins. The specific goals were:

- To assess the suitability of hot melt extrusion to prepare ovalbumin-loaded PLGA- and lipid-based implants
- To characterize the release of OVA-loaded PLGA-based implants and to identify the reasons for protein instability and release incompleteness
- To improve protein release completeness from PLGA-based implants
- To evaluate the characteristics and performance of lipid-based implants, with special emphasis on polymorphic changes of the lipidic matrix, dissolution profile and protein stability
- To optimize the dissolution of OVA from lipid-based implants by identifying key formulation parameters and by implementing Design of Experiments (DoE)
- To investigate the effect of gamma-irradiation, as terminal sterilization approach, on the characteristics of PLGA- and lipid-based implants

2. Materials and methods

2.1 Materials

2.1.1 Proteins

Ovalbumin lyophilized powder (OVA) (Sigma-Aldrich Chemie GmbH, Munich, Germany); lyophilized hen egg white lysozyme (LYS) (Carl Roth GmbH & Co. KG, Karlsruhe, Germany)

2.1.2 Biodegradable matrices

Poly(D,L-lactide-co-glycolide acid) (5050 DLG2A, un-capped 50:50 PLGA, log MP 4.064 ± 0.020 (g/mol), Tg 38.9°C), inherent viscosity 0.2 dlg^{-1}, Lakeshore Biomaterials ™ Evonik Industries AG, Essen, Germany); glycerol trimiristate (Dynasan 114), glycerol tristearate (Dynasan 118) and hydrogenated palm oil (Dynasan P 60) (Cremer Oleo, GmbH & Co. KG, Hamburg, Germany).

2.1.3 Co-excipients

Shellac (SSB® 57 Pharma Flake Shellac, Tg 37.9°C, SSB Stroever GmbH & Co. KG, Bremen, Germany); magnesium carbonate (Fagron GmbH & Co. KG, Barsbüttel, Germany); magnesium hydroxide (Sigma-Aldrich Chemie GmbH, Munich, Germany); Poloxamer 407 (Lutrol F127), Polyethylene glycol 400, 1500, 4000 and 6000 (Lutrol® E), polyvinylpirrolidone (PVP, Kollidon 17PF) (BASF AG, Ludwigshafen, Germany); calcium chloride ($CaCl_2$), sodium chloride (NaCl), D-(+)-sucrose (Carl Roth GmbH & Co. KG, Karlsruhe, Germany), mannitol (Fluka Sigma-Aldrich Chemie GmbH, Munich, Germany); Poly(D,L-lactide acid) (PDL02A, inherent viscosity 0.2 dlg^{-1}, Corbion, Gorinchem, The Netherlands); glycerol dibehenate (Compritol® 888ATO), glycerol distearate (Precirol™ ATO5) (Gattefossé GmbH, Bad Krozingen, Germany).

2.1.4 Reagents and kits

1-anilino-8-naphthalene sulfonate (ANS), deuterated chloroform ($CDCl_3$), formic acid, guanidinium chloride (GnHCl), hydroxylammonium chloride, sodium azide (NaN_3), tetramethylsilane ($SiMe_4$), (Sigma-Aldrich Chemie GmbH, Munich, Germany); disodium hydrogen phosphate, ethanol, hydrochloric acid, potassium dihydrogen phosphate, sodium chloride, sodium hydroxide (NaOH), sodium dodecyl sulfate (SDS), tetrahydrofuran (THF) (Carl Roth GmbH & Co. KG, Karlsruhe, Germany); ethyl acetate (Merck KGaA, Darmstadt,

Germany); acetonitrile (ACN), dithiothreitol (DTT), methanol (VWR Chemicals GmbH, Darmstadt, Germany); ultrapurified water purified by a Milli-Q-apparatus (Merck-Millipore, Merck KGaA, Darmstadt, Germany); Pierce™ 660nm Protein Assay for total protein quantification (Thermo Fisher Scientific Inc., USA).

2.2 Methods

2.2.1 Preparation of Implants

2.2.1.1 PLGA-based implants

2.2.1.1.1 Freeze drying of OVA and co-excipients prior extrusion

For some formulations, OVA was freeze dried together with the co-excipients prior the extrusion process. For this, the solids were co-dissolved in 10 mM phosphate buffer, pH 7.4 (1:4 protein: co-excipient ratio); usually 2 mL of this aqueous solution was charged into 25 mL glass vials. The solutions were frozen into liquid nitrogen and subsequently lyophilized using a Martin Christ Gamma 2-20 (Martin Christ Gefriertrocknungsanlagen; Osterode, Germany) with a shelf temperature of -30°C, a condensor temperature of -90°C and a pressure of 0.270 mBar. Samples were equilibrated for 1 hour under those conditions. Primary drying was conducted by increasing the temperature to 0°C during 4 hours (pressure of 0.370 mBar), and the process continued under these conditions for another 18 hours. Subsequently, the shelf temperature and pressure were raised to +15°C and 0.470 mBar, and the samples were kept under these conditions for another 6 h. OVA alone in solution was freeze dried under the same settings and serve as a control.

2.2.1.1.2 Hot-melt extrusion with a mini-ram extruder

Blends of OVA, PLGA and other co-excipients, when required, were prepared by physical mixing in a mortar with pestle. Implants were prepared with a syringe-die extrusion device (mini-ram extruder) (Ghalanbor et al., 2010) heated at 100ºC for 7 to 12 minutes depending on the formulation. Cylindrical matrices with diameter of around 1.5 mm were obtained after the molten blends were manually extruded. The matrices were cut into 20 mg implants and evaluated for release kinetics, and degradation and interaction experiments. PLGA-only implants were used as control.

2.2.1.1.3 Hot-melt extrusion with a twin-screw extruder

Blends of OVA, PLGA and shellac, were prepared by physical mixing in a mortar with pestle. The mixture (~5 g) was manually fed into the preheated barrel (85°C) of the twin-screw extruder (HAAKE MiniLab Rheomex CTW5 co- rotating twin-screw extruder, Thermo Scientific, Karlsruhe, Germany). A 30-rpm screw speed and a 1.5 mm die diameter were used during extrusion. Cylindrical strands with diameter between 1.5 and 1.6 mm were

obtained and cut into 20 mg implants. These were evaluated for release kinetics, protein stability and storage stability.

2.2.1.2 Lipid-based implants

Blends of OVA, the lipid matrix (Dynasan 114, Dynasan 118 or Dynasan P 60) and other co-excipients, when required, were prepared by physical mixing in a mortar with pestle. Implants were prepared with a syringe-die extrusion device (Ghalanbor et al., 2010) heated at 100ºC for 4 to 8 minutes depending on the lipid matrix used. Cylindrical matrices with diameter of around 1.5 mm were obtained after the molten blends were manually extruded. The matrices were cut into 20 mg implants and further processes and/or characterized. The Dynasan 118-based and Dynasan P 60-based implants were further cured by incubating them in an oven (Heraeus Instruments, Osterode, Germany) at 40, 45 or 50 ºC for 30, 60 and 90 min. Lipid-only implants were used as control.

2.2.2 Determination of Implant Morphology by Optical Light Macroscope

Implant morphology was studied using a macroscope (Inteq Informationstechnik GmbH, Berlin, Germany). The magnification of macroscope was adjusted to obtain a clear observation. The images were recorded by image analysis software (EasyMeasure, Inteq Informationstechnik GmbH, Berlin, Germany).

2.2.3 Mechanical properties of implants

Mechanical properties (hardness and energy required to break the implants) were determined using a texture analyzer (TAXT.Plus, Winopal Forschungsbedarf, Ahnsbeck, Germany). A flat-faced cylindrical probe (6mm diameter) was fixed on the load cell (5 kg) and driven downwards towards the implant at a speed of 0.01 mm/s (flat surface towards the implant). Load versus displacement curves were recorded until implant rupture and used to determine the energy required to break the systems as follows:

$$Energy\ at\ break\ per\ unit\ volume\ = \frac{AUC}{V}$$

where AUC is the area under the load versus displacement curve and V the volume of the implant. Hardness was considered as the maximum force reached prior to the implant's fracture. Mechanical properties of 6 replicates were analyzed using Student's t-test for paired data with Microsoft® Excel program. A *p*-value <0.05 was considered as statistically significant.

2.2.4 Differential scanning calorimetry (DSC)

Thermograms of implants and lipid powders were recorded using a DSC 6000 (PerkinElmer, Inc. Waltham, MA, USA). Samples of ~10 mg were accurately weighed in 50µL aluminum pans with pierced lid. DSC scans were recorded using a heating rate of 5 ºC/min within -10 and 100ºC. For bulk lipids two heating rates were applied with a cooling at 20ºC/min between them.

2.2.5 X-ray diffraction (XRD)

The lipids and ground implants were analyzed by X-ray diffraction using a Philips X-ray generator PW 1830 (Philips Industrial and Electroacoustic Systems Division, Almelo, The Netherlands) with a diffraction angle range between 4° and 40° and a step size of 0.02°.

2.2.6 Protein extraction from implants

2.2.6.1 PLGA-based implants

Protein was extracted from the implants by precipitation with ethyl acetate and re-dissolution in buffer as described previously (Körber and Bodmeier, 2008). Briefly, the implants (~20 mg) were dissolved in 1.5 ml ethyl acetate and then centrifuged for 20 min at 20°C and 17000 rpm (Heraeus Biofuge stratos Haemo, Heraeus Instruments, Osterode, Germany). About 1 ml of the supernatant (dissolved polymer in ethyl acetate) was removed, and the washing cycle was repeated three more times. The protein precipitates were then dried under vacuum for 180 min (Heraeus oven VT 5042 EKP, Hanau, Germany, coupled with a chemistry hybrid pump, Vacuubrand GmbH, Wertheim, Germany) to remove residual ethyl acetate, and were then dissolved in 1 ml release medium (10 mM phosphate buffer, pH 7.4 containing 0.02% sodium azide). Quantification of soluble OVA was performed using the Pierce™ 660nm Protein Assay for total protein quantification (Thermo Fisher Scientific Inc., USA) and/or by HPLC as described in section 2.4.

2.2.6.2 Lipid-based implants

Protein was extracted from the implants as described before (Sax and Winter, 2012). Briefly, the implants were ground, suspended in phosphate buffer, pH 7.4, and heated to 60ºC for 10 min. The samples were cooled down and centrifuged for 20 min at 20°C and 17000 rpm (Heraeus Biofuge stratos Haemo, Heraeus Instruments, Osterode, Germany). Quantification of soluble OVA was performed spectrophotometrically at a wavelength of 280 nm (UV-VIS scanning spectrophotometer 2101 PC, Shimadzu, Kyoto, Japan).

2.2.7 Protein quantification and structural integrity of ovalbumin

Size exclusion chromatography (SEC) was performed by HPLC (SCL-10A VP, Shimadzu, Japan) using a G2000SW$_{XL}$ column (Tosoh Bio-science, USA). The mobile phase consisted of 0.05 M potassium dihydrogen phosphate with 0.3 M sodium chloride at pH 6.6, at a flow rate of 1 ml/min for 18 minutes and a column temperature of 30ºC. Samples were injected (60µL) and protein detection by UV was done at 214 nm. Retention times of roughly 7.5, 6.4 and 5.2 min were obtained for OVA, its dimer and the soluble aggregates, respectively.

2.2.8 Fourier transform infrared spectroscopy (FTIR)

FTIR spectra were generated with an Excalibur 3100 FTIR spectrophotometer (Varian Inc., Palo Alto, USA). The spectra from protein powder, PLGA, ground implants (with mortar and pestle) or dried implants after release, were collected using a horizontal ATR accessory with a single reflection diamond crystal (Pike Miracle, Pike Technologies, Madison, USA). Sixty-four scans at 4 cm^{-1} resolution were averaged, and spectral contributions coming from water vapor in the light pass were subtracted using Varian software (Resolution Pro 4.0). All spectra were treated with a 13-point smoothing function.

2.2.9 Circular dichroism (CD)

CD measurements were performed using a Jasco J810 spectropolarimeter at 20ºC (Hachioji city, Japan). Spectra were recorder over 190-250 nm using a cuvette of 2mm path length and scan rate of 100 nm/min under nitrogen flow. Three measurements were performed and averaged. The CD spectra obtained was expressed in terms of ellipiticity. Ellipticity of all spectra was corrected for the molarity of the solution. OVA-free implant formulations were included for subtraction of matrix and/or buffer effects.

2.2.10 Fluorescence spectroscopy

Fluorescence spectra were recorded at 25ºC with a Fluoromax-4 spectrofluorometer (Horiba Jobin Yvon, Longjumeau, France) using a 1 cm cuvette. An excess of ANS (fluorescent probe) at 50 µM was titrated with protein solutions prior the measurement. The emission spectra (460 – 520 nm) were obtained at an excitation wavelength of 378 nm, with an excitation and emission slit widths of at 2 and 5 nm, respectively. All fluorescence spectra were normalized and corrected for matrix or buffer contributions.

Surface hydrophobicity parameter (S_O) were measured using the method of Kato and Nakai (Kato and Nakai, 1980). Relative fluorescent intensity (F_R) was calculated as follows:

$$F_R = \left[\frac{F - F_O}{F_O}\right] \times 10$$

Where F and F_O are the fluorescence intensities of the sample and blank, respectively, at 480 nm. This value was plotted as a function of protein concentration and the slope of the regression line was taken as S_O.

2.2.11 Ovalbumin release

Implants (~20 mg) were incubated in vertical position in vials containing 1 mL of phosphate buffer (10mM, pH 7.4, + 0.02 wt.% sodium azide, n=3) at 37°C in a horizontal shaker (Gemeinschaft für Labortechnik, Burgwedel, Germany). At predetermined time intervals, complete medium exchange with fresh buffer was performed. OVA concentrations in the release samples were determined as already described. In the case of lipid-based implants lipid-only implants were used as blanks for the spectrophotometric quantification.

All in vitro release experiments were performed in triplicate and the data is presented as the sample mean ± standard deviation (SD).

The pH in the release medium was monitored with a pH-meter at each sampling point (Sartorius, Sartorius AG, Göttingen, Germany). The difference of the measured pH (pH_t) and the original pH of the release medium (t_0 = pH 7.4) was used for the calculation of the cumulative pH changes (in %) during release (Ghalanbor et al., 2013, 2012; Körber, 2010):

$$Cumulative\ \Delta pH_t = \frac{100 \times \sum_t^{t_0}(7.4 - pH_t)}{\sum_t^{t_0}(7.4 - pH_t)}$$

where the final t (t_f) is the time near the end of release, when pH of release medium remains unchanged (pH 7.4).

2.2.12 Determination of lipid composition

2.2.12.1 Nuclear magnetic resonance (NMR)

^1H and ^{13}C NMR spectra were recorded in $CDCl_3$ using a Bruker Avance 300 spectrometer with a QNP probe head (^1H: 300 MHz, ^{13}C: 75 MHz) or Bruker Avance 400 (^1H: 400 MHz, ^{13}C: 100 MHz) (Bruker Corporation, Rheinstetten, Germany). The calibration of the spectra was carried out and referenced with residual solvent shifts ($CDCl_3$, ^1H = 7.26, ^{13}C = 77.16) and were reported as parts per million relative to $SiMe_4$. All the NMR samples were measured at 297 K.

2.2.12.2 Electrospray ionization/Time-of-flight mass spectrometry (ESI/TOF-MS)

ESI-TOF spectra were recorded using an Agilent 6220 TOF liquid chromatographer mass spectrometer ESI/TOF-LC/MS (Agilent Technologies, Santa Clara, CA, USA). The samples were dissolved dichloromethane and the eluent consisted in a mixture of methanol: 0.1% formic acid in water (90:10) at a flow of 0.5 mL/min. The fragmentor voltage was 180V and

the capillary voltage 4000 V. Parameters for analysis were set using negative ion mode with spectra acquired over a mass range from *m/z* 50 – 1000.

2.2.13 Polymer molecular weight determination

Implants (~20 mg) were incubated as described in 2.8 and at predetermined points two samples were withdrawn for polymer molecular weight evaluation. After removal of the buffer, these degradation samples were vacuum-dried for 24 h, dissolved in THF, and analyzed for mass and the molecular weight distribution of the remaining polymer.

Gel permeation chromatography (GPC) analysis was carried out using a Shimadzu (Shimadzu, Tokyo, Japan) LD-10 liquid chromatograph in combination with a Viscotek triple detector (TDA-300, Viscotek, Malvern Instruments Ltd., Malvern, UK) operated in double mode (differential refractive index, viscosimetry), using a column with a linear range from 1000 g/mol to 20,000 g/mol (Mesopore 7.5 µm x 300 mm; Varian Inc., Darmstadt, Germany). THF was used as mobile phases at a flow rate of 1 mL/min and a column and detector temperature of 30ºC. 25 µL of the samples (20% concentration) were injected and a universal calibration method (third-order polynomial fit, R2 = 0.99996) was applied to determine the molecular weights of PLGA, which was obtained from polystyrene standards with peak molecular weights of 1,260 g/mol, 2,360 g/mol, 4,920 g/mol, 9,920 g/mol, 19,880 g/mol (Varian Inc., Darmstadt, Germany). Data acquisition was performed using Omnisec software (Viscotek, Malvern Instruments Ltd., Malvern, UK).

2.2.14 Protein-polymer interaction

To identify the nature of the interaction between the polymer and the protein a series of tests with different reagents was performed. Samples that presented a residual mass after more than 70 days of release, were vacuum-dried for 24 h and were exposed to the different treatments described in Table 4.

Table 4 Reagents used and their expected effect on residual mass of implants after release

Reagent; concentration	Expected effects	Reference
THF; 100%	PLGA Solvent	(Ghalanbor et al., 2012)
Ethanol; 100%	Shellac solvent	(Limmatvapirat et al., 2007)
SDS; 2%	Dissociation of non-covalent bonds and protein adsorbed to PLGA by hydrophobic interaction; solubilization of aggregates	(Park et al., 1998; Stanković et al., 2015b; Wang, 1999)
GnHCl; 6 M	Dissociation of non-covalent bonds	(Park et al., 1998; Wang, 1999)
ACN: H2O 50:50	Disruption of protein–protein contacts formed by hydrogen bonding formation; denaturation of protein	(Gekko et al., 1998; Wang, 1999)
NaOH; 1 M	Alkaline hydrolysis of esters; disruption of strong ionic interactions	(Ghalanbor et al., 2012)
DTT; 0.01 M	Cleaving disulfide bridges and thioester bonds at an intra- and intermolecular level	(Fenton and Fahey, 1986; Ghalanbor et al., 2012; Stanković et al., 2015b; Wang, 1999)
Hydroxylamine; 0.2 M	Hydrolyzing thioesters but not disulfide bridges	(Fenton and Fahey, 1986; Ghalanbor et al., 2012; Stanković et al., 2015b; Wang, 1999)

3. Part I: PLGA based implants - Results and discussion

3.1 Introduction

The development of delivery systems for peptides and proteins is still a lively research topic due to the growing number of therapeutic macromolecular candidates (Teekamp et al., 2015; Vaishya et al., 2014). The parenteral route is the preferred for their administration, because peptides and, specially, proteins possess a complex structure that results in physical and chemical stability issues and poor membrane permeability (Ibraheem et al., 2014). The development of sustained releasing systems has arisen from the need to prolong protein circulation and avoid its rapid clearance from the metabolism (Teekamp et al., 2015). Therefore, the suitability of many biodegradable and non-biodegradable carriers have been studied in the last decades. Poly(lactide-co-glycolide acid) (PLGA) is the most common biodegradable polymer, being used in different FDA approved products (Ghalanbor et al., 2012). However, the complete release of therapeutic proteins in their native form from PLGA-based formulations poses a challenge due to the complexity and variety of denaturation mechanisms caused by manufacturing processes and the nature of this polymeric matrix (i.e. hydrophobicity), its degradation mechanism and its degradation products (Giteau et al., 2008; Houchin and Topp, 2008; Teekamp et al., 2015).

Different manufacturing routes have been studied for the preparation of PLGA-based drug delivery systems, aiming to achieve stable protein-loaded formulations. Preparation of micro- and nanoparticles is one of the most investigated approaches, due to the easiness of administration (i.e. sc, im, iv), and because potentially higher protein stability within a polymeric matrix could be reached when considering the physiological metabolization by enzymes (Vaishya et al., 2014). However, this formulation approach usually involves the use of organic solvents and the creation of interfaces that compromise stability (Ghalanbor et al., 2013; Teekamp et al., 2015).

Hot melt extrusion (HME) is a manufacturing process that overcomes this issue, since it does not involve the use of solvents and the protein can be incorporated on its -more stable- dry state (Ghalanbor et al., 2010; Stanković et al., 2015a). It allows the encapsulation of high drug loadings within the matrix, and it is easier to scale up as it is a single-step

manufacturing process. However, the use of high temperatures and shear forces characteristic of this process might impact protein integrity as well (Breitenbach, 2002; Ghalanbor et al., 2010; Repka et al., 2012; Stanković et al., 2015a). In this part of the thesis the feasibility of HME to prepare OVA-PLGA-based implants is investigated; it is divided in three subchapters as follows:

- **Understanding the incomplete release of ovalbumin**
  OVA is a globular glycoprotein with 386 aminoacids and a molecular weight of 45 kDa. It is more hydrophobic than other proteins such as bovine serum albumin (BSA) (Ianeselli and Zhang, 2010), having a hydrophobic core buried into its structure that can be exposed depending on the environmental conditions (i.e. high temperatures, pH < 4.9, which is OVA's isoelectric point (pI)), leading to protein aggregation and detrimental interactions with other molecules in the system (Hu and Du, 2000; Huntington et al., 1995; Ianeselli and Zhang, 2010). Furthermore, previous studies with other two globular proteins, lysozyme (Ghalanbor et al., 2010) and BSA (Ghalanbor et al., 2012) have shown that incomplete release from PLGA-based implants, might be related to the presence of free cysteine groups in the protein (Ishimaru et al., 2014), which can mediate protein-polymer interactions, as it was observed in the case of BSA but not of lysozyme. Since OVA has four cysteine residues, it is expected that some interaction between the protein and the polymer could happen. Therefore, this chapter aimed to evaluate the stability of OVA within the PLGA matrix and to identify the reasons for its incomplete release from PLGA-based implants.
- **Improving release completeness of OVA from PLGA-based implants**
  Different co-excipients have been successfully used to improve release completeness from PLGA implants. The use of plasticizers (Ghalanbor et al., 2013), basic additives (Zhu and Schwendeman, 2000) and pre-degraded PLGA (Ghalanbor et al., 2013, 2012), have shown promising results in the case of BSA-loaded implants. Although OVA and BSA are both globular proteins, the highest hydrophobicity of OVA may lead to differences in both, its stability within the polymeric matrix, and the effectivity of these excipients to improve release completeness. Hence, the objective of this chapter was to evaluate and to improve the protein release by the addition of stabilizing excipients.
- **Use of shellac as novel co-excipient: upscaling and stability evaluation**
  The objective of the last chapter of this section was to upscale and to fully characterize the formulation that showed the best dissolution profile in the previous study (by incorporating shellac, a pH responsive polymer barrier, as co-excipient in the polymer matrix). The upscaling of a formulation usually involves the adjustment

of manufacturing parameters, which in the case of HME might involve additional stress factors such as higher shear forces and longer residence time within the extruder that could be detrimental for the protein (Breitenbach, 2002; Ghalanbor et al., 2010). Moreover, since this type of formulations are usually intended for parenteral use, its sterility must be guaranteed. Usually terminal sterilization techniques are advised because the implementation of aseptic processing might be too challenging (Burgess et al., 2002). Nonetheless, terminal sterilization could result in the degradation of the polymer, denaturation of the protein and overall loss of formulation's performance (Carrascosa et al., 2003; Dorati et al., 2005; Kumar and Palmieri, 2010; Rothen-Weinhold et al., 1997; Tracy, 1998). Hence, this chapter also aimed to study the suitability of gamma irradiation as terminal sterilization procedure to sterilize the prepared implants.

3.2 Understanding the incomplete release of ovalbumin

3.2.1 Ovalbumin stability after extrusion

The use of high temperatures during hot melt extrusion might be detrimental for the formulation's components, most critically for the integrity of proteins (Rajagopal and Wood, 2013; Stanković et al., 2013), specially for proteins such as OVA, with a denaturation temperature (T_c) of 84.5°C (Donovan and Mapes, 1976), which is lower than the process temperature. Therefore, evaluation of protein' structural integrity was performed with different methods to characterize its secondary and primary structure, as well as the formation of aggregates or changes in hydrophobicity of the protein. CD spectra of the protein in solution and the one extracted from the implant showed comparable spectra with two minima at 222 nm and 210 nm (Figure 7, left), which are representative of the mixture of α-helix and β-sheet structures commonly present in OVA (Hu and Du, 2000). The FTIR spectra of the standard and the extracted OVA from implants were also comparable (Figure 7, right), both showing the characteristic amide I (1630 and 1627 cm^{-1}) and amide II (1545 and 1543 cm^{-1}) peaks at around the same wavenumber (Kong and Yu, 2007); these results indicate that the secondary structure of OVA remained unaltered. Further evaluation of the extracted OVA by SEC-HPLC indicate that neither additional aggregation nor hydrolysis were caused by the extrusion process. These results suggest that the PLGA matrix served as a protection against the temperature stress inherent to the implant manufacturing process; as the biodegradable matrix melts during the process, it may act as a "protective cushion" for the protein by reducing its mobility (Lang et al., 2014).

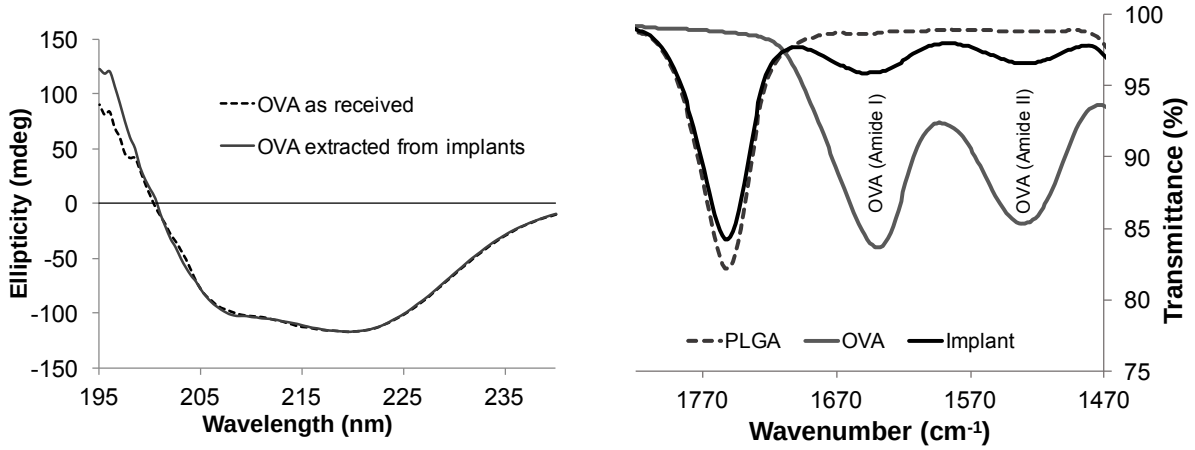

Figure 7 CD spectra [left] and FTIR spectra [right] of OVA standard and 10% OVA-loaded PLGA based implants

3.2.2 Release incompleteness of Ovalbumin

Release of OVA from PLGA implants showed a burst followed by a slow but sustained release up to 14 days, which can be attributed to diffusional processes out of the polymeric matrix (Figure 8). Cumulative release concentrations of ≤50% were achieved, except for loadings ≥25% where higher cumulative release was observed. This could be attributed to the achievement of the percolation threshold of the PLGA matrix that allowed a higher burst release (Figure 8). For all formulations, the release rate plateaued after 21 d, indicating release incompleteness.

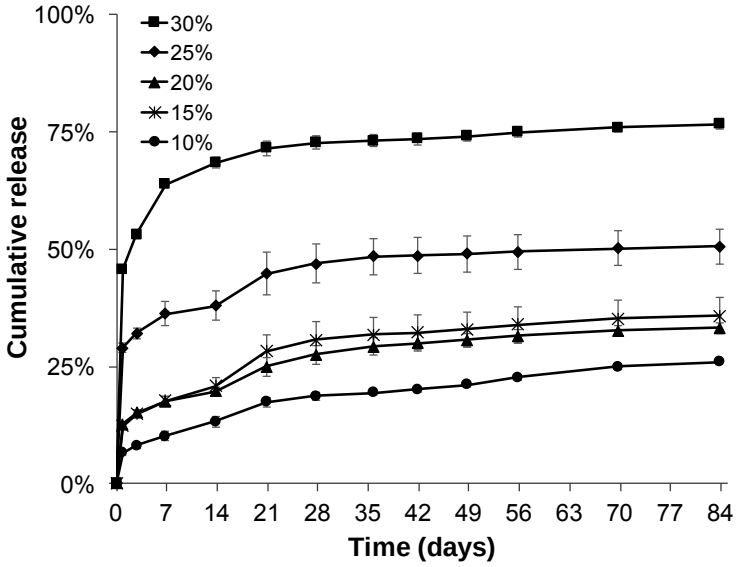

Figure 8 Release profile of PLGA-based implants loaded with different concentrations of OVA

Release incompleteness from PLGA-based formulations is a known problem for peptides and proteins, and often attributed to the acidic microclimate created by the autocatalytic nature of PLGA hydrolysis that can induce protein denaturation (Giteau et al., 2008; Houchin and Topp, 2008; Teekamp et al., 2015) and degradation (Ghalanbor et al., 2013, 2012). That the acidic degradation products of PLGA was related to the release incompleteness of OVA, was indicated by a drop of the medium pH to <3.8 after 21 d (Figure 9, left), which is below to the pI of OVA (Jones et al., 2005). Exposure to acidic conditions can induce structural transformations in OVA, increase its hydrophobicity and enhance its propensity to produce insoluble aggregates (Hu and Du, 2000; Weijers et al., 2002) that ultimately led to release incompleteness from the implants. As it can be seen in Figure 10, the fluorescence emission spectra of OVA at different pH values present a proportional increase in intensity as the pH decreases (Figure 10, left). This can be explained by the increase in surface's hydrophobicity of the protein, which can bind more to ANS giving a higher relative intensity (Capelle et al., 2007; Cardamone and Puri, 1992; Hawe et al., 2008). Moreover, CD spectra of OVA at different pH (Figure 10, right) showed a shift of one of the minima from 222 to 218

nm, indicating an increase in β-sheet content within the protein (Determan et al., 2006). This increases the mobility of the protein chains and facilitates the formation of aggregates as well as the likeliness for non-covalent and covalent interactions with PLGA or its degradation products (Determan et al., 2006; Koseki et al., 1988).

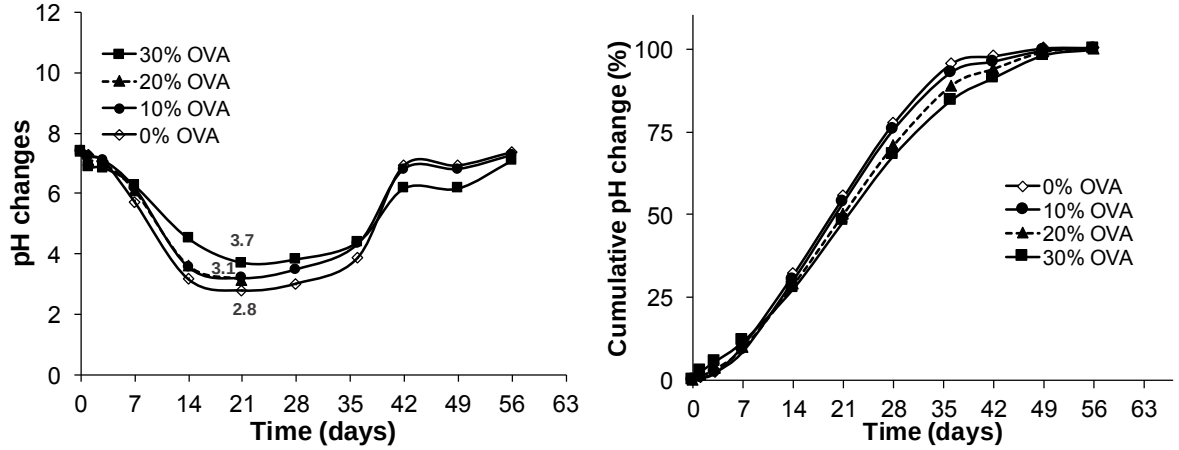

Figure 9 Absolute [left] and relative cumulative [right] pH changes during OVA release from implants with different protein loadings

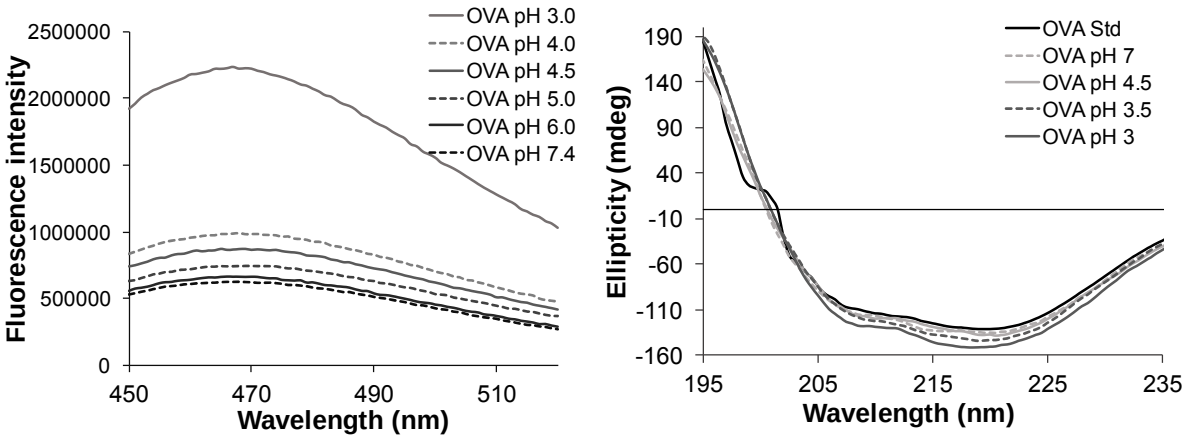

Figure 10 Fluorescence emission spectra [left] and CD spectra [right] of OVA at different pH

In line with these observations, an insoluble mass was formed during release of OVA from the implants, which remained for more than 70 days (vide infra), whereas no residual mass was visible after 56 days in control experiments (PLGA-only implants). Furthermore, slightly higher medium pH values were measured during release with increasing OVA loading (Figure 9), indicating that OVA exerted a buffering effect (Ghalanbor et al., 2013; Zhu et al., 2000). To corroborate this hypothesis, changes of PLGA's molecular weight were followed up during the dissolution time. Figure 11 shows how the molecular weight of PLGA decreased over the time, being faster when no protein was encapsulated within the PLGA-

based implants. Moreover, slower degradation was observed for implants loaded with 30% of the protein than for the ones loaded with 10%. Thus, OVA certainly decreased the autocatalytic rate of the polymer hydrolysis (Ghalanbor et al., 2013; Körber, 2010). The residual mass, which was insoluble in dissolution buffer and THF (polymer solvent), was further characterized in order to find out its nature and the mechanism of its formation. FTIR spectra revealed that this insoluble mass was mainly formed by protein residues and a small amount of PLGA (Figure 12). It was also observed that the wavenumber and shape of the amide II characteristic peak were different from the initial implant, suggesting a change in protein conformation. Furthermore, the fact that the residue was not soluble in THF indicated that the remaining PLGA and/or its oligomers are entrapped or bonded to the OVA aggregates.

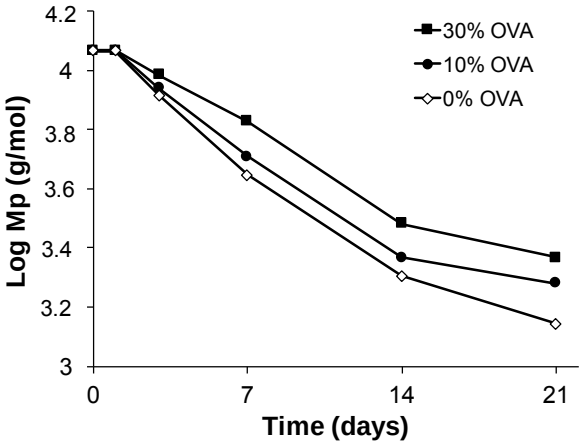

Figure 11 Semi-log plot of the peak molecular weight of PLGA implants during degradation in phosphate buffer, pH 7.4, as a function of OVA content (n=2)

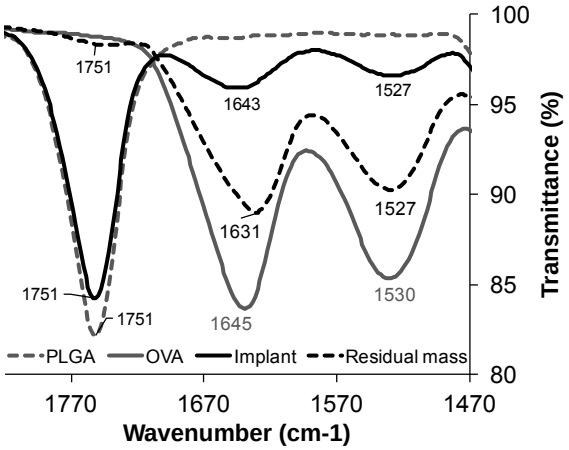

Figure 12 FTIR spectra of PLGA, OVA, OVA-loaded implants and residual insoluble mass

A series of tests were additionally performed to identify the nature of the residual mass; the findings are summarized in Table 5. NaOH was capable of dissolving the residual mass and

increasing the recovery of OVA to ≥90%, indicating the presence of ester bonds and/or strong ionic interactions between protein-protein and/or protein-polymer residues (Ghalanbor et al., 2012; Stanković et al., 2015b). Although OVA possesses four free thiol groups that can covalently interact with the polymer (Ishimaru et al., 2014), no thioester or disulfide bridge formation were found to be the cause for incomplete release, as neither DTT nor hydroxylamine were able to solubilize the residue (Fenton and Fahey, 1986; Ghalanbor et al., 2012). Probably this reactive groups interact between them inducing protein-protein interactions faster and strongly than protein-polymer ones. Furthermore, SDS and GnHCl solutions were able to dissolve the residue almost completely implying the presence of ionic interactions between the protein and polymer, non-covalent aggregation of the protein caused by its increase in hydrophobicity at low pH, and the adsorption of the protein on PLGA as the causes of the incomplete release obtained with the prepared formulations. The possible adsorption to PLGA, and even in a larger extent to its degradation products, is also supported by the loss of OVA recovery over the time shown in Figure 13. These findings are in line with the causes of release incompleteness reported before (Giteau et al., 2008); a schematic representation is shown in Figure 14.

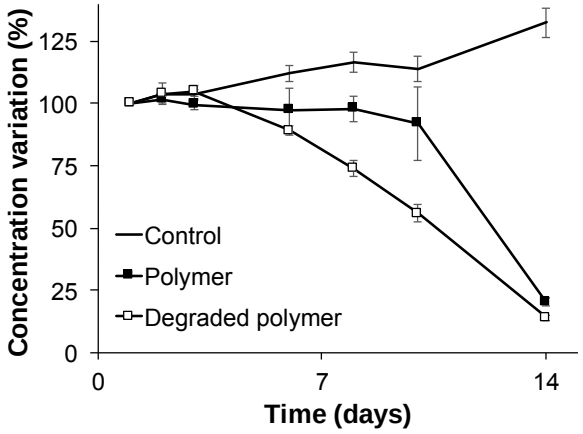

Figure 13 Recovery of OVA (1 mg/ml) in the presence of 18 mg of polymer or pre-degraded polymer (polymer exposed to 40°C/75% RH over 4 days) in release medium

However, it is important to notice that the removal of water by vacuum drying during sample preparation, could also have an influence on the quality of the residue. It is known that this process causes dehydration of proteins, which might promote its denaturation and exposure of hydrophobic regions inducing covalent or non-covalent aggregation (Abdul-Fattah et al., 2007; Crowe et al., 1990). Therefore, aggregation caused by the drying process cannot be completely excluded.

Table 5 Series of treatments used to find the mechanism of formation of insoluble residual mass

Reagent; concentration	**Observed effects**	**Conclusion**
THF; neat	No dissolution	No PLGA remaining or completely entrapped within protein aggregates Interaction/adsorption protein-protein or protein-PLGA
NaOH; 1 M	Solubilized	Ester bonds and/or strong ionic interactions are formed between Protein-protein and/or protein-PLGA
DTT; 0.01 M	Breaks down precipitate aggregates but it does not dissolve it	Protein-protein aggregation not likely caused by thioester and disulfide bridges formation
Hydroxylamine; 0.2 M	No dissolution	No thioester formation
SDS; 2%	Solubilized	Non-covalent bonds and protein adsorption to remaining PLGA are responsible
GnHCl; 6 M	Solubilized	
ACN: H_2O 50:50	Breaks down precipitate aggregates but it does not dissolve it	Protein-protein aggregation partially caused by hydrogen bonding formation

Incomplete release of OVA from PLGA-implants could be attributed to the formation of insoluble protein aggregates probably due to an interaction between protein and acidic polymer degradation products. An increase of OVA hydrophobicity and denaturation at pH values below the protein's pI, could have been triggered solely by the acidic microenvironment generated during PLGA hydrolysis. The following studies were therefore designed to manipulate the micro-environmental pH around the protein and/or to reduce the contact of protein to the acidic degradation products of PLGA.

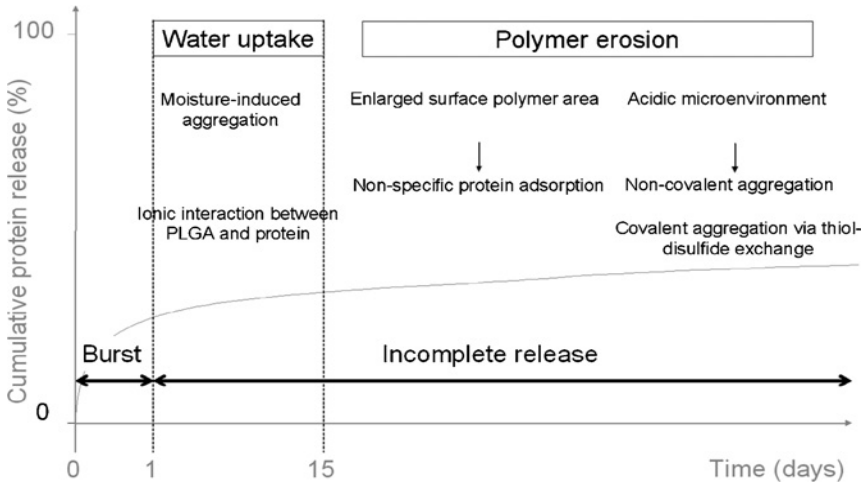

Figure 14 Schematic illustration of protein release profile and mechanism of incomplete release from PLGA microspheres (taken from (Giteau et al., 2008))

3.3 Improving release completeness of OVA from PLGA based implants

After having identified the causes for incomplete release, different strategies were selected to assess their effectivity on stabilizing the protein during release. Some of these are represented in the framed areas of Figure 15 (Giteau et al., 2008). Since chemical modification of the protein was not possible (i.e. PEGylation, carboxymetilation), additional co-excipients such as pore formers and pH modifiers were evaluated.

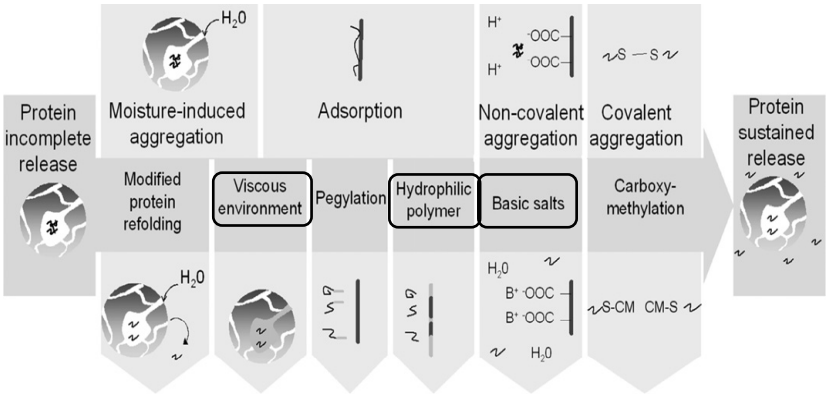

Figure 15 Schematic illustration of some strategies stabilizing the protein during the release period (Taken from (Giteau et al., 2008))

3.3.1 Creation of a viscous environment

Moisture-induced aggregation and adsorption could be prevented, or at least minimized, by the use of a more viscous environment that avoids the direct contact between the protein and the polymer (Giteau et al., 2008). PVP (Wang et al., 1999) and Poloxamer 407 (Sturesson and Carlfors, 2000) have been reported as appropriate excipients to increase inner viscosity in PLGA microspheres, reducing the contact between protein and polymer and, therefore, maintaining protein' stability and improving the release completeness. Thus, these two excipients were incorporated in the PLGA-based implants and evaluated for their suitability. To increase the contact between the protein and PVP or Poloxamer, they were dissolved together in MilliQ water (1:4 OVA: co-excipient ratio) and freeze dried. OVA alone was also freeze dried to evaluate the effect of the process on protein integrity and dissolution. The powders obtained were free-flowing with the presence of small agglomerates. PLGA-based implants were prepared as described before.

The CD spectra of OVA and freeze-dried OVA (OVA FD) were comparable indicating that no appreciable changes in the secondary structure were caused by the freeze-drying process (Figure 16, left). However, the fluorescence emission spectra indicated an increase in protein's hydrophobicity caused by the process, as evidence by the higher intensity of the OVA FD when compared to OVA as received (Figure 16, right) (Gabellieri and Strambini,

2006). Freeze drying could create stress to the protein due to the rapid freezing and dehydration inherent to the method (Abdul-Fattah et al., 2007). Denaturation of the protein might occur together with its partial unfolding (Eckhardt et al., 1991; Strambini and Gabellieri, 1996), which, in the case of OVA, could represent the exposure of the hydrophobic core and thus, increase on its surface hydrophobicity. It has also been reported before that the denaturation caused by this process might be partial affecting the tertiary structure but not the secondary one (Abdul-Fattah et al., 2007; Franks et al., 1988; Privalov, 1990), which is in line with the results obtained.

The incorporation of both co-excipients, PVP and Poloxamer, showed an effect on the secondary structure of the protein (Figure 16, left). In the case of PVP the two minima were more marked indicating a decreased of order structure and the conversion from α-helix to β-sheet (Hagolle et al., 1997; Hu and Du, 2000; Moon and Song, 2001), probably caused by strong interaction between PVP and OVA. On the contrary, in the case of Poloxamer changes in the CD spectra (Figure 16, left) indicated the formation of a more organized structure with a higher amount of α-helix within the protein. Poloxamer could have inhibit aggregation and/or unfolding of the protein by decreasing its mobility during the freeze drying process (Wang, 1999)

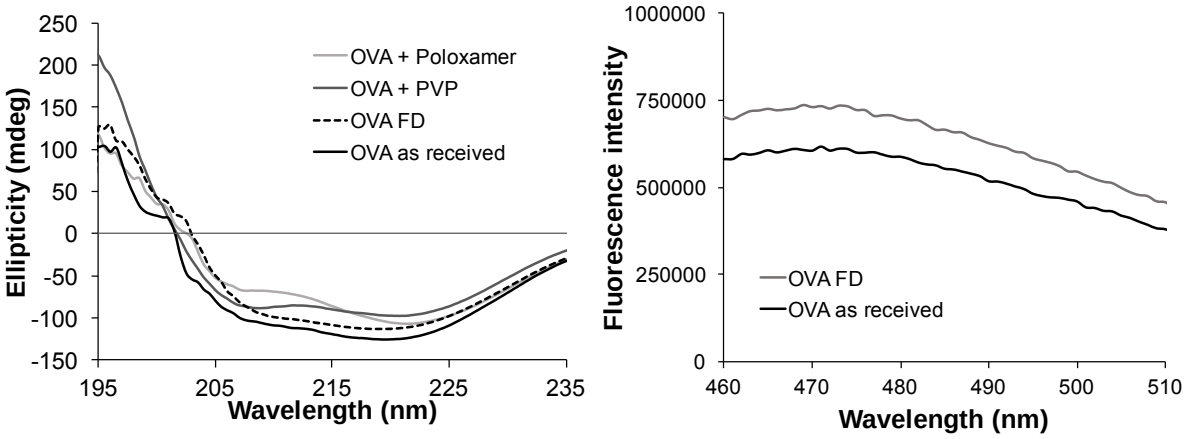

Figure 16 CD spectra of OVA after freeze drying alone and with Poloxamer or PVP as co-excipients to create a viscous environment [left] and fluorescence emission spectra of OVA before and after freeze drying [right]

No substantial differences in the dissolution profile between OVA as received and OVA FD were observed (Figure 17), except for a slightly decrease on the release rate during 7 and 21 days. This could be related to the increase of protein's hydrophobicity and decrease on its solubility that could upturn the likelihood of protein-protein ad protein-polymer interactions. With the inclusion of both co-excipients, higher burst release was observed

releasing more than 45% and 75% when using PVP and Poloxamer, respectively. The greater effect of Poloxamer than PVP might be related to the fact that Poloxamer is capable of avoid adsorption to PLGA due to its surface active properties (Paillard-Giteau et al., 2010), which allowed higher amount of protein to be released. Although some protein was still released during the following weeks, release completeness was not achieved most probably caused by the acidic microclimate created and changes in protein conformation, which induced OVA aggregation.

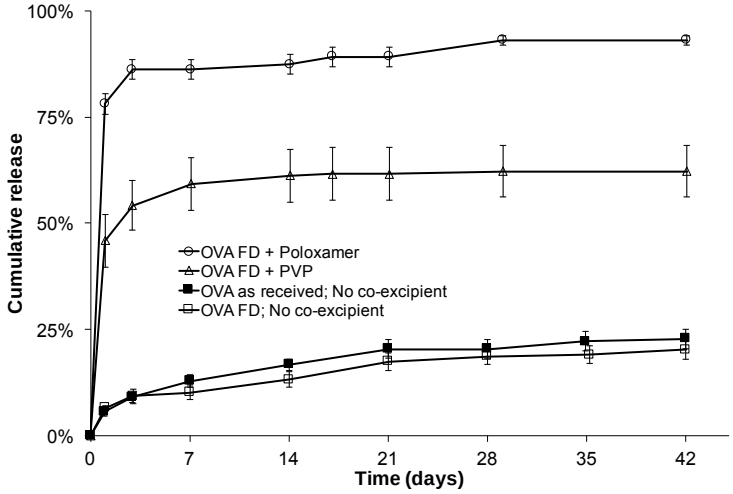

Figure 17 Release profile of OVA-loaded PLGA-based implants after protein's freeze drying alone and with Poloxamer or PVP as co-excipients

While the creation of a more viscous inner environment within the implant may help to achieve higher cumulative protein release, the dissolution profile achieved might not be the most suitable for a sustained release parenteral formulation, where lower burst releases and longer releasing periods are desired. Besides, the freeze-drying process required generates additional destabilization of the protein and creates a more challenging manufacturing process, which is undesirable.

3.3.2 Pore formers

3.3.2.1 Polyethylene glycols (PEG) with different molecular weights

Low- and medium-molecular weight PEGs are hydrophilic excipients that can act as pore formers and plasticizers of PLGA. They generally increase the burst release and the diffusion of the protein thanks to the pores formed and an efflux of the acidic species formed during PLGA degradation (Ghalanbor et al., 2010; Jiang and Schwendeman, 2001; Kang and Singh, 2001). Therefore, PEGs with average molecular weight of 400, 1500 and 4000 Da were tested as co-excipients within the PLGA-based implants at a concentration of 10 wt.%.

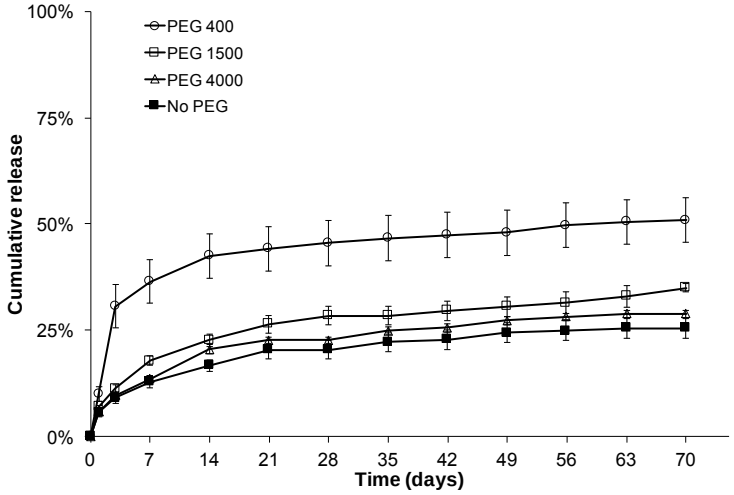

Figure 18 Release profile of OVA-loaded PLGA-based implants using PEGs with different molecular weights as co-excipients

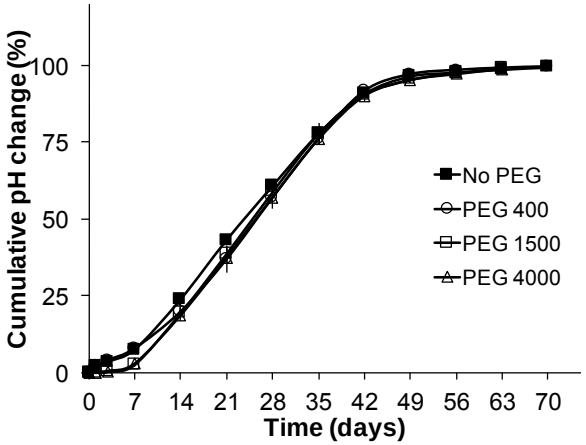

Figure 19 Relative cumulative pH changes during OVA release from implants using PEGs with different molecular weights as co-excipients

At lower PEG's molecular weight higher cumulative release was obtained (Figure 18), which could be explained by the higher aqueous solubility of PEG with lower molecular weight. As they dissolved, they formed pores that facilitate the diffusion of the protein, which occurs during the first weeks of release. However, release completeness was still not achieved, most probably caused by pore closure that can occur within the swelled PLGA matrix (Kang and Schwendeman, 2007). As the pores close, not only diffusion of the protein is impaired, but also the efflux of the acidic species formed. As shown in Figure 19, differences in the cumulative pH changes were observed during the first weeks of release (up to 21 days), where the pores left by the PEG allowed the efflux of the acidic species causing a pH drop to less acidic values than when PEG was not incorporated. However, after 21 days, when pore closure most probably occurred, the pH of the release medium of the different formulations

became comparable, with values below OVA's pI. In the case of acid-labile proteins like OVA, the incorporation of PEG within the implant formulation does not seem suitable since the acidic microclimate cannot be influenced, and therefore, protein aggregation cannot be prevented.

3.3.2.2 Sugars and ionic salts

Pore formation can also be achieved by the inclusion of osmotic agents within the PLGA matrix such as sugars and ionic salts (Ahmed and Bodmeier, 2009; Lee and Sah, 2016; Reinhold et al., 2012; Sahoo et al., 2005). To assess this approach 10% of sodium chloride (NaCl), calcium chloride ($CaCl_2$), sucrose or mannitol where incorporated within the implant formulation. Surprisingly, none of the above-mentioned excipients improved the release of OVA (Figure 20). In the case of the salts two factors could have being the cause of this: increase of ionic strength within the matrix, which is known to cause OVA aggregation (Veerman et al., 2003; Weijers et al., 2003), and the possible ionic interaction between the cations of the salts and the protein, which has a negative charge at neutral pH (Ianeselli and Zhang, 2010). The coordination between the protein donor atoms (oxygen, nitrogen, sulfur) with the hard calcium ions is stronger and more probable that in the case of sodium, explaining why the implants containing $CaCl_2$ only reached 10% of protein cumulative release. Furthermore, a faster pH drop was observed with $CaCl_2$ than with NaCl (Figure 21) indicating that aggregation and interaction of the protein with the salt occurred from the beginning of dissolution. As the acidic microclimate was not improved, incomplete release was also observed when using these two salts.

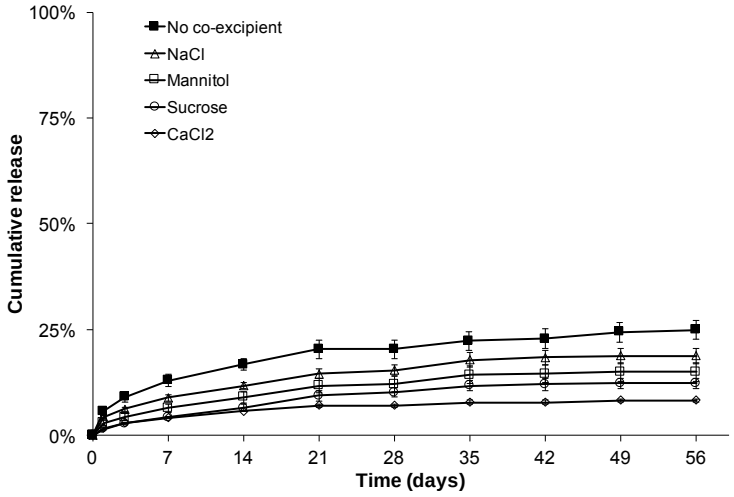

Figure 20 Release profile of OVA-loaded PLGA-based implants using sugars and ionic salts as co-excipients

Although sugars are reported to avoid direct contact of the protein with PLGA by their preferential hydration (Kang and Schwendeman, 2002; van de Weert et al., 2000), no effect was observed in the release completeness of OVA (Figure 20). Since no control of the acidic microclimate was achieved (Figure 21), OVA aggregation was not prevented. Moreover, it has been reported that hydrolysis of non-reducing sugars (i.e. sucrose and mannitol) might be accelerated under acidic conditions (i.e. PLGA degradation) producing species that might hamper the stability of the protein (Sánchez et al., 1999; van de Weert et al., 2000).

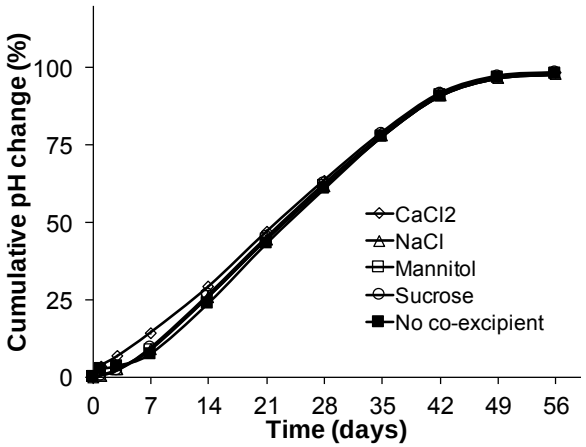

Figure 21 Relative cumulative pH changes during OVA release from implants using sugars and ionic salts as co-excipients

Though the co-excipients tested are capable of create pores, their effect is not sufficient in the case of OVA-loaded implants since there is no control of the acidic microclimate or the ionic strength within the matrix. Furthermore, pore-closure of the swelled matrix cannot be disregarded. Thus, stabilizing co-excipients should be selected based on their capability to avoid direct contact of OVA with the degrading species of PLGA and to maintain a microclimate that is not below OVA's pI.

3.3.3 pH-stabilizers

3.3.3.1 Weak basic salts as proton scavengers

The acidic microenvironment is the primary trigger for the incomplete release of OVA from PLGA. Therefore, proton scavenging additives were used as excipients at a loading of 3.5% to neutralize the produced acidic species as suggested previously (Zhu and Schwendeman, 2000). In the case of OVA-implants, the release was only increased up to 46% and 36% with the use of the weak basic salts $MgCO_3$ and $Mg(OH)_2$, respectively (Figure 22). This could be attributed to the concomitant increase in ionic strength within the matrix that also promotes OVA aggregation (Ianeselli and Zhang, 2010). Release of OVA was constant for the 5-7

weeks, plateauing afterwards, which correlates well with the pH changes measured during the release (Figure 22 and Figure 23, left). In both cases the pH minimum was achieved at 28 days, one week later than in the other formulations, reaching values of 3.4 and 4.0 for $Mg(OH)_2$ and $MgCO_3$, respectively. Cumulative pH changes correlate well with the changes of PLGA molecular weight by showing the 1-week delay on the erosion onset (Figure 23, right and Figure 24), which was caused by the neutralization effect of the weak bases during the first weeks of dissolution. This shift in medium pH curve was predominantly caused by the neutralization effect of the weak bases and not by an off-set of the acidic (auto-)catalysis.

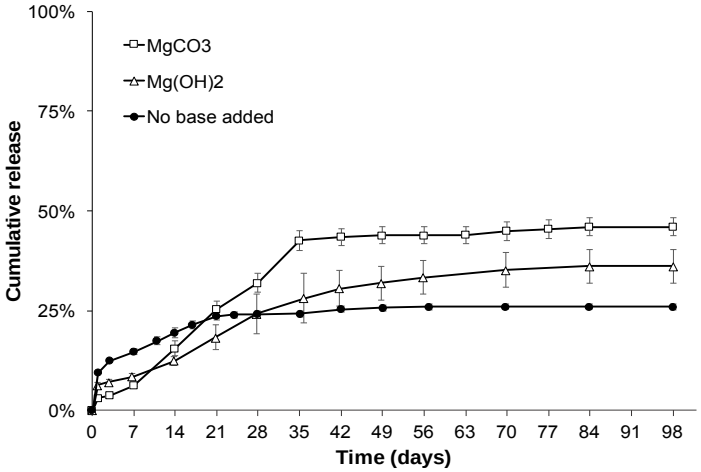

Figure 22 Release profile of 10% OVA-loaded PLGA-based implants with/without addition of weak bases

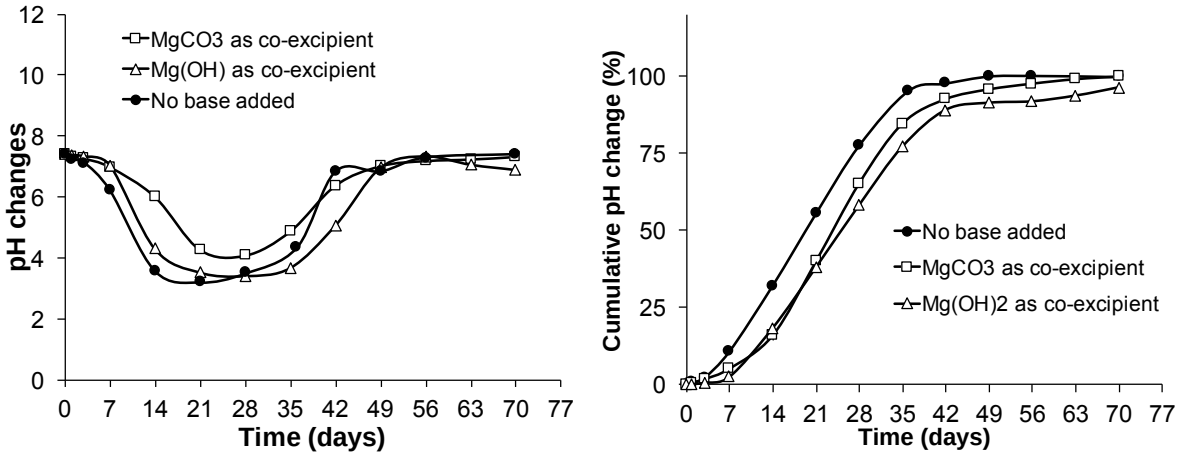

Figure 23 Absolute [left] and relative cumulative [right] pH changes during OVA release from PLGA-based implants using $Mg(OH)_2$ and $MgCO_3$ as excipients

The differences observed in the pH changes between the two bases used can be attributed to differences in the solubility of these weak bases; $MgCO_3$ is more soluble in water than

$Mg(OH)_2$ (~100 µg/ml vs. ~6.0 µg/mL), leaching out of the matrix sooner and leaving open pores from where the acidic species formed during PLGA's degradation could diffuse out. This yields to less accumulation of this products and thus, a less acidic environment. This observation is corroborated by the release profile of the prepared implants (Figure 22), where the formulation containing $MgCO_3$ releases more of the protein than the formulation containing $Mg(OH)_2$, due to a combination of the pore formation effect and the less acidic pH observed. However, the synergy of these effects was not enough to achieve release completeness, because the pH was not kept above the protein's pI. Although protein stability could be improved to some extent, higher amounts of weak bases would be required to prolong the neutralization effect to the entire degradation / erosion and hence release phase of PLGA matrices. If we consider that solubility of the oligomers is attained when they reach a critical molecular weight of 1000 g/mol (Körber, 2010), then the amount of base should be enough to neutralize ~11.6 equivalents of polymer. This means that for a 20 mg implant loaded with 10% of OVA, app. 0.52 mg of $Mg(OH)_2$ or 1.52 mg of $MgCO_3$ would be required. The amounts used are in the former hardly above the stoichiometrically required, while in the later is sub-stoichiometric. Moreover, the addition of higher amounts of weak bases induces porosity and thus dramatically shortens the feasible release time frames due to an increased diffusional release as shown previously (Liu and Schwendeman, 2012; Reinhold et al., 2012; Zhu and Schwendeman, 2000). This methodology might work only in cases where a slower-degrading PLGA grade is used, where the pH drops slowly and its minimum is reached after complete protein release. Nonetheless, special care should be taken to avoid increase in hydrophobicity and water impermeability that could also induce protein destabilization (Jiang and Schwendeman, 2001; Reinhold et al., 2012; Zhu and Schwendeman, 2000).

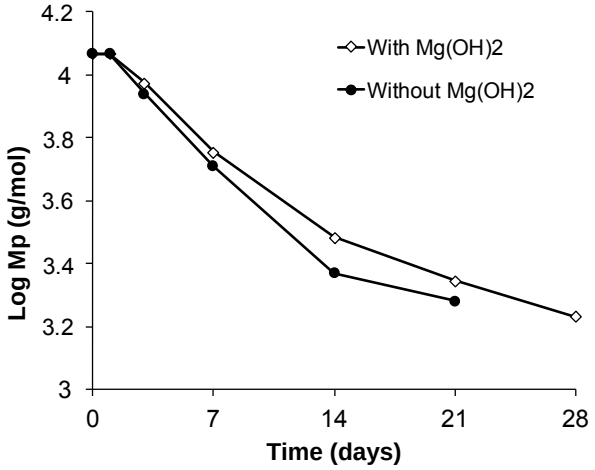

Figure 24 Semi-log plot of the peak molecular weight of PLGA implants with and without $Mg(OH)_2$ during degradation in phosphate buffer, pH 7.4 (n=2)

3.3.3.2 pH responsive polymeric barriers

In an attempt to avoid the detrimental effect on the protein by the acidic microclimate, shellac was included in the implant formulation. Shellac is insoluble at low pH values, soluble at high pH and is used for enteric coatings of peroral dosage forms (Pearnchob et al., 2003). Moreover, shellac is used in coatings of drug-eluting stents, and hence is proven suitable and safe regarding its parenteral administration (Byrne et al., 2014; Karimi et al., 2013; Peters et al., 2012).

Shellac was incorporated at three different ratios: 1, 5 and 10 shellac: OVA, and stability and dissolution were also evaluated (Figure 25 and Figure 26). OVA extracted from these implants did not show any additional aggregation or hydrolysis, as indicated by the SEC-HPLC chromatograms. Only one glass transition temperature (Tg) was obtained during DSC evaluation of the implants; a slight decrease on it was observed when shellac was incorporated, but this did not affect their shape or hardness (Figure 27). Furthermore, the fluorescence emission spectra of OVA before and after extrusion, and with and without shellac in the matrix, were comparable (Figure 25), indicating that no changes in hydrophobicity have occurred. The addition of shellac resulted in a higher burst release and a slow sustained release during 7 weeks (Figure 26, left). Interestingly, when shellac was used at a ratio of 5:1 or 10:1 compared to OVA, higher amounts of the protein were released during the three following weeks. This was in accordance with the pH changes measured (Figure 26, right): the pH drop occurred also at 21 days, but it recovered faster than when shellac was not added; and after 49 days the pH reached values ≥7.0 allowing the diffusion of the remaining amount of protein out of the shellac portion. The higher burst release might have contributed to lower accumulation of acidic species thanks to the pores formed as the protein was released, which in turn allowed a faster pH recovery having a less detrimental effect on the protein and decreasing the interactions between OVA and PLGA. OVA was still released even after three months showing a total protein recovery of ≥75%. Consequently, the mechanism by which shellac protects the protein and allows higher OVA release could be described as follows: when the implants are incubated in the PB, pH 7.4, shellac can swell and partially dissolve (Limmatvapirat et al., 2007; Pearnchob et al., 2003) surrounding the neighboring protein molecules; when the pH within the implant drops as a consequence of the PLGA degradation, shellac, due to its low solubility at acidic pH, entraps the protein molecules, hampering its interaction with the acidic microclimate. Then, when the pH is again ~7.0, shellac starts to dissolve allowing the diffusion of the protein molecules, resulting in a higher recovery. With increasing amounts of shellac inside the implant a higher total OVA release may be achieved since more protein molecules can be surrounded and protected by the shellac matrix. Nonetheless, an exceeding amount will lead to higher burst

releases, which, depending on the application, might be undesirable. An OVA: shellac ratio between 1:5 and 1:10 seem to be a good compromise between these features.

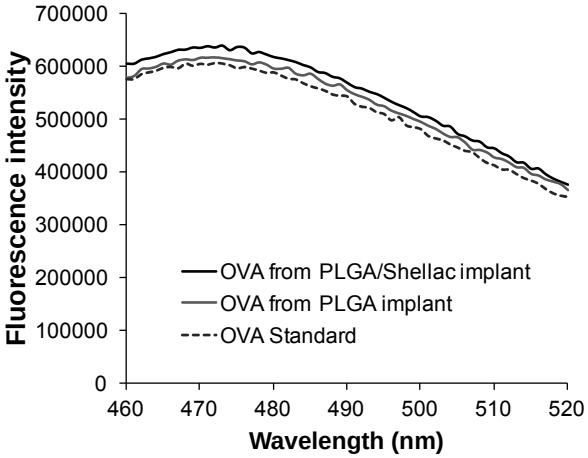

Figure 25 Fluorescence emission spectra of extracted OVA from implants with and without shellac

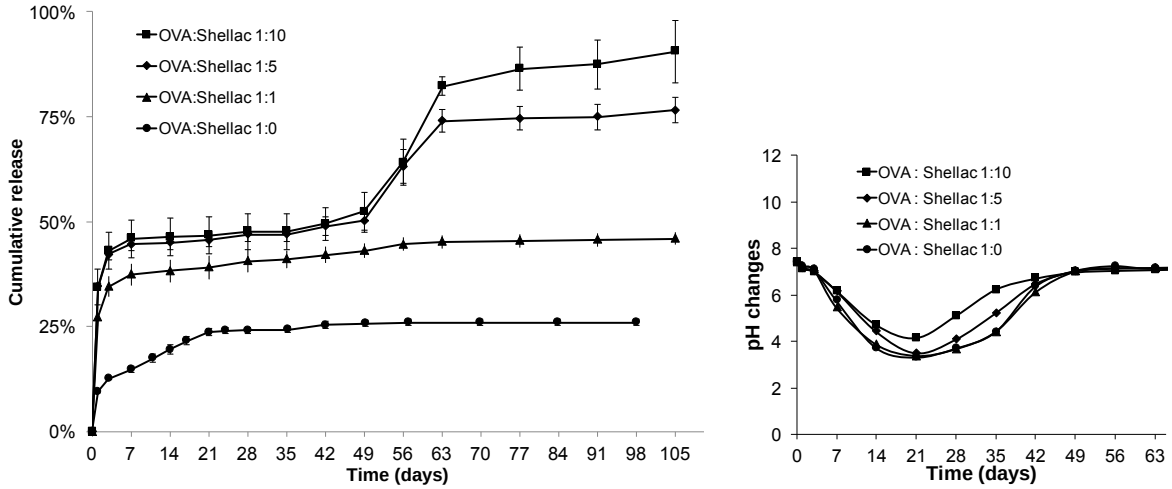

Figure 26 Release profile of OVA-loaded PLGA-based implants using shellac at different ratios [left] and pH changes during OVA release from PLGA-based implants using shellac at different ratios [right]

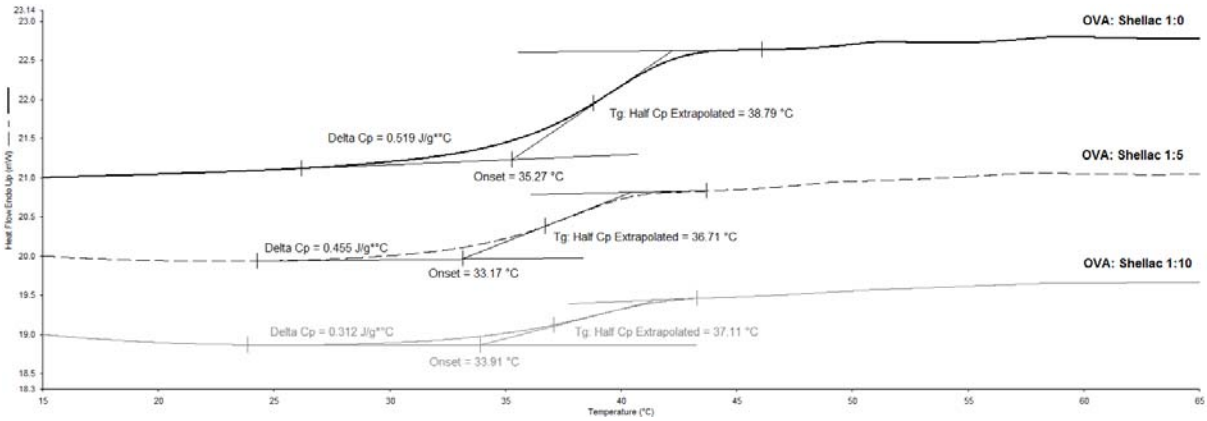

Figure 27 DSC thermograms of OVA-loaded PLGA-based implants using shellac at different ratios

3.4 Use of shellac as novel co-excipient in OVA-loaded PLGA-based implants

Based on the previous findings and the proven suitability of shellac as co-excipient to improve release completeness of OVA from PLGA-based implants, up-scaling, evaluation of terminal sterilization and formulation stability was performed.

3.4.1 Upscaling from the mini-ram extruder to a twin-screw extruder

The formulation with a 1:5 OVA: shellac ratio was selected for up-scaling; a scale-up size factor of 15 was used. Although both extrusion methods required heat to melt and to extrude the formulation, twin-screw extrusion might have a more detrimental effect on protein' stability caused by the longer residence time required at high temperature (22 min at 85°C vs. 8 min at 100°C) and the presence of shear forces caused by the screws. Interestingly, neither signs of additional aggregation or hydrolysis were detected in the SEC-HPLC chromatograms, nor substantial differences in the fluorescence emission spectra (Figure 28) were observed. This suggested that no changes in the primary structure of the protein or in its hydrophobicity occurred as a consequence of the upscaling. As stated earlier, this can be attributed to a protective effect that the polymeric matrix could exert by melting before the protein does (Lang et al., 2014).

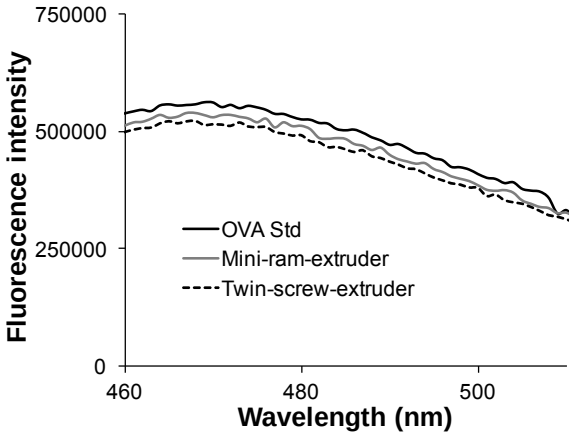

Figure 28 Fluorescence emission spectra of extracted OVA from implants prepared by the two extrusion methods evaluated

The implants prepared with the twin-screw extruder showed a slightly higher Tg and onset temperature than the ones prepared with the mini-ram extruder (Figure 29). However, the change of heat capacity (ΔCp) of the twin-screwed implants was less than in the other case (0.390 vs. 0.455 J/g°C), indicating that less energy was required to melt or deform this formulation. This could be related to the fact that stronger interactions between the polymers could have been achieved, thanks to the shear forces (Lang et al., 2014; Repka et al., 2012; Stanković et al., 2015a), obtaining a more homogeneous matrix and full miscibility of PLGA

with shellac. Both formulations were comparable on their ease of handling and absence of deformation during e.g. implant cutting.

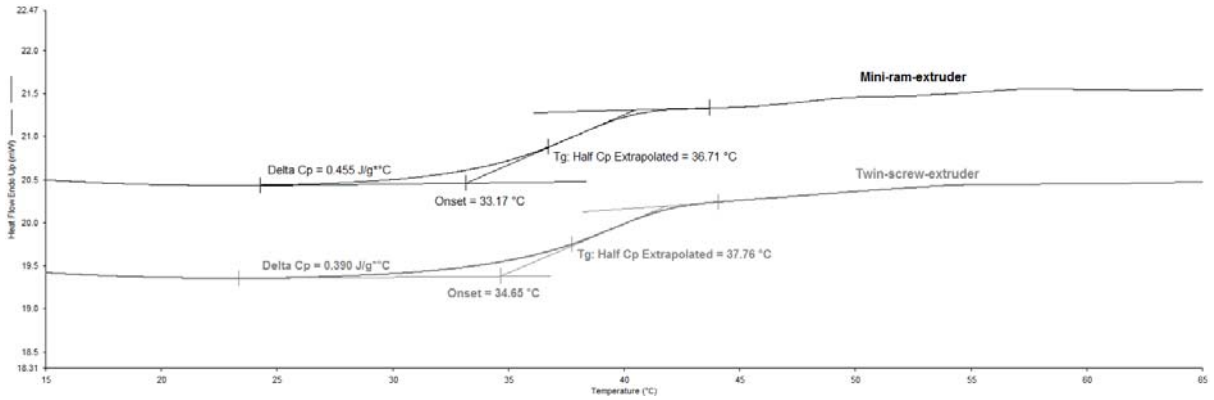

Figure 29 DSC thermograms of OVA-loaded PLGA: shellac-based implants prepared by the two extrusion methods evaluated

The dissolution of OVA also showed a multiphasic profile for the up-scaled formulation. However, the burst release was lower, accounting only for the 10% of the release (Figure 30, left). This can be attributed to densification of the matrix (lower porosity) that happened during the twin-screw hot melt extrusion process. The slow diffusion phase that followed up to 49 days was comparable in both cases. Moreover, a rapid diffusion of the protein after this time point was also observed, thanks to the recovery of the pH (Figure 30, right), which allowed the solubilization of shellac. In the case of the twin-screwed formulation, a slower dissolution of the protein during the erosion phase was observed. Nonetheless, both formulations presented similar recovery upon release (ca. 77%) (Figure 30, left). This could be related to the lower burst release of the twin-screwed implant formulation, and thus less pore formation that slowed down the protein's diffusivity.

In both cases an insoluble mass remained after the release. However, evaluation with FTIR of this mass (Figure 31) indicated that it was mainly conformed by undissolved shellac and the small portion of the protein that was not released. In agreement with these findings, the residual mass was completely soluble in NaOH, 1 M, and almost fully solubilized in ethanol, which indicated that it was primarily composed of shellac residues.

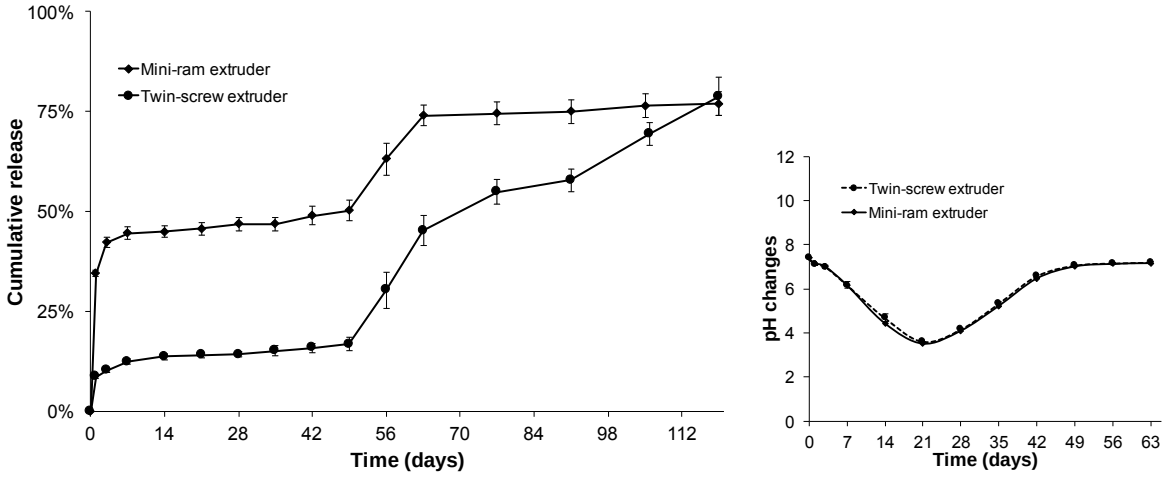

Figure 30 Release profile of OVA-loaded PLGA: shellac-based implants prepared by the two extrusion methods evaluated [left] and absolute pH changes during OVA release from PLGA: shellac-based implants prepared by the two extrusion methods evaluated [right]

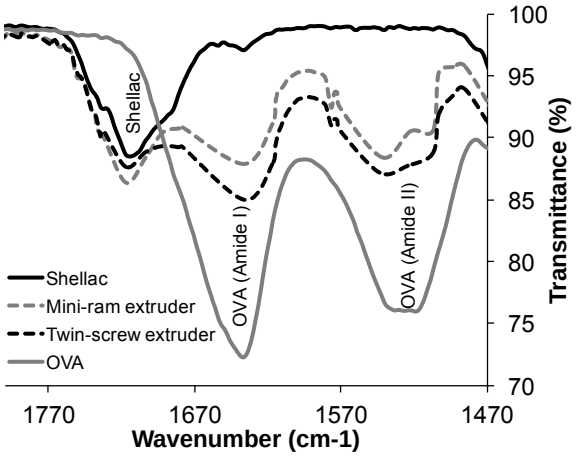

Figure 31 FTIR spectra of shellac, OVA and residual mass of implants prepared with the mini-ram and the twin-screw extruder (dashed lines)

The use of shellac as co-excipient has shown its feasibility at a larger scale as well being a promising approach to optimize the dissolution profile of acid-labile proteins from PLGA-based implants. Since the burst release is decreased when up-scaling, it could be advisable to increase the amount of shellac inside the matrix to allow a higher recovery. However, additional information regarding their degradation time should be retrieved to assess its suitability as a depo formulation with multiple doses (i.e. treatment of chronical diseases or a vaccination scheme with various doses).

3.4.2 Storage stability of the up-scaled formulation

As a next step, the storage stability of the formulation was tested at three different temperatures (4-8, 25 and 40°C) and at different time points. Humidity was not considered since the implants were packaged in sealed and water-impermeable blisters prior storage. Appearance, changes in aggregation/hydrolysis, in tertiary structure (hydrophobicity), thermal properties and dissolution kinetics were stablished as the stability indicators.

Implants retained their shape after storage at either 4-8°C or 25°C. However, after 1 week of storage at 40°C, the implants lost their cylindrical shape and became rounded and softer. Upon further storage at that temperature the implants lost completely their shape, they were molten and it was not possible to handle them. Nonetheless, in all the cases no phase separation or segregation of the implant components was observed. This is in line with the changes in the thermal properties of the implants after storage (Table 6). Only one Tg was detected for all the implants, indicating that the polymeric matrix kept its homogeneity. Furthermore, a decrease in the Tg and onset temperature was observed for all the samples after storage at either 25°C or 40°C; implants stored refrigerated presented comparable thermal properties to the initial state. When stored at 25°C these changes were not as drastic as in the case of 40°C, where at the later time points no Tg was detected at $\geq$ 0°C. This was caused by the storage at a temperature above the implants' Tg, which caused mobility of the polymer chains and re-arrangements into a less rigid structure.

The surface hydrophobicity of OVA was of 12.66 μM^{-1} (Figure 32), which agreed well with reported values in literature (Chaudhuri et al., 1993; Rather and Gupta, 2013). Taking this into account, if protein concentration is kept constant, changes in hydrophobicity of the protein (i.e. tertiary structure) are reflected as higher absorbance in the fluorescence emission spectra. When the implants were stored at $\leq$ 25°C, no significant changes in OVA's hydrophobicity were observed (Figure 33, left). However, when the implants were stored at 40°C, an increase of protein's hydrophobicity was observed after 1 week (Figure 33, right). This was caused by the conformational changes induced by the high temperature that could have exposed the hydrophobic core of OVA (Hu and Du, 2000; Huntington and Stein, 2001; Ianeselli and Zhang, 2010; Weijers et al., 2003). Interestingly, after 2 and 4 weeks of storage at 40°C the fluorescence intensity did not increase but the spectra presented a shift on its maximum and a different shape (Figure 33, right). This could be ascribed to changes in the tertiary and/or secondary structure of the protein and/or increase of interactions between the matrix and the protein, which are catalyzed by the higher temperature. This changes affected the electrostatic interactions between the cationic sites of the protein and the dye, which led to less fluorescence intensity and changes in intensity (Capelle et al., 2009; Hawe

et al., 2008). None of the storage conditions had an impact on formation of additional aggregates or protein hydrolysis as indicated by the SEC-HPLC chromatograms.

Table 6 Thermal characterization of the implants stored at different temperatures

Storage temperature / Time point	**Tg (°C)**	**Onset (°C)**	**ΔCp (J/g°C)**
- **/ Before storage (t_0)**	37.76	34.65	0.390
4-8°C / 12 weeks	37.12	33.13	0.387
25°C / 2 weeks	36.67	32.97	0.513
25°C / 4 weeks	35.49	31.21	0.507
25°C / 8 weeks	35.04	30.44	0.507
25°C / 12 weeks	34.75	30.31	0.612
40°C / 1 week	26.98	23.85	0.312
40°C / 2 weeks	13.31	5.0	0.468
40°C / 4 weeks	*ND*	*ND*	*ND*
40°C / 8 weeks	*ND*	*ND*	*ND*

ND: not detected

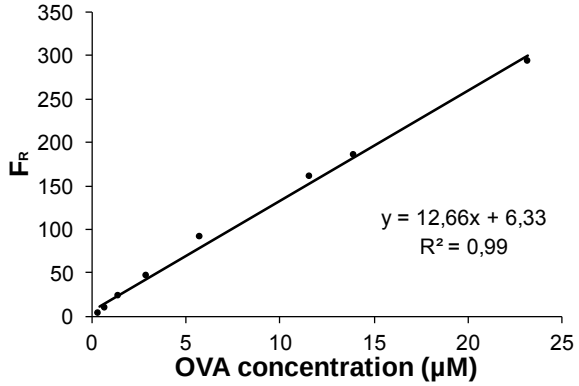

Figure 32 Surface hydrophobicity measurements by ANS titration

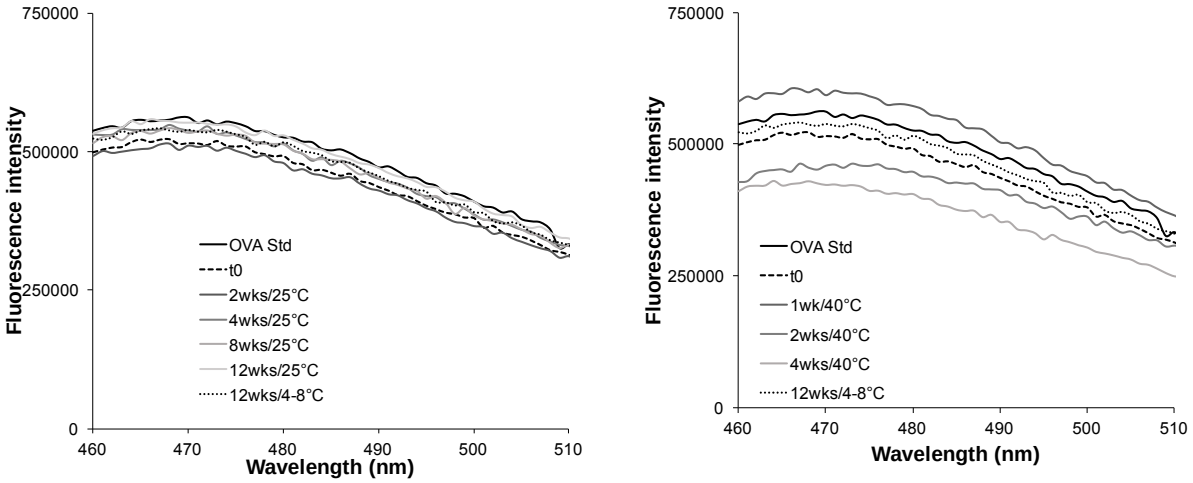

Figure 33 Fluorescence emission spectra of extracted OVA from implants stored at ≤25°C [left] and at 40°C [right]

The dissolution kinetics was comparable for all the implants prior and after storage (Figure 34) showing the typical multiphasic behavior described before. Samples stored longer than 2 weeks at 40°C were not evaluated, since they lost their shape and could not be handled properly. A slightly faster dissolution after 49 d was observed for the implants stored for 1 week at 40°C. Moreover, with a longer storing time at 25°C a faster dissolution was observed during the erosion phase This could be attributed to the decrease in the Tg (Table 6), which could have allowed a better contact with the release medium and thus higher protein's diffusivity. Implants stored at 4-8°C presented comparable profile to the freshly prepared implants.

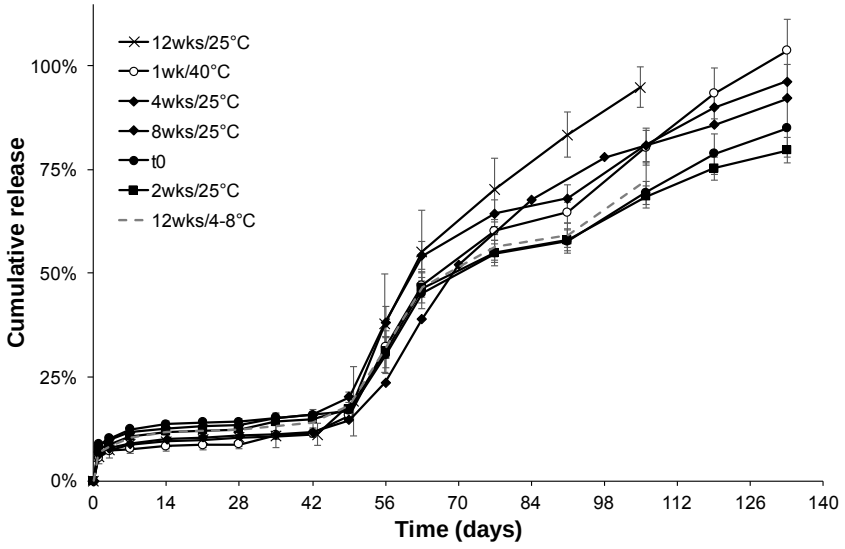

Figure 34 Release profile of OVA-loaded PLGA: shellac-based implants after storage under different conditions and duration of time

Although no considerable changes occurred in the appearance and protein's conformation of the implants after storing them at 25°C, the small variations in the thermal properties and release kinetics under these conditions cannot be neglected; they could have a negative impact on the formulation's characteristics after long-term storage. Therefore, the implants should be stored at refrigerated conditions to guarantee their proper performance.

3.4.3 Effect of terminal sterilization on PLGA: shellac-based implants

Sterility of parenteral delivery systems must be ensured as part of the product development. Aseptic manufacturing or terminal sterilization should be considered early in the formulation phase to bypass the stability issues of the delivery system (Burgess et al., 2004; Volland and Wolff, 1994). Aseptic manufacturing requires that the production area and needed tools are sterile and under controlled environmental conditions (i.e. process designed into an isolator) (Tracy, 1998), which can be expensive, labor intensive and more challenging depending on the equipment used and the complexity of the steps required to prepare the formulation. Hence, terminal sterilization is preferred from a microbiological and cost-effectiveness point of view (Volland and Wolff, 1994). However, the methods used for terminal sterilization can cause detrimental effects on the formulation such as hydrolysis, degradation and/or deformation of the delivery system and its components altering its performance (Burgess et al., 2004; Dorati et al., 2005; Volland and Wolff, 1994). Therefore, the suitability of gamma-irradiation as terminal sterilization technique was assessed for the PLGA: Shellac implants prepared. Implants were packaged in sealed blisters and exposed to an irradiation dose of ≥25 kGy, which is enough to guarantee sterility (Montanari et al., 2001). Hence, the evaluation of the implants was done at a physicochemical level and not a microbiological one. Two conditions during irradiation were tested: Low temperature during sterilization (LTS) and High temperature during sterilization (HTS); LTS corresponded to the blisters surrounded by dry ice during the irradiation and HTS to blisters without any cooling agent (i.e. uncontrolled temperature). This was done to evaluate possible alterations caused by the increase of temperature that takes place during the sterilization process (Fernández-Carballido et al., 2004).

Implants kept their shape and appearance after gamma-irradiation. However, their Tg decreased after sterilization (Figure 35), being more noticeable for the samples without cooling agent than the others. This most probably was caused by some polymer breakdown that might have occurred as consequence of the high-impacted energy (Montanari et al., 2001, 1998).

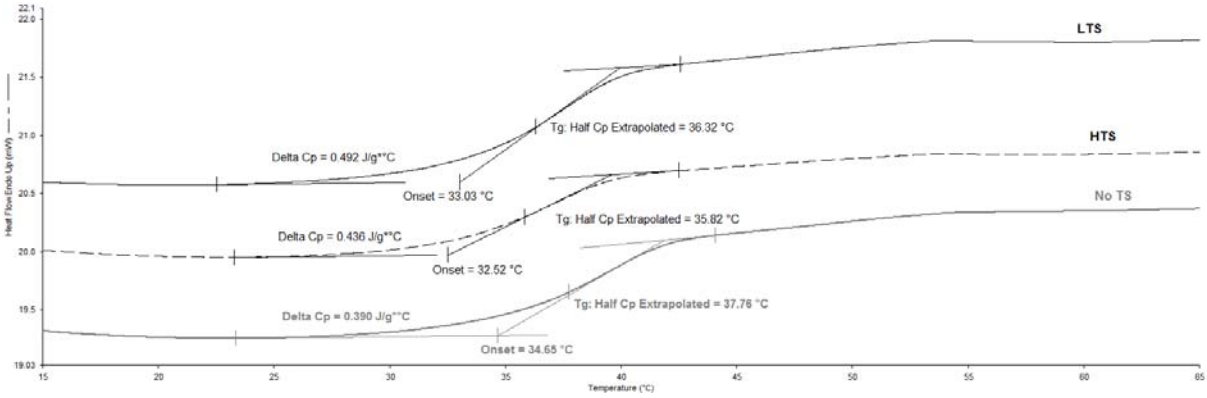

Figure 35 DSC thermograms OVA-loaded PLGA: shellac-implants before (No TS) and after terminal sterilization (LTS and HTS)

Increase in protein's hydrophobicity was detected after gamma-irradiation for both sterilization conditions, and for the lab-scale (Figure 36, left) and up-scaled (Figure 36, right) batches. This was more pronounced for the case of HTS, as probably uncontrolled temperature led to OVA aggregation and conformational changes. It has been previously reported that gamma-irradiation can disrupt the ordered structure of proteins like OVA due to the oxygen radicals generated by the sterilization process (Moon and Song, 2001), which could exposed the hydrophobic core of the protein. Furthermore, additional covalent/non-covalent interaction with the polymer matrix cannot be disregarded since mobility of the molecules is increased during irradiation and protein molecules can absorb energy, producing free radicals (Carrascosa et al., 2003; Rothen-Weinhold et al., 1999a).

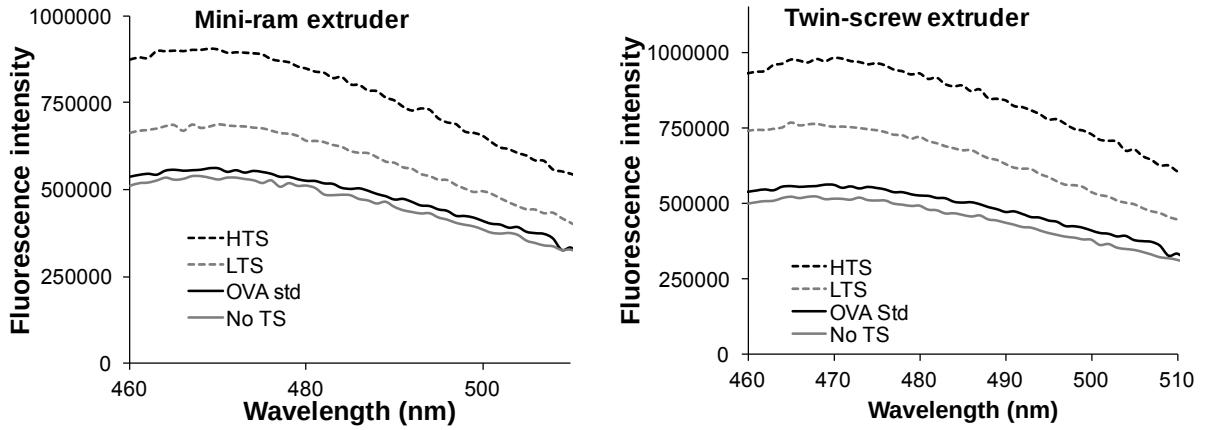

Figure 36 Fluorescence emission spectra of extracted OVA from PLGA: shellac-based implants prepared at lab-scale [left] and up-scaled [right] before (No TS) and after terminal sterilization (LTS and HTS)

Burst release was decreased as a consequence of the sterilization process in all the formulations tested (Figure 37 and Figure 38). This could be related to the increased

hydrophobicity of OVA, and thus lower solubility in water, and to stronger non-covalent interactions between the polymeric matrix and the protein. A decreased in OVA release from PLGA/PEG microspheres after gamma-irradiation has also been reported previously (Dorati et al., 2005). Authors attributed this behavior to morphological changes of the microspheres and increased interaction with the PLGA matrix and its degradation products.

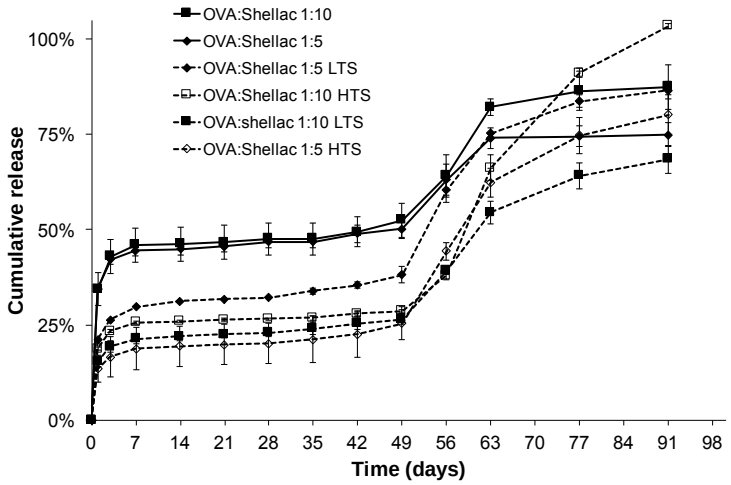

Figure 37 Release profile of OVA-loaded PLGA: shellac-based implants, prepared with the mini-ram extruder, before and after terminal sterilization

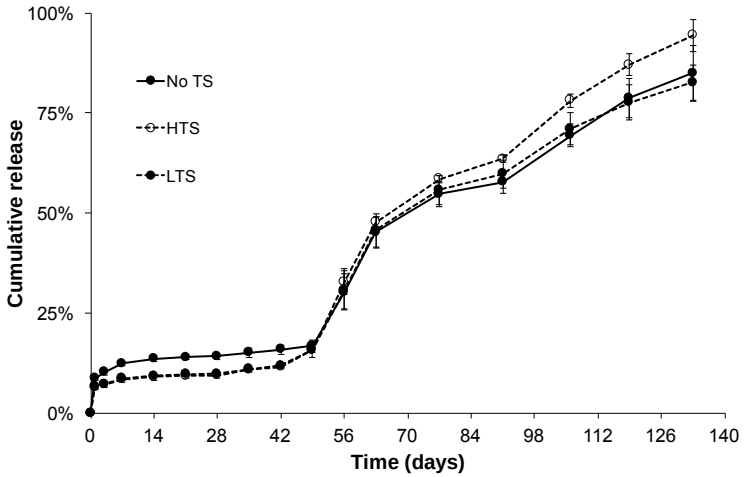

Figure 38 Release profile of OVA-loaded PLGA: shellac-based implants, prepared with the twin-screw extruder, before and after terminal sterilization

Irradiated implants prepared with the mini-ram extruder (Figure 37) showed bigger differences than those prepared with the twin-screw extruder (Figure 38). This might be due to the higher porosity of the implants prepared with the mini-ram extruder, which allowed higher mobility of the protein molecules. The variation is more noticeable during the fast dissolution phase of the protein (i.e. erosion phase after 49 d). However, no clear correlation

could be established between the irradiation condition or the OVA: shellac ratio and the release. Higher protein recovery during dissolution was observed for all the implants after irradiation under HTS conditions (Figure 37 and Figure 38), whereas under LTS conditions it remained similar to the non-sterilized samples. It could be expected that shellac also went through molecular weight changes after irradiation, which induced a more rapid solubilization of it in the release medium, releasing the protein molecules that have surrounded before due to the acidic microclimate. These changes were exacerbated by the higher increase in temperature during HTS than LTS, which might have promoted higher molecular mobility within the matrix. In general, irradiation induced OVA aggregation during release, but these were soluble aggregates capable of diffusing out of the matrix.

Gamma-irradiation affected the performance of the formulations prepared and it proved not to be suitable for the OVA-loaded PLGA: shellac-based implants. Further evaluation of the polymers molecular weight distribution and free radical formation would be ideal to fully understand the effect of irradiation on the implants and to assess whether the incorporation of other co-excipients (e.g. antioxidants) could maintain the physicochemical characteristics of the formulation after irradiation or not. Also the evaluation of a low-bioburden sterilization process (Gèze et al., 2001) could be useful to determine its suitability to produce sterile implants that maintain their physicochemical properties after irradiation at a lower dose.

3.5 Conclusions

The incomplete release of OVA from PLGA-implants was caused by ionic interactions between protein and PLGA, non-covalent aggregation and adsorption of the protein on PLGA. These reactions were triggered by the acidic microenvironment generated during PLGA hydrolysis. The creation of a more viscous environment within the matrix or the inclusion of pore formers was not successful to improve release completeness. These co-excipients were not able to control the acidic microclimate and did not avoid OVA aggregation. Besides, in the case of the ionic salts, protein aggregation was also induced by the increase in ionic strength and interaction of the OVA with the cations. Even though the use of weak bases as co-excipients doubled the release, the neutralization of all the acidic species formed was not possible and, thus, OVA aggregation could not be prevented.

The use of co-polymeric composites (i.e. PLGA and shellac), not only avoided the formation of insoluble protein aggregates but also led to a protein sustained release for longer periods of time. The formulation was up-scaled by a factor of 15, without changes in protein stability. The dissolution profile was comparable for both, lab-scale and up-scale formulations, with differences in the burst release caused by densification of the matrix. The prepared implants remained stable after three-months storage at 25°C regarding appearance and protein stability. However, due to changes in dissolution kinetics and thermal properties, it is advisable to store them at temperatures $<$10°C. Terminal sterilization by gamma-irradiation had an impact on protein' stability and conformation, and physicochemical characteristics of the implants. Therefore, an aseptic production process or a low-bioburden one should be considered for further product development.

This is the first successful application of the rather ubiquitous shellac in protein-releasing implants. This promising formulation approach is a step forward towards effective protein PLGA-based release systems, which up to now, have remained elusive.

4. Part II: Lipid based implants – Results and discussion

4.1 Introduction

The use of controlled release systems for the delivery of peptides and proteins aims not only to have a sustained release of the active compound, but also to protect these labile compounds from detrimental conditions upon administration (i.e. pH variations and enzymatic activity across the body) (Kreye et al., 2008; Teekamp et al., 2015). Therefore, the matrix in which the peptide or protein is embedded should be compatible with it and offer good mechanical, degradation and physicochemical properties to be able to be formulated as the required dosage form (Mitragotri et al., 2014). PLGA is the most common biodegradable material used for the preparation of protein-loaded formulations (Ghalanbor et al., 2012). However, as studied before, its acidic degradation hinders the stability of the protein and leads to incomplete release (Giteau et al., 2008; Houchin and Topp, 2008; Teekamp et al., 2015). Specially in the case of an acid-labile proteins like ovalbumin (OVA), where the acidic microclimate induces the formation of insoluble aggregates (see 3.2). Lipids are an interesting alternative to PLGA because they do not create an acidic microclimate during their degradation (Kreye et al., 2008). Moreover, they are biodegradable and biocompatible and have shown their suitability for the release of proteins (Almeida and Souto, 2007; Di Sabatino et al., 2012; Even et al., 2015; Guse et al., 2006c; Herrmann et al., 2007a; Ho et al., 2005; Koennings et al., 2007; Sax et al., 2012; Sax and Winter, 2012; Schulze and Winter, 2009).

Different manufacturing routes can also be used to prepare lipid-based formulations proving their versatility. Emulsification or spray-congealing are some of the studied processes to prepare nano- and microparticles (Almeida and Souto, 2007; Di Sabatino et al., 2012; Kathe et al., 2014; Maschke et al., 2007; Zaky et al., 2010). However, the creation of larger interfaces and shear forces (i.e. vigorous stirring and atomization) inherent to both methods, might compromise the stability and activity of the protein (Oh et al., 2014; Teekamp et al., 2015). HME is a good choice to avoid the presence of interfaces and to produce a more homogenous formulation (i.e. implants) (Kreye et al., 2008; Stanković et al., 2015a). Nonetheless, the temperature inherent to this process might have an impact not only on the protein but also on the stability of the lipidic matrix. Lipids present a complex structure that

can undergo polymorphic changes affecting the dissolution characteristics and overall performance of the formulation (Windbergs et al., 2009a, 2009b, 2009c). Thus, special care must be taken when using methods that involved the use of heat to prepare lipid-based implants. In this part of the thesis the feasibility of HME to prepare Ovalbumin (OVA)-lipid-based implants is investigated; it is divided in three subchapters as follows:

- **Understanding the release from lipid-based implants**
  Dissolution of proteins from lipid-based implants is mainly governed by diffusion processes: influx of water to dissolve the available protein molecules causing their efflux (Guse et al., 2006b; Kreye et al., 2011b; Sax et al., 2012). This diffusion process might be affected by the matrix composition and its possible interaction with the protein. Therefore, this subchapter aimed to evaluate the variations in implant characteristics depending on the lipidic matrix used.
- **Exploring formulation approaches to modulate the dissolution of OVA from lipid-based implants**
  To modify the dissolution kinetics from implants different approaches can be followed including the blending with other lipid materials (Guse et al., 2006c; Kreye et al., 2011c; Schulze and Winter, 2009), the use of PEG as release modifier (Güres and Kleinebudde, 2011; Herrmann et al., 2007a, 2007b; Sax and Winter, 2012) or tempering of the implants after preparation (Even et al., 2015; Kreye and Siepmann, 2011). These strategies not only affect the dissolution kinetics but they may also influence the overall characteristics of the formulation, especially the stability of the protein and lipidic matrix. Thus, the objective of this subchapter was to evaluate the impact of these approaches, among others, on the protein dissolution and stability of the main implant components. Moreover, the effect of gamma-irradiation as terminal sterilization technique on the formulation's characteristics is also assessed here.
- **Design of experiments (DoE) to optimize the release of OVA from lipid-based implants**
  These last subchapter presents the implementation of a DoE as a tool to optimize the dissolution of OVA from lipid-based implants, aiming to have a prolonged and sustained release of the protein. The Taguchi method was selected with the aim to reduce the number of experimental runs required to evaluate the interactions between responses (i.e. implant characteristics) and process/formulation variables (Bolboacă and Jäntschi, 2007; Yu et al., 2014). The information gathered through this evaluation could help to understand better the formulation and find means to optimize it.

4.2 Understanding the release from lipid-based implants

4.2.1 Characterization of the lipids used as biodegradable matrix

Glycerol trimirystate (D114), glycerol tristearate (D118) and hydrogenated palm oil (DP60) were selected as biodegradable matrices for the OVA-loaded implants. Composition of these triglycerides was evaluated with ESI/TOF-MS (Figure 39, Figure 40 and Figure 41), ^{1}H-NMR (Figure 42, Figure 44 and Figure 46) and ^{13}C-NMR (Figure 43, Figure 45 and Figure 47) indicating that D114 and D118 were composed of only one triglyceride, trimirystate and tristearate respectively, whereas DP60 was a mixture of mostly palmitic/stearic di- and triglycerides (Table 7).

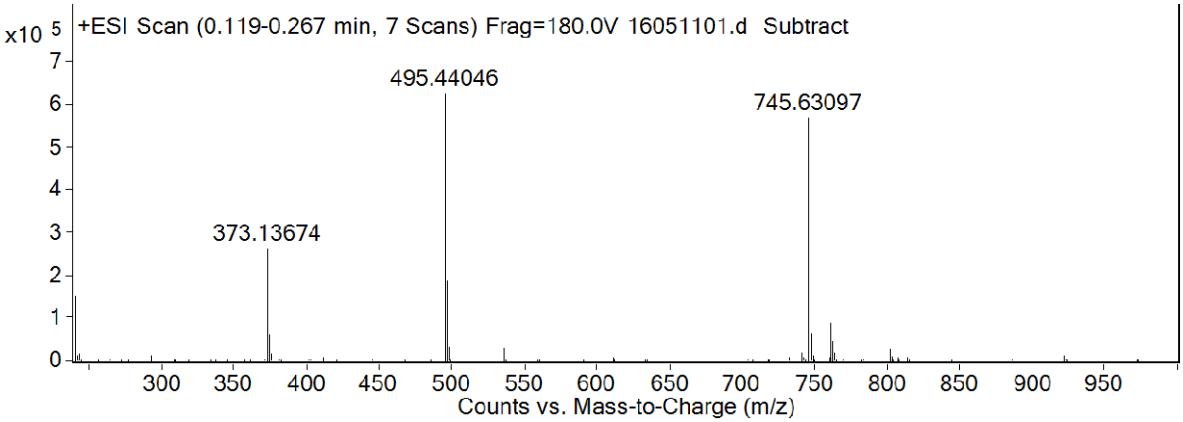

Mass-to-charge (m/z)	Assignation (refer to Table 7)
495.440	[*Structure 2* – H_2O + H]$^+$
745.631	[*Structure 1* + Na]$^+$

Figure 39 ESI/TOF-MS spectrum of D114 and its mass assignation

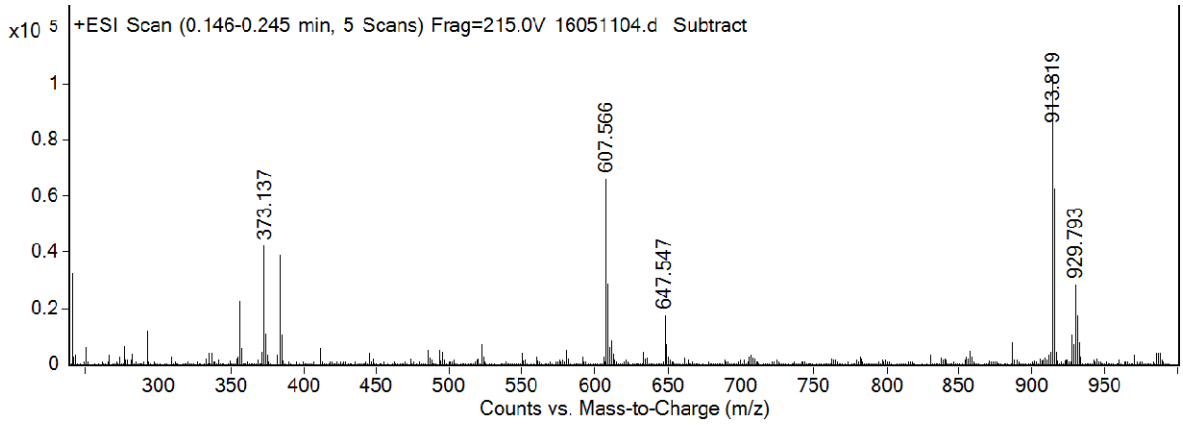

Mass-to-charge (m/z)	Assignation (refer to Table 7)
607.566	[*Structure 4* – H_2O + H]$^+$
647.547	[*Structure 4* + Na]$^+$
913.819	[*Structure 3* + Na]$^+$
929.793	[*Structure 3* + K]$^+$

Figure 40 ESI/TOF-MS spectrum of D118 and its mass assignation

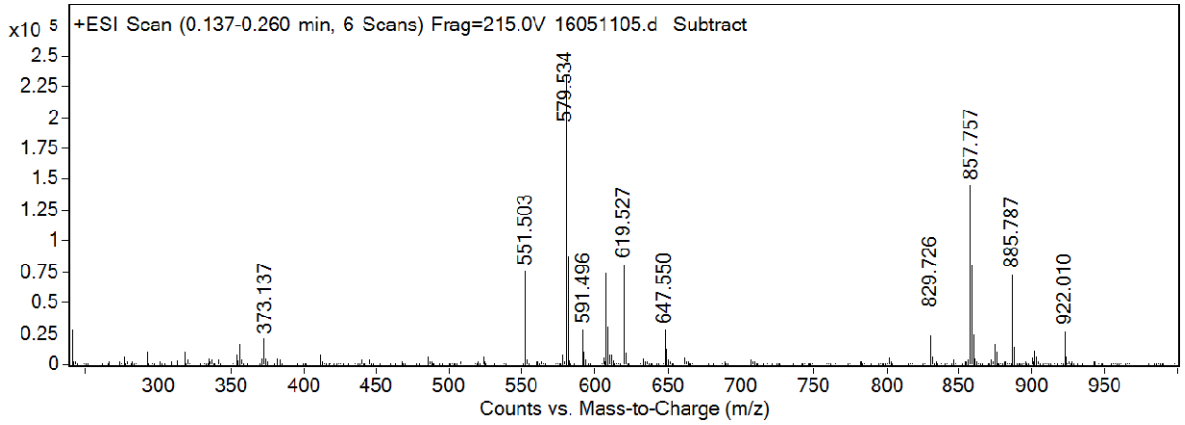

Mass-to-charge (m/z)	Assignation (refer to Table 7)
551.503	[*Structure 8* – H_2O +H]$^+$
579.534	[*Structure 9* – H_2O +H]$^+$
591.496	[*Structure 8* +Na]$^+$
619.527	[*Structure 9* +Na]$^+$
647.550	[*Structure 10* +Na]$^+$
829.726	[*Structure 5* +Na]$^+$
857.757	[*Structure 6* +Na]$^+$
885.787	[*Structure 7* +Na]$^+$

Figure 41 ESI/TOF-MS spectrum of DP60 and its mass assignation

Table 7 Lipid composition

Lipid	Structure #	Composition	
D114	1	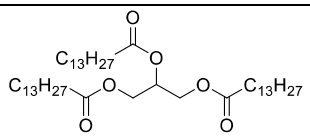	Glycerol trimirystate
	2	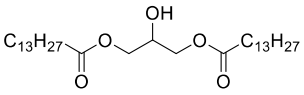	Glycerol dimirystate
D118	3	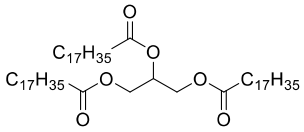	Glycerol tristearate
	4	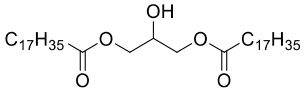	Glycerol distearate

DP60	5	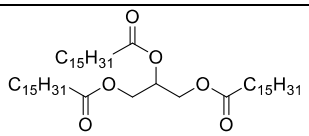	Glycerol tripalmitate
	6	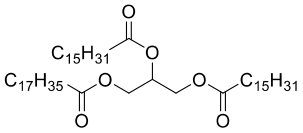	Glycerol dipalmitate stearate
	7	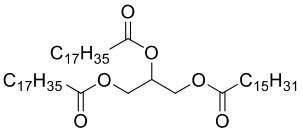	Glycerol palmitate distearate
	8	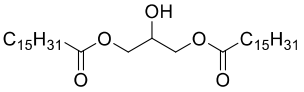	Glycerol dipalmitate
	9	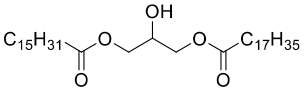	Glycerol palmitate stearate
	10	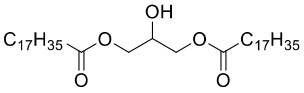	Glycerol distearate

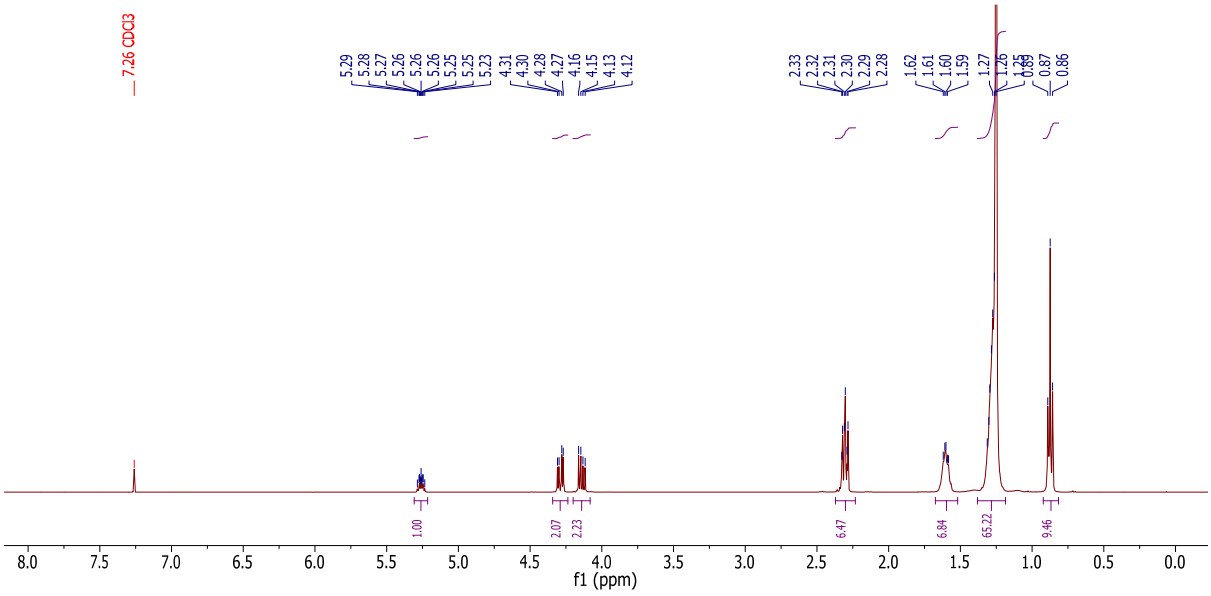

Figure 42 ^{1}H-NMR spectra of D114 (400 MHz, Chloroform-*d*) δ 5.26 (tt, *J* = 6.0, 4.3 Hz, 1H), 4.29 (dd, *J* = 11.9, 4.3 Hz, 2H), 4.14 (dd, *J* = 11.9, 6.0 Hz, 2H), 2.31 (td, *J* = 7.5, 2.4 Hz, 6H), 1.61 (tt, *J* = 6.9, 3.6 Hz, 7H), 1.38 – 1.19 (m, 65H), 0.87 (t, *J* = 6.8 Hz, 9H).

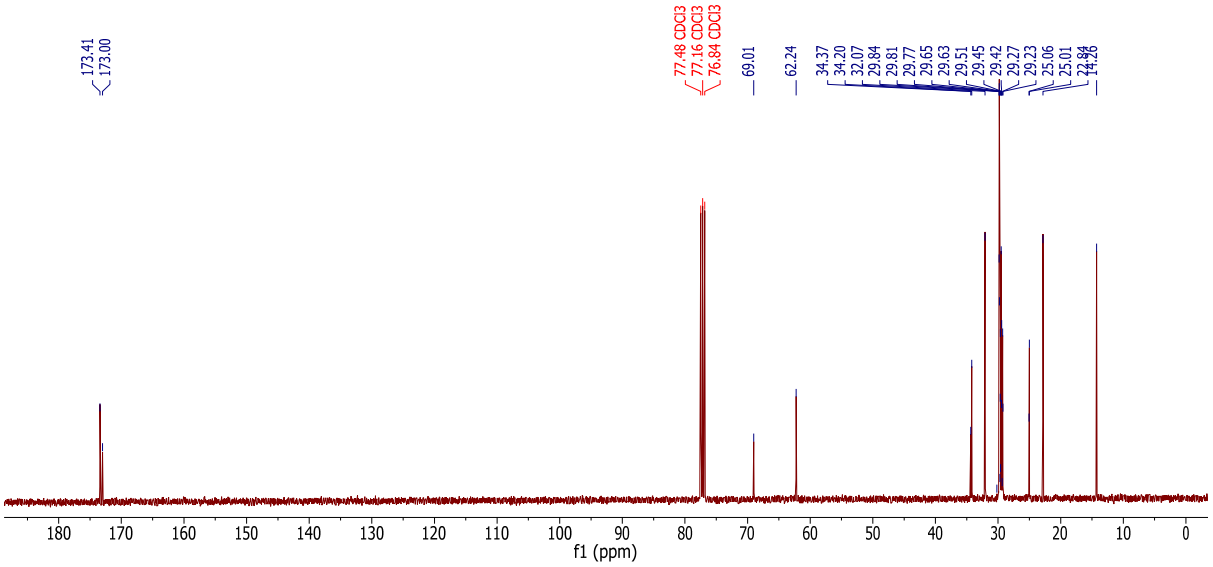

Figure 43 ^{13}C-NMR spectra of D114 (101 MHz, Chloroform-*d*) δ 248.01, 173.41, 173.00, 77.48, 77.16, 76.84, 69.01, 62.24, 34.37, 34.20, 32.07, 30.20, 29.84, 29.81, 29.77, 29.70, 29.65, 29.63, 29.60, 29.51, 29.45, 29.42, 29.34, 29.27, 29.23, 25.06, 25.01, 22.84, 14.26.

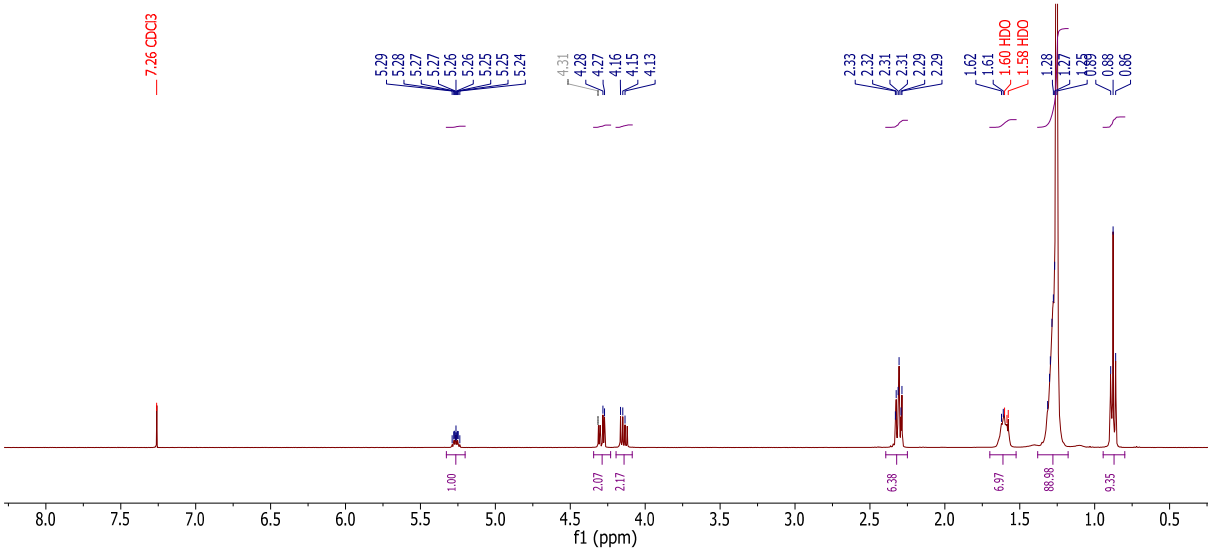

Figure 44 ^{1}H-NMR spectra of D118 (400 MHz, Chloroform-*d*) δ 5.26 (tt, *J* = 5.9, 4.3 Hz, 1H), 4.34 – 4.23 (m, 2H), 4.20 – 4.09 (m, 2H), 2.31 (td, *J* = 7.5, 2.4 Hz, 6H), 1.63 (dd, *J* = 7.2, 4.3 Hz, 7H), 1.25 (s, 89H), 0.88 (t, *J* = 6.7 Hz, 9H).

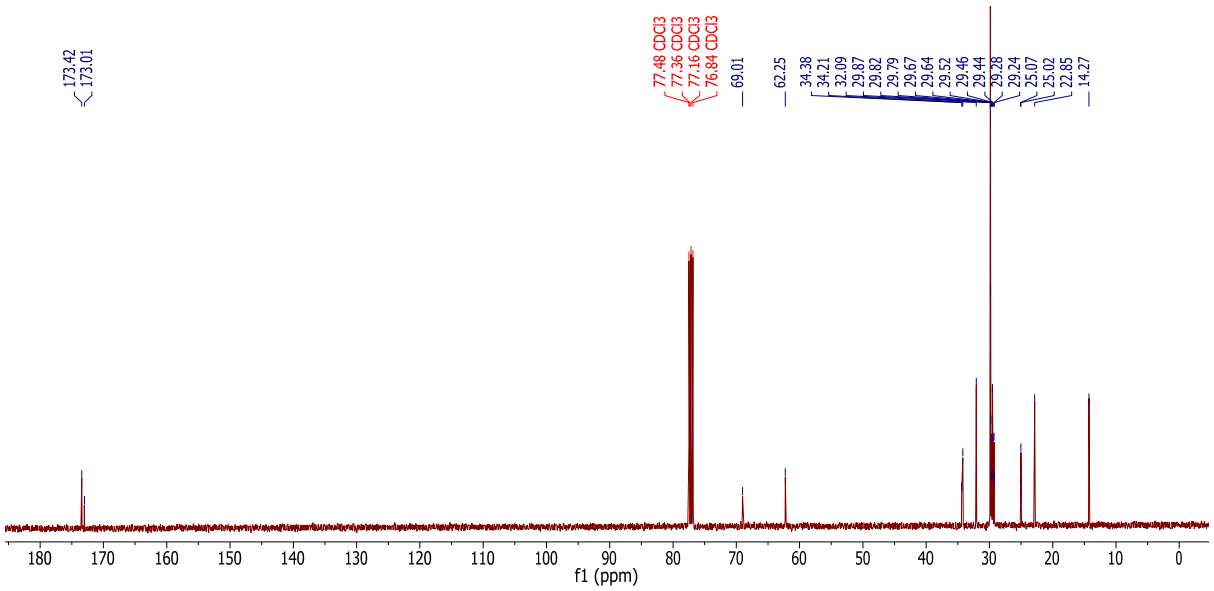

Figure 45 ^{13}C-NMR spectra of D118 (101 MHz Chloroform-*d*) δ 173.42, 173.01, 77.48, 77.36, 77.16, 76.84, 69.01, 62.25, 34.38, 34.21, 32.09, 29.87, 29.82, 29.79, 29.67, 29.64, 29.52, 29.46, 29.44, 29.28, 29.24, 25.07, 25.02, 22.85, 14.27.

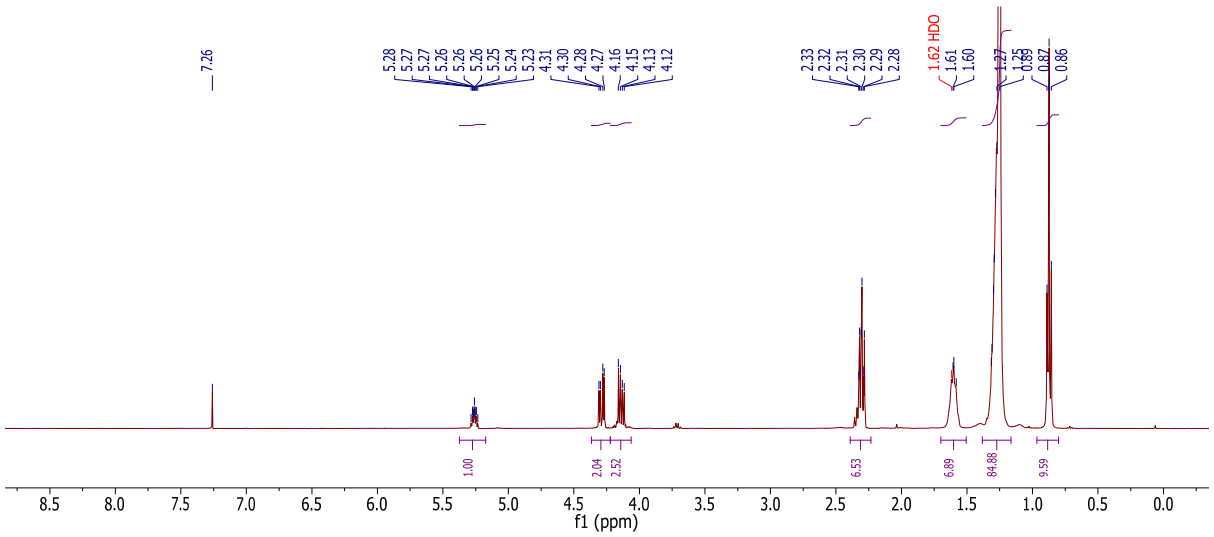

Figure 46 ^{1}H-NMR spectra of DP60 (400 MHz, Chloroform-*d*) δ 5.26 (tt, *J* = 5.9, 4.3 Hz, 1H), 4.29 (dd, *J* = 11.9, 4.3 Hz, 2H), 4.14 (dd, *J* = 11.9, 6.0 Hz, 3H), 2.30 (td, *J* = 7.5, 2.4 Hz, 7H), 1.70 – 1.51 (m, 7H), 1.25 (s, 85H), 0.97 – 0.80 (m, 10H).

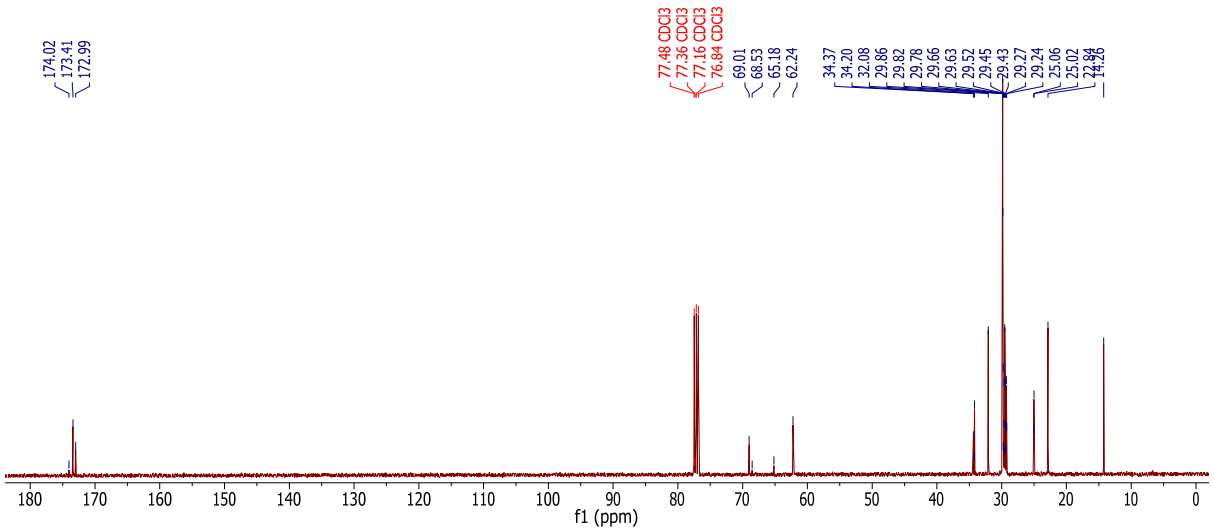

Figure 47 ^{13}C-NMR spectra of DP60 (101 MHz, Chloroform-*d*) δ 174.02, 173.41, 172.99, 77.48, 77.36, 77.16, 76.84, 69.01, 68.53, 65.18, 62.24, 34.37, 34.25, 34.20, 32.08, 29.86, 29.82, 29.78, 29.75, 29.66, 29.63, 29.60, 29.52, 29.45, 29.43, 29.40, 29.27, 29.24, 25.06, 25.02, 22.84, 14.26.

The X-ray diffraction pattern of D114 (not shown) and D118 showed the three dominant reflections that are typical for β-modification (Sato, 2001; Schulze and Winter, 2009; Severino et al., 2012) whereas the diffraction pattern of the DP60 showed only one reflection, resulting from its less crystalline nature (Figure 48). This indicated differences in crystallinity of the lipids, which might play a role on protein dissolution and implant performance.

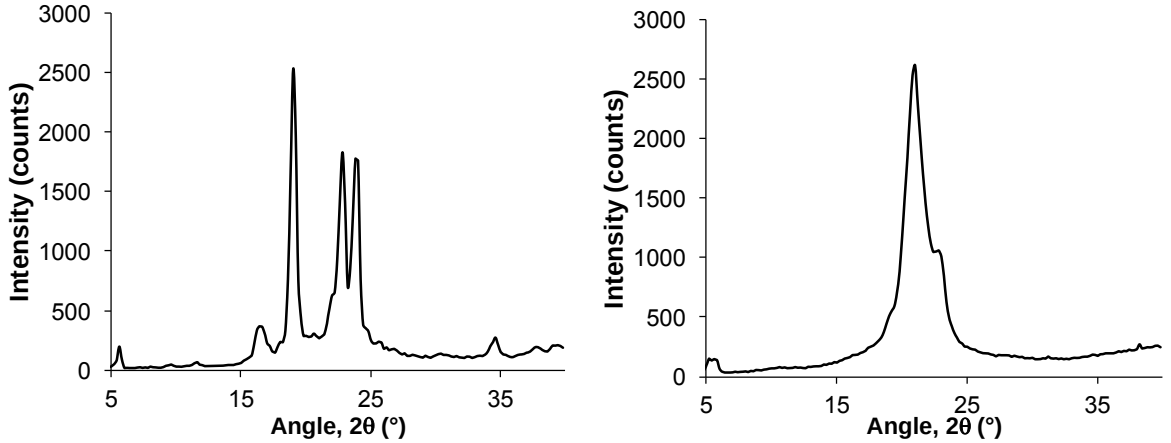

Figure 48 XRPD patterns of D118 as received [left] and of DP60 as received [right]

Thermal characterization indicated one single melting temperature (Tm) for D114 and D118 (β-stable modification) and two melting peaks for DP60, which indicated that this lipid is composed of more than one crystalline form of triglycerides (Figure 49). After rapid cooling and melting again, DP60 recrystallized in two stable modifications, with slightly lower Tm

than during the first run, but keeping the same behavior as shown during the first melting. In contrast, D118 showed an additional melting temperature corresponding to its metastable α-form, followed by the recrystallization of the β-modification (Sato, 2001; Schulze and Winter, 2009). In the case of D114, the low melting α-hexagonal form was observed, followed by its recrystallization into its β-metastable form (Reitz and Kleinebudde, 2007; Sato, 2001). These are indicators of lipid unstable modifications after they have been completely molten. Moreover, for all the three lipids evaluated, lipid crystallinity decreased after melting and cooling as indicated by the drop in their melting enthalpies (ΔH) (Table 8). This is of importance during the HME process, since high temperatures are used and the biodegradable matrix should be molten to prepare the implants. Therefore, polymorphic changes arising from the manufacturing process need to be monitored.

Table 8 Thermal characterization of D114, D118 and DP60

Lipid	1st heating run				Cooling run	2nd heating run				
	Tm_1 (°C)	ΔH_1 (J/g)	Tm_2 (°C)	ΔH_2 (J/g)	T_{cryst} (°C)	Tm_1 (°C)	ΔH_1 (J/g)	T_{cryst} (°C)	Tm_2 (°C)	ΔH_2 (J/g)
D114	56.84	193.81	-	-	-	32.20	14.72	35.38	53.54	179.90
D118	70.00	200.85	-	-	46.14	54.24	138.37	-	69.03	17.64
DP60	50.02	4.87	56.82	87.39	40.66	49.37	12.74	-	56.40	36.21

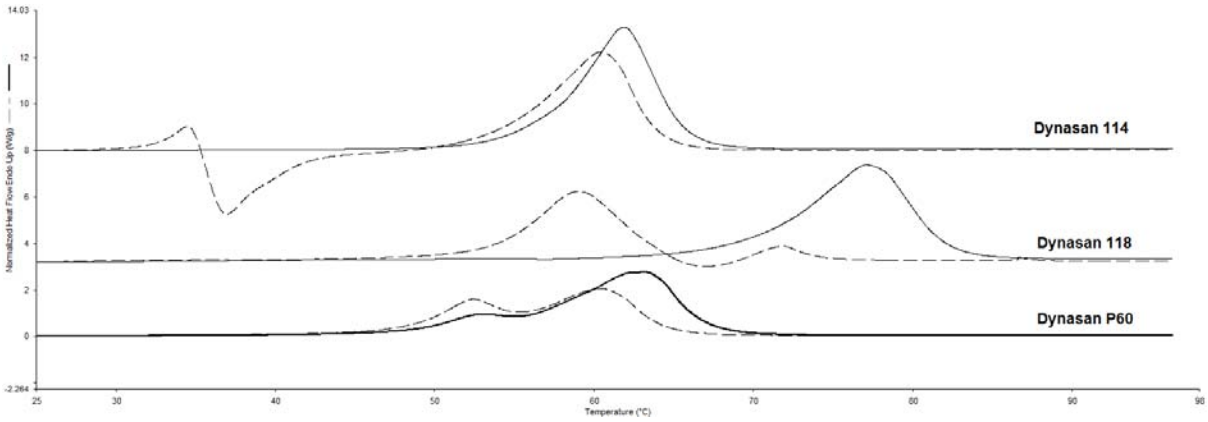

Figure 49 DSC thermograms of D114, D118 and DP60 [first heating cycle: continuous line; second heating cycle: dashed line]

4.2.2 Implant characterization

4.2.2.1 Appearance and mechanical properties

Implants with and without OVA were prepared with the mini-ram extruder. All three matrices were well extrudable requiring slightly more time (4.5 vs. 4 min for DP60 and 8 vs. 7 min for D118) under 100°C when OVA was incorporated. The surface of the D118- and DP60-based implants was smooth and slightly shiny, whereas the surface of the D114-based implants was rough. No pores or cracks were evident in any of the formulations (Figure 50). Protein particles were observed on the surface of the implants when OVA was incorporated (Figure 50, right, shiny dots), and in the case of the D118-based implants, the surface was rougher than when the protein was not present. This can be attributed to the fact that OVA particles were not completely melted under the extrusion conditions forming a solid dispersion within the lipidic matrix.

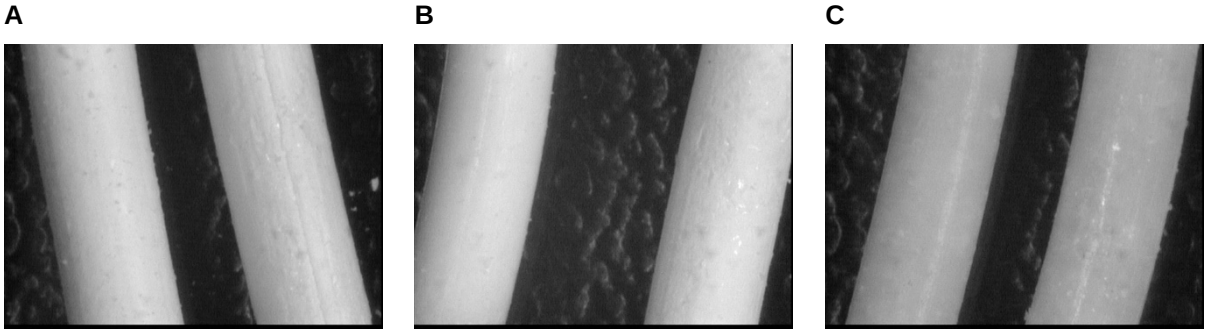

Figure 50 Comparison of the morphology of lipid-only [left] and 5% OVA-loaded [right] implants based on D114 [A], D118 [B] and DP60 [C] right after extrusion

All the implants presented good mechanical stability to be handled during the experiments. Extrudates of D118 alone were more rigid and easier to cut than the ones based on DP60 and D114 lipids. The hardness was significantly different ($p<0.001$) between the three lipid-only implants evaluated (Figure 51) and could be ranked as D118> DP60> D114. D118 showed the highest strength probably due to its higher melting temperature that confers higher stability to the matrix. Additionally, its homogeneous composition allowed a more effective molecule packaging with a higher Van der Waals contact within the chains and higher cohesion among them. Interestingly, when OVA was incorporated into this matrix the hardness and energy at break of the implant decreased significantly (Figure 51). As stated before, the dispersion of protein molecules within the lipidic matrix could decrease the cohesion forces between the lipid molecules causing these differences. In the case of D114 and DP60 matrices the hardness was comparable but the energy at break was higher when OVA was incorporated than when it was not (Figure 51). In this case, the ranking was DP60>D118>D114. It could be hypothesized that the differences between D114 and D118,

and DP60 were caused by the less crystalline structure of DP60, which allowed a stronger physical interaction with the protein due to a more homogeneous distribution within the amorphous matrix.

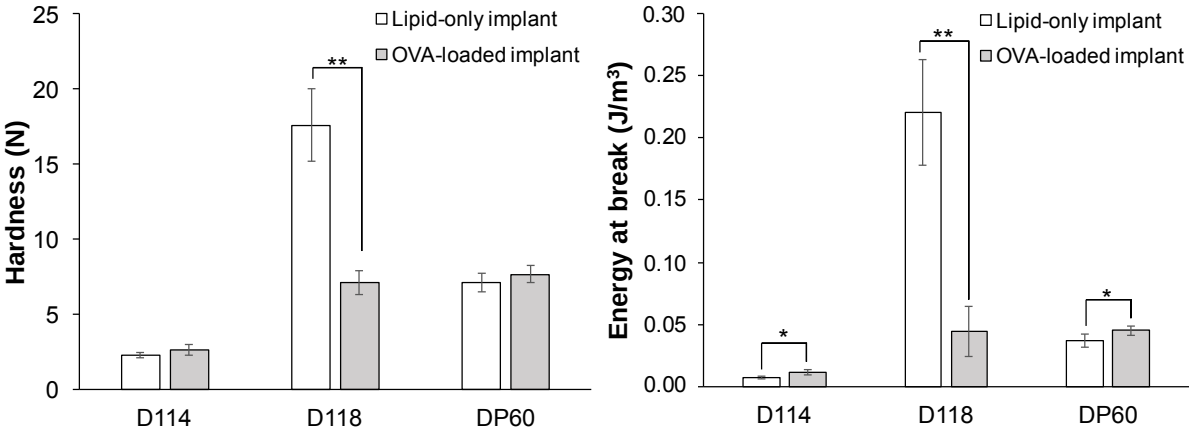

Figure 51 Hardness [left] and energy required to break the implants [right] either lipid-only or with 5% OVA-loading as measured with the texture analyzer (n=6; mean ± SD; *$p < 0.05$, **$p < 0.001$)

4.2.2.2 Thermal properties

Implants prepared with D114 and D118 presented similar thermal properties to the lipids as received. Neither the HME process nor the incorporation of OVA changed the Tm or the ΔH of the lipid matrix (Figure 52 vs. Table 8), indicating that no polymorphic changes occurred as a consequence of the extrusion process and/or the inclusion of the protein within the matrix. In the case of DP60-based implants, only one melting peak was observed instead of the two shown initially. Moreover, an increase of ΔH was also detected for this formulation (Figure 52). These changes might be attributed to a reordering of the lipid chains structure into a more stable structure (i.e. highest Tm among the two initial ones), after melting have occurred during the hot melt extrusion process (Sax and Winter, 2012).

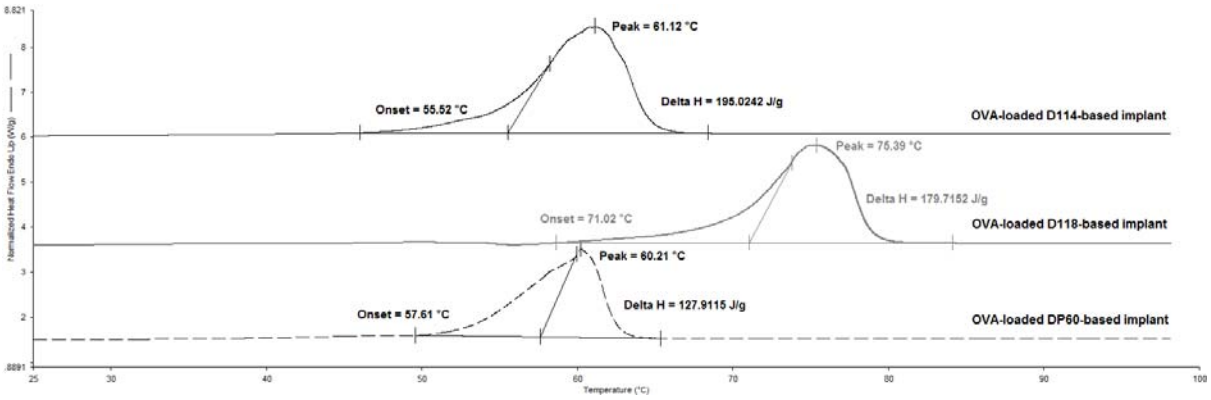

Figure 52 DSC thermograms of D114-, D118- and DP60-based implants loaded with 5% OVA

4.2.3 OVA stability after extrusion

As explained in section 3.2.1, the use of high temperatures during hot melt extrusion might be detrimental for proteins like OVA (denaturation temperature 84.5ºC) (Donovan and Mapes, 1976; Rajagopal and Wood, 2013; Stanković et al., 2013). Thus, stability characterization was performed after implant preparation as well. OVA remained stable after extrusion as indicated by the SEC-HPLC, which indicated that neither additional aggregation nor hydrolysis were caused by the extrusion process. Furthermore, comparable CD spectra of the protein as received and extracted from the implants were obtained (Figure 53, left). The two minima at 222 nm and 210 nm, representative of the α-helix and β-sheet structures commonly present in OVA (Hu and Du, 2000), were observed suggesting that the secondary structure remained unaltered and that the lipid matrix could protect the drug against the temperature stress inherent to the HME manufacturing. In contrast, OVA after heating presented a shift towards the minima at 210 nm, indicating an increase in the β-sheet conformation (Hu and Du, 2000). Since the lipid melts first during the extrusion process, it might act as cushion from heat towards the protein. This is in line with the appearance of the implants, were protein particles were visible on the surface (Figure 50).

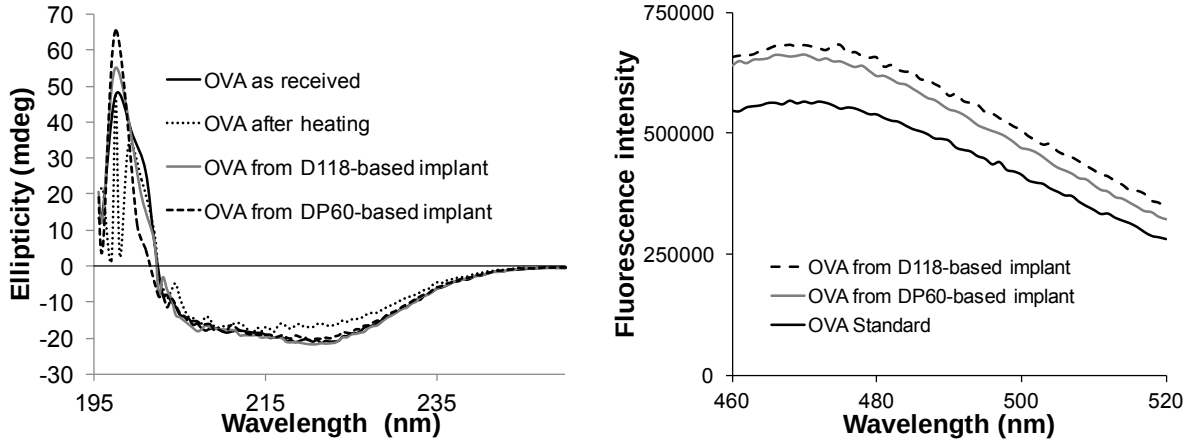

Figure 53 CD spectra [left] and fluorescence emission spectra [right] of OVA standard and OVA extracted from D118-based and DP60-based implants

The fluorescence spectra of the protein showed a slightly higher intensity for the protein extracted from the implants (Figure 53, right) than the standard. This could have been caused by non-covalent interactions between the protein and the lipophilic matrix that induced small rearrangements of OVA's tertiary structure and, thus, additional exposure of the protein's hydrophobic areas. This has been reported for other hydrophobic molecules, like PEG, before (Farruggia et al., 2000; Lee and Lee, 1987)

4.2.4 Dissolution behavior of OVA from lipid-based implants

Since the lipid matrices do not erode, protein release is mainly governed by diffusional processes of the protein out of the matrix and/or water into the matrix (Guse et al., 2006b; Kreye et al., 2011b; Siepmann and Siepmann, 2011). Although the three lipid matrices evaluated are composed by long-chain glycerides, substantial differences in protein dissolution were observed. The burst release was comparable between the three lipids (<25% after 3 hours), indicating that the amount of protein molecules located on the surface of the implant was similar. Release of OVA from D114 and D118 matrices was relatively fast with more than 75% of the protein released during the first week, followed by a slow diffusion of the remaining protein over the next 2 and 5 weeks for D114 and D118, respectively (Figure 54), recovering the total amount of the protein. In contrast, DP60 matrix released OVA in an extended fashion over a period of 10 weeks at a release rate of about 5.0-6.5% per week, followed by an even slower diffusion phase during the remaining time. In this case, no more than 75% of the protein was released after 175 days. This could be explained by the possible interaction between the protein and the lipid matrix and/or by a limited penetration of water into these hydrophobic systems, impairing the dissolution of all the protein molecules contained within the implant (Kreye et al., 2011b). Nonetheless, extraction of the remaining protein fraction was possible after the release study was completed, as opposed to the PLGA based implants (see 3.2.2), showing the suitability of the lipids as releasing matrices.

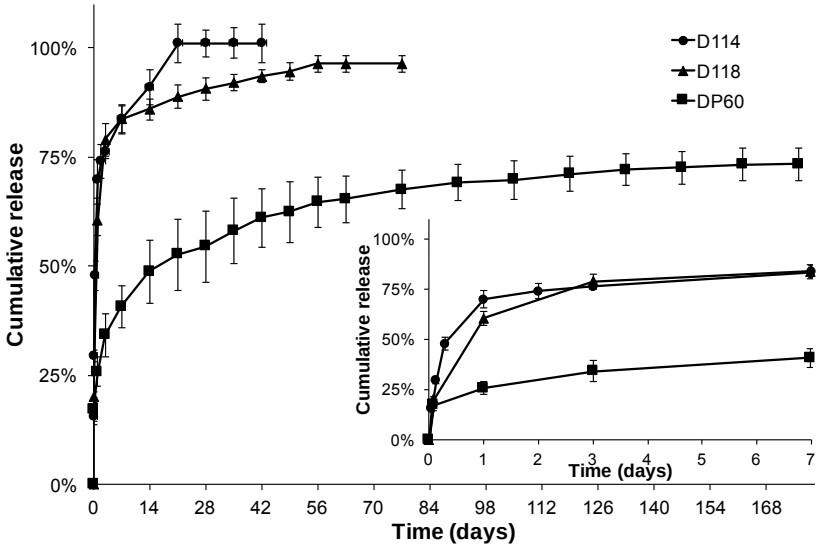

Figure 54 Release profile of 5% OVA-loaded lipid-based implants using different lipids as matrix

The differences between the three matrices could be attributed to differences in the degree of crystallinity of the lipids. Since DP60 is less crystalline than the other two lipids, stronger physical interaction between the matrix and the dissolved protein could have occurred,

delaying its diffusion (Crotts et al., 1997; Maschke et al., 2007). In contrast, the presence of crystallites within the structure of D114 and D118 leads to a higher anisotropy of the protein distribution yielding to a faster release. These results are in line with the mechanical properties found before, were DP60-based implants were stronger than the D114- and D118-based ones (Figure 51), indicating higher cohesion forces for D118.

4.2.5 Effect of protein loading on implant properties

To evaluate the effect of OVA loading on its dissolution from lipid-based implants, D118 and DP60 were selected as matrices because they showed similar mechanical properties when OVA was incorporated but significant differences in their dissolution profile.

4.2.5.1 Thermal properties

For D118-based matrix the increase in the loading of OVA did not alter the Tm or the polymorphic form of the lipid matrix (Figure 55). A slight decrease in the ΔH was detected when more OVA was incorporated (Table 9), which could be explained by the fact that less lipid was present in the formulation. In the case of the DP60-based implants the melting peak became narrower when more protein was incorporated (Figure 56). Moreover, ΔH increased with increases in protein loading (Table 9). This suggested the formation of crystal structures with closer distribution of melting peaks. In all the three cases the thermograms showed only one melting peak as shown previously (see 4.2.2.2).

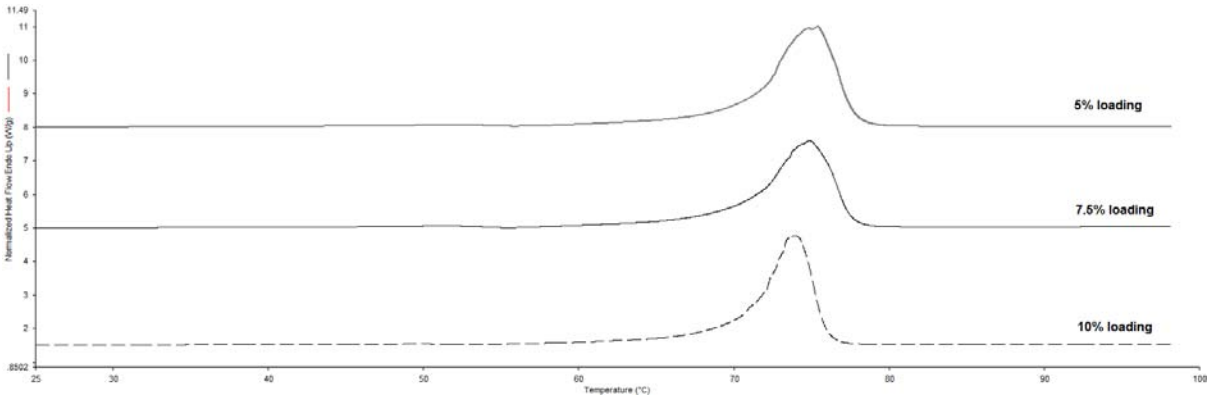

Figure 55 DSC thermograms of D118-based implants loaded with different loadings of OVA

Table 9 Thermal characterization of D118- and DP60-implants loaded with different OVA loadings

OVA loading (%)	D118		DP60	
	Tm (°C)	ΔH (J/g)	Tm (°C)	ΔH (J/g)
0	70.0	200.9	56.8	92.3
5	71.0	189.1	58.2	127.9
7.5	72.1	163.2	58.9	130.4
10	71.6	164.4	57.0	136.1

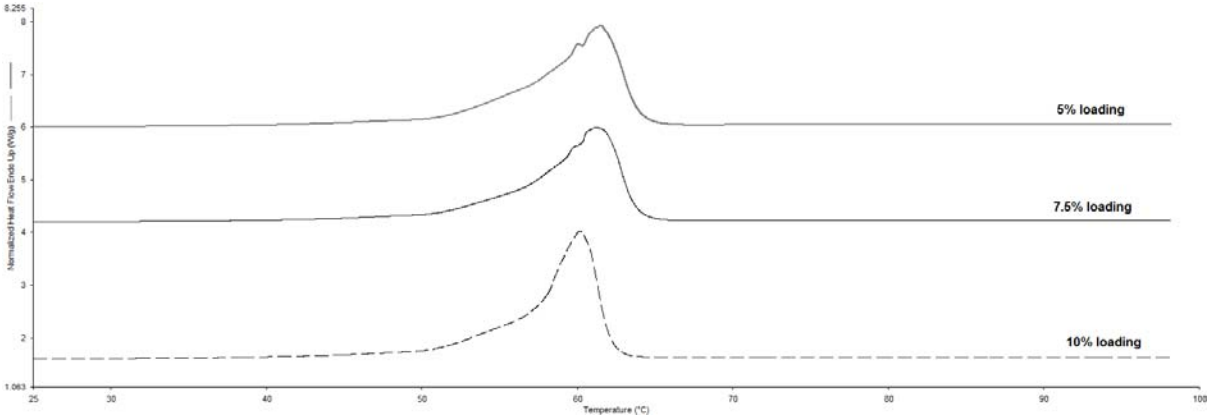

Figure 56 DSC thermograms of DP60-based implants loaded with different loadings of OVA

4.2.5.2 Protein stability

No indication of aggregation or hydrolysis was observed for any of the formulations after SEC-HPLC evaluation. Hydrophobicity measurements showed that in the case of DP60-based implants no major differences were observed between the three loadings evaluated (Figure 57, right). In all three cases the fluorescence intensity was higher than in the case of the standard, probably caused by the interaction between the lipid matrix and the non-polar residues of the protein, as stated before (Mohl and Winter, 2004). Interestingly, in the case of D118-based implants by increasing the loading, the hydrophobicity of the protein decreased, reaching comparable intensities with the standard when 10% OVA was loaded (Figure 57, left). This could be attributed to a higher differentiation between the hydrophilic (protein-rich) and hydrophobic areas (lipid-rich) within the matrix caused by the presence of lipid crystallites that difficult the interaction with the protein molecules (Kreye et al., 2012).

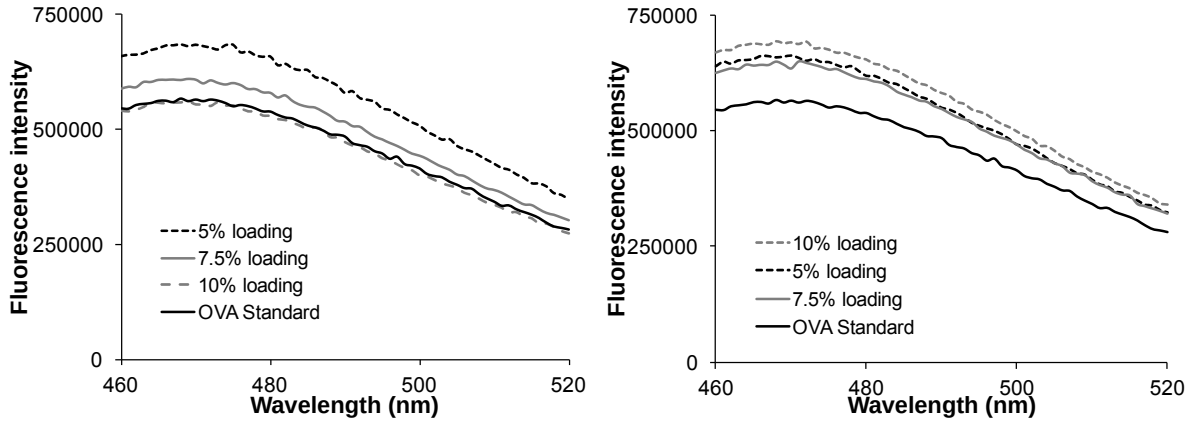

Figure 57 Fluorescence emission spectra of OVA extracted from D118-based [left] and DP60-based [right] implants with different protein loadings

4.2.5.3 Protein release

For both matrices evaluated there was an increase in the dissolution rate when higher loadings were used (Figure 58 and Figure 59), as a result of the higher porosity created after the protein starts to release. This was in agreement with previous studies on lipid-based implants (Guse et al., 2006b; Kreye et al., 2011b). Release from D118-based implants was faster than the DP60 ones, with the main fraction being released during the first three days (Figure 58). Since bigger pores are created at higher loadings, the proteins molecules buried in the core of the implant can be accessed faster by water, facilitating their release (Kreye et al., 2011b). Thus, complete protein recovery was achieved after two weeks for the 10 and 7.5% loadings, and after four weeks for the 5% one. The differences in release rate could also be related to the changes in hydrophobicity observed (Figure 57, left), where less protein-lipid physical interactions seemed to happen at higher protein loading, yielding to faster release.

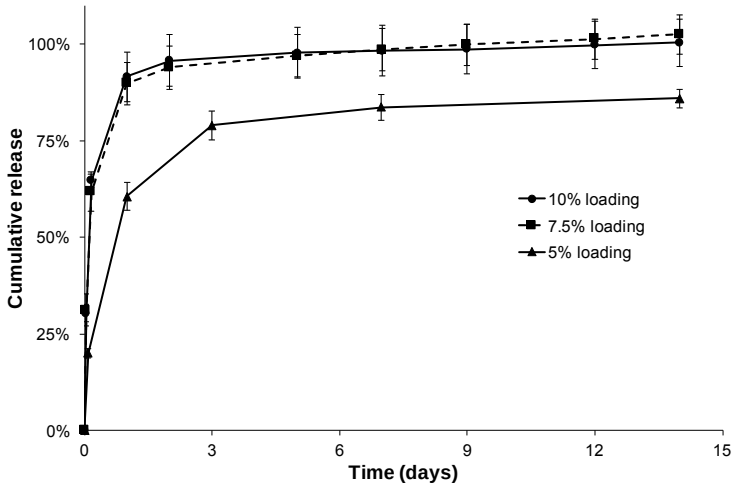

Figure 58 Release profile of OVA-loaded D118-based implants with different protein loadings

In contrast, DP60-based implants released the main fraction of protein during the first two, four or ten weeks for the 10%, 7.5% and 5% loadings, respectively (Figure 59). These results are in line with the hydrophobicity measurements (Figure 57, right), which indicated some interaction of OVA with the DP60 matrix that could have delayed its diffusion out of the matrix. Furthermore, the increase in matrix crystallinity observed at a higher protein loadings (Table 9) might have influenced this behavior as well: faster release is obtained when the crystallinity of the matrix increases. Complete protein release was observed for the 7.5 and 10% loadings after 98 days, whereas in the case of the 5% OVA-loading, less than 75% was released, caused by the limited influx of water through the implant.

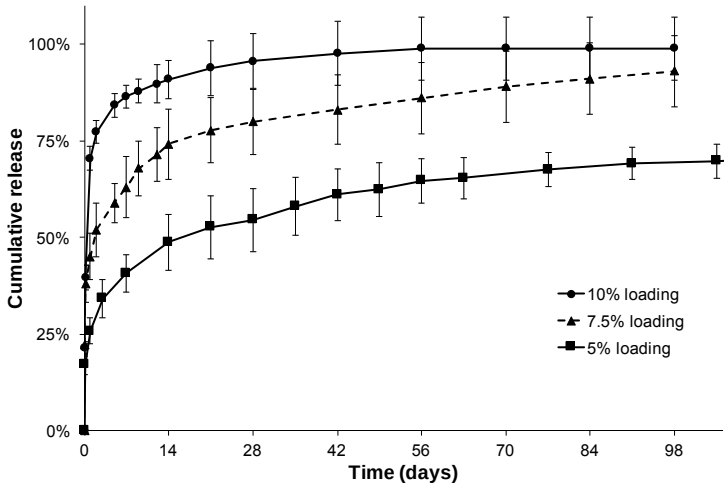

Figure 59 Release profile of OVA-loaded DP60-based implants with different protein loadings

Both matrices, D118 and DP60, showed their suitability for preparing OVA-loaded implants with dissolution profiles controlled by diffusion of protein and water molecules, and with durations between few days and several weeks depending on the lipid used.

4.2.6 Loading a smaller protein leads to longer release: the case of lysozyme

Previous reports have shown extended release of lysozyme (LYS) from D118-based implants (Sax and Winter, 2012), which is in contrast with the results found here (see sections 4.2.4 and 4.2.5) and by other researches for OVA (Even et al., 2015). Therefore, LYS was incorporated at a 5% loading in D114, D118 or DP60 matrices to assess its influence on implant properties, especially on dissolution.

The surface of the implants was rougher in the case of D114-based formulations than in the case of the D118 and DP60 ones (Figure 60), showing some irregularities and possibly pores. The surface of the other two implants was smooth and even, and no protein particles were visible under the macroscope.

Figure 60 Comparison of the morphology of the lipid-only [left] and 5% LYS-loaded [right] implants based on D114 [A], D118 [B] and DP60 [C] right after extrusion

The implants that presented the higher mechanical stability were the D118 ones, followed by the DP60 and the D114, most probably caused by the higher melting point of D118 when compared to the other two. In the three cases, the incorporation of LYS led to a lower hardness and energy at break of the implants (Figure 61), being significant only for the D118-based implants ($p<0.001$) and the hardness of the D114-one ($p<0.05$). As in the case of OVA, the incorporation of protein molecules within the matrix could have decreased the cohesion forces within the lipid molecules causing these differences. Interestingly, implants were significantly weaker when LYS was incorporated than when OVA was incorporated ($p<0.05$), probably because OVA is more hydrophobic than LYS (Cardamone and Puri, 1992), so the chances of physical interactions between the matrix and the protein, which could confer mechanical stability as well, are bigger (Maschke et al., 2007).

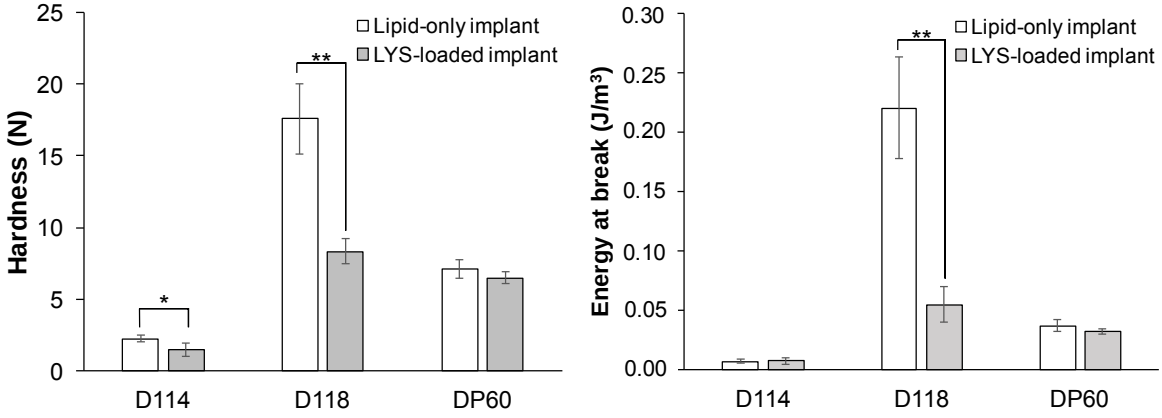

Figure 61 Hardness [left] and energy required to break the implants [right] either lipid-only or with 5% LYS-loading as measured with the texture analyzer (n=6; mean ± SD; *$p<0.05$, **$p<0.001$)

D114-based implants released the protein the fastest, reaching 100% release within one week (Figure 62). This correlated well with the mechanical properties measured, where these implants showed bigger fragility and the presence of uneven areas on the surface, which could have led to a rapid diffusion of the protein. This behavior was similar to the OVA-loaded D114-based implants. Remarkably, no substantial differences in the dissolution of LYS were found between D118 and DP60 (Figure 62). In both cases, the release of LYS was slow and continuous for more than 28 weeks. These findings correlated well with previous reports, where D118 was used in combination with other lipidic materials, yielding prolonged and sustained released over several days (Sax and Winter, 2012). For these two formulations, the remaining amount of LYS (35-25%) was recovered after extraction from the matrix.

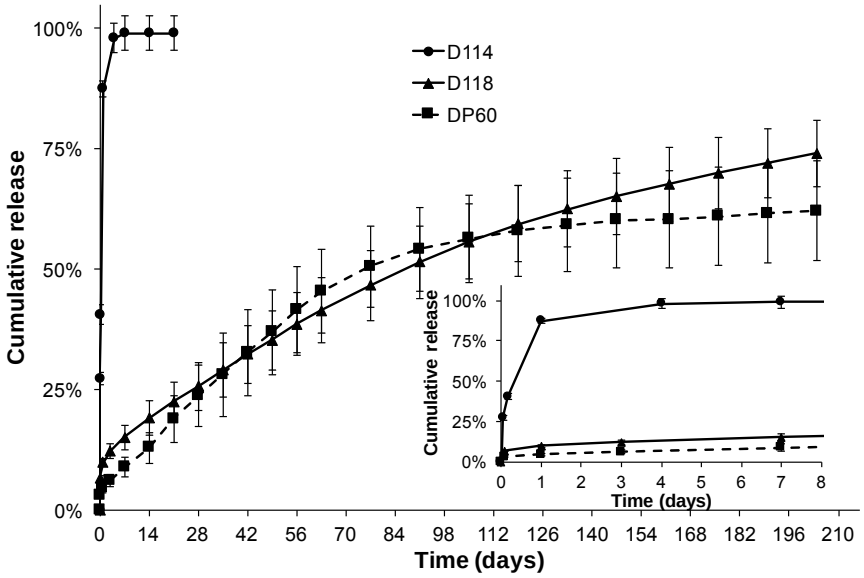

Figure 62 Release profile of 5% LYS-loaded lipid-based implants using different lipids as matrix

The differences between OVA and LYS could be attributed to differences in the molecular weight of the proteins (44.3 vs. 14 KDa). Since LYS is smaller, its distribution within the matrix could have been more homogeneous than in the case of OVA, avoiding the formation of protein-rich areas. Hence, the pores formed during diffusion of the protein were less interconnected than in the case of OVA, decreasing the water influx within the lipidic matrix and thus, the dissolution of the protein molecules.

Protein size and hydrophobicity play a role in the implant properties. Differences in the inner structure of the implant, in the distribution of the protein and the possible physical interaction between the matrix and the implant, are critical factors that impact the performance of the formulation and that should be considered during the development of controlled release systems for the proteins.

4.3 Exploring formulation approaches to modulate the release of OVA from lipid-based implants

Different strategies have been reported before as alternatives to adjust the release of the drug from lipid-based implants. These approaches included the use of more hydrophilic excipients like PEG (Herrmann et al., 2007a, 2007b; Mohl and Winter, 2006), use lipidic blends as releasing matrix (Even et al., 2015; Kreye et al., 2011c; Sax et al., 2012; Sax and Winter, 2012; Schulze and Winter, 2009) and curing after implant preparation (Even et al., 2015; Kreye and Siepmann, 2011). Thus, diverse approaches were explored to modulate the release of OVA from D118-based implants, as an example of a fast releasing matrix, and from DP60-based implants, as a slow releasing one.

4.3.1 Effect of co-excipients on dissolution kinetics

4.3.1.1 PLA as a release-delaying excipient

To slower the release rate of OVA from D118-based implants, PLA was incorporated as co-excipient at a loading of 10 or 20%. A 10% loading of OVA was selected because this was the fastest releasing formulation (Figure 54). Since PLA degrades slower than PLGA (i.e. higher crystallinity, pH drops slower) (Jain, 2000; Jiang and Schwendeman, 2001), no incomplete OVA release was expected as it was observed before for PLGA-based implants (see section 3.2).

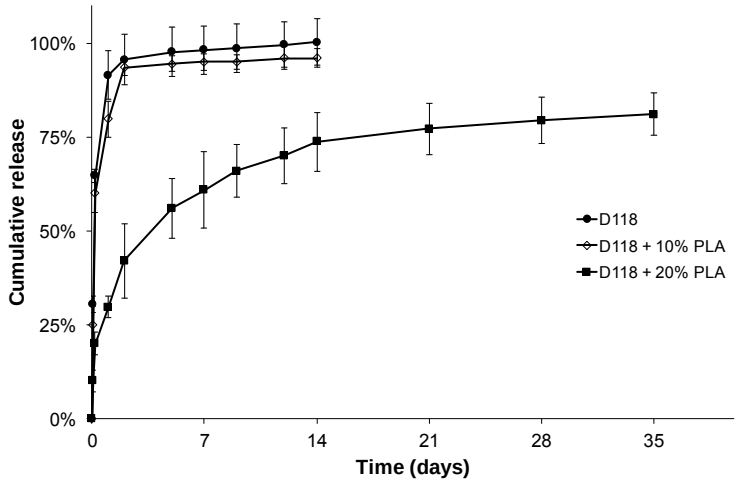

Figure 63 Release profile of 5% OVA-loaded D118-based implants using PLA as co-excipient

The implants were well extrudable requiring slightly longer processing time at 100°C when PLA was present (8, 9 and 12 min for 0, 10 and 20% PLA loading respectively). All the formulations were mechanically stable and easy to handle. A decrease in the burst release was observed when PLA was present in the matrix. It decreased from 30% to 25 and 10%

when PLA was incorporated at 10 or 20% respectively (Figure 63). In these three formulations, the drug release was driven mainly by diffusion and it was at a lower rate when PLA was present than when it was not. This decrease in the release rate was considerable lower for the 20% PLA yielding to a sustained release for over 1 month (Figure 63). The polymer decreased the diffusion of the protein by acting as a barrier against the water available to dissolve the protein particles (Jiang and Schwendeman, 2001). The remaining amount of protein (~19%) was recovered after the release, so no aggregation was induced by the presence of PLA. This could be related to the fact that the pH was always >6.8 during the whole study, avoiding the degradation induced by the acidic microclimate of the polymer's degradation products (Crotts and Park, 1997; Jiang and Schwendeman, 2001).
The use of PLA as a co-excipient of the D118-lipid matrix is a suitable approach to prolong the release of OVA from 1 week to 1 month without the detrimental effects that the polymeric matrix could have on the protein.

4.3.1.2 PEG with different molecular weights to accelerate the dissolution of OVA

In the case of DP60 a faster dissolution was aimed. It has been shown previously that PEG at a 10% loading is enough to create an interconnected porous network that allows the diffusion of the protein out of the lipidic matrix (Herrmann et al., 2007a, 2007b). Therefore, PEG with different molecular weights was incorporated at this concentration.

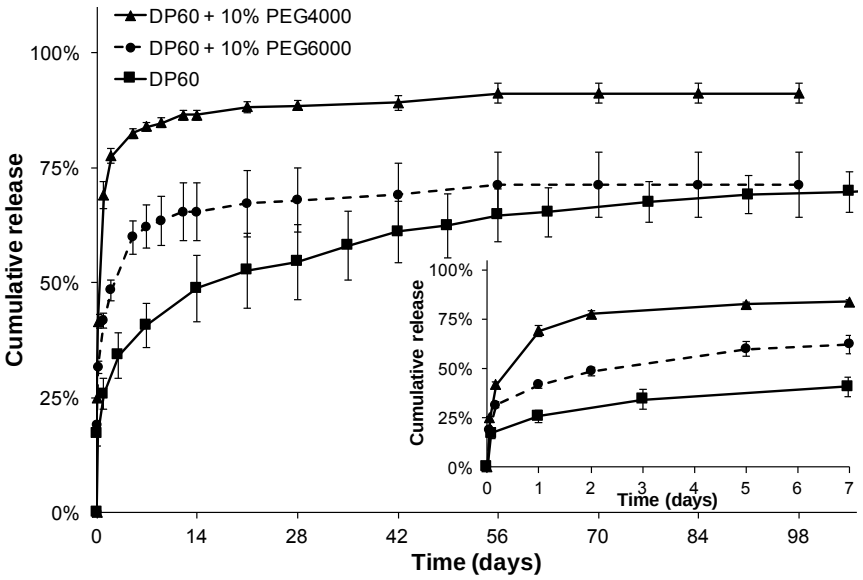

Figure 64 Release profile of 5% OVA-loaded DP60-based implants using PEG with different molecular weights as co-excipient

Implants were extruded using the same conditions with slightly less time required at 100°C when PEG was incorporated than when it was not (3.5 min vs. 4 min, respectively). The

implants surface was smooth and non-porous, and presented good mechanical properties for all the three formulations. The burst release presented some small differences being the highest when PEG 4000 (25%) was incorporated, followed by PEG 6000 (19%) and no PEG (17%) as the latest (caption Figure 64). At lower PEG's molecular weight, faster protein release was observed during the first week of dissolution. This can be attributed to differences in aqueous solubility of PEG. They leave pores in the lipidic matrix after solubilizing, allowing the diffusion of more protein molecules. However, this rapid diffusion phase occurred only during the first 21 days of release, probably because complete solubilization of PEG molecules have occurred by then, and the porosity of the lipid matrix could not be increase any further. Hence, the protein molecules buried in the core of the implant were not reached by water. Previous studies showed complete recovery of the protein when PEG was incorporated (Herrmann et al., 2007a; Mohl and Winter, 2004). However, in these studies the implants were prepared by compression instead of hot melt extrusion. Differences in water uptake and erosion between these two methods have been reported before showing that the melting of lipids leads to a more dense and compact matrix than the ones prepared by compression (Kreye et al., 2008; Pongjanyakul et al., 2004), which can explain the differences. Nonetheless, the remaining fraction of protein (9-27%) was recovered after protein extraction. PEG might be an interesting approach when faster diffusion is required at the beginning of the release period.

4.3.1.3 Blends with other lipidic materials to tune the release

Another approach to tune the dissolution kinetics from lipid-based implants is by using blends of different lipidic materials (Kreye et al., 2011c; Schulze and Winter, 2009). Binary blends of DP60 with other lipid (D114, D118, Precirol^{TM} ATO5 (Prec) or Compritol$^{®}$ 888ATO (Comp) were prepared by physically mixing the lipids prior OVA incorporation to achieve higher homogeneity within the matrix. All the formulations were well processable with extrusion times varying between 3 and 4 minutes. In all the cases the dissolution was faster than when DP60 was used alone (Figure 65). As expected, with less amount of DP60 present in the matrix (i.e. 25%) the release of OVA was faster probably caused by less interactions between the protein and the matrix. Furthermore, the blend DP60:D118 (25:75) and DP60:D114 (50:50) released faster than the DP60:Comp (25:75), most probably because the protein can interact more with the hydrophilic components of the Comp (mono- and diglycerides) than with the homogeneous and crystalline structure of the D114 or D118 (Aburahma and Badr-eldin, 2014; Reitz et al., 2008). In the 50:50 blends prepared, the dissolution speed was ranked as: D114 > Prec > D118 > Comp, which corresponds with their length of the fatty acid chain (C_{14} > C_{16}/C_{18} > C_{18} > C_{22}). Thus, the increase in lipophilicity

within the system, delays the release of OVA because of a water influx decrease across the matrix (i.e. higher impermeability) (Kreye et al., 2011b, 2011c) to dissolve the protein. Although both Prec and Comp have a more heterogeneous composition (mono-, di- and triglycerides) expecting similar behavior during OVA dissolution, differences in their release were observed. This could be attributed to differences in their erosion and water uptake behavior, being more pronounced for Prec than Comp (Kreye et al., 2011c).

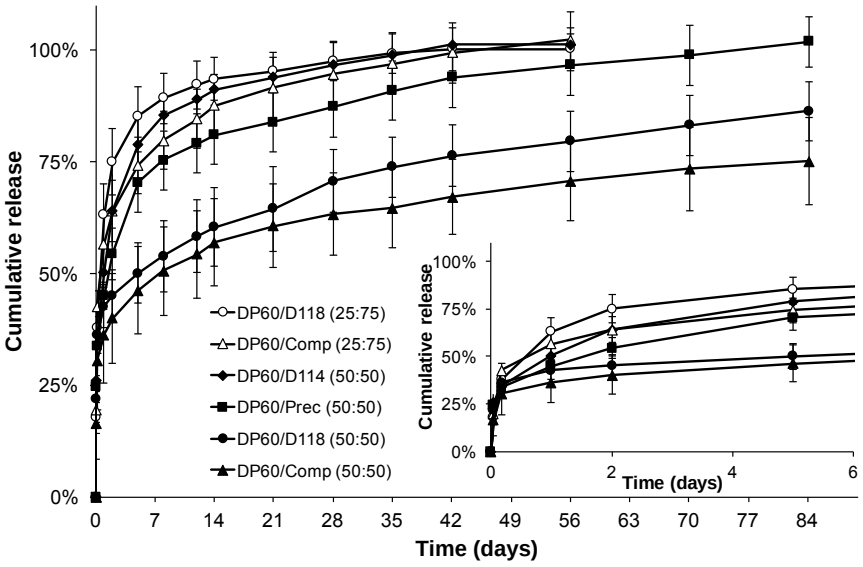

Figure 65 Release profile of 5% OVA-loaded implants using lipid blends as matrix

A broad but single melting temperature was observed when DP60 was blended with either D114 or Prec, whereas in the case of D118 and Comp more than one melting transition was observed (Figure 66). This could have been caused by differences in melting temperature between the components of the binary blend. While in the case of D114 and Prec the melting range is closer to DP60 (53-57°C, 55-58°C and 58-62°C, respectively), D118 and Comp present higher differences (70-73°C and 69-74°C vs. 58-62°C); thus, achieving a single phase between these last ones is more difficult during the extrusion process, especially because the extruder used (mini-ram) does not allows compounding of the molten materials hampering the creation of one single phase and probably leading to phase separation (Kreye et al., 2011c; Sprengholz, 2014).

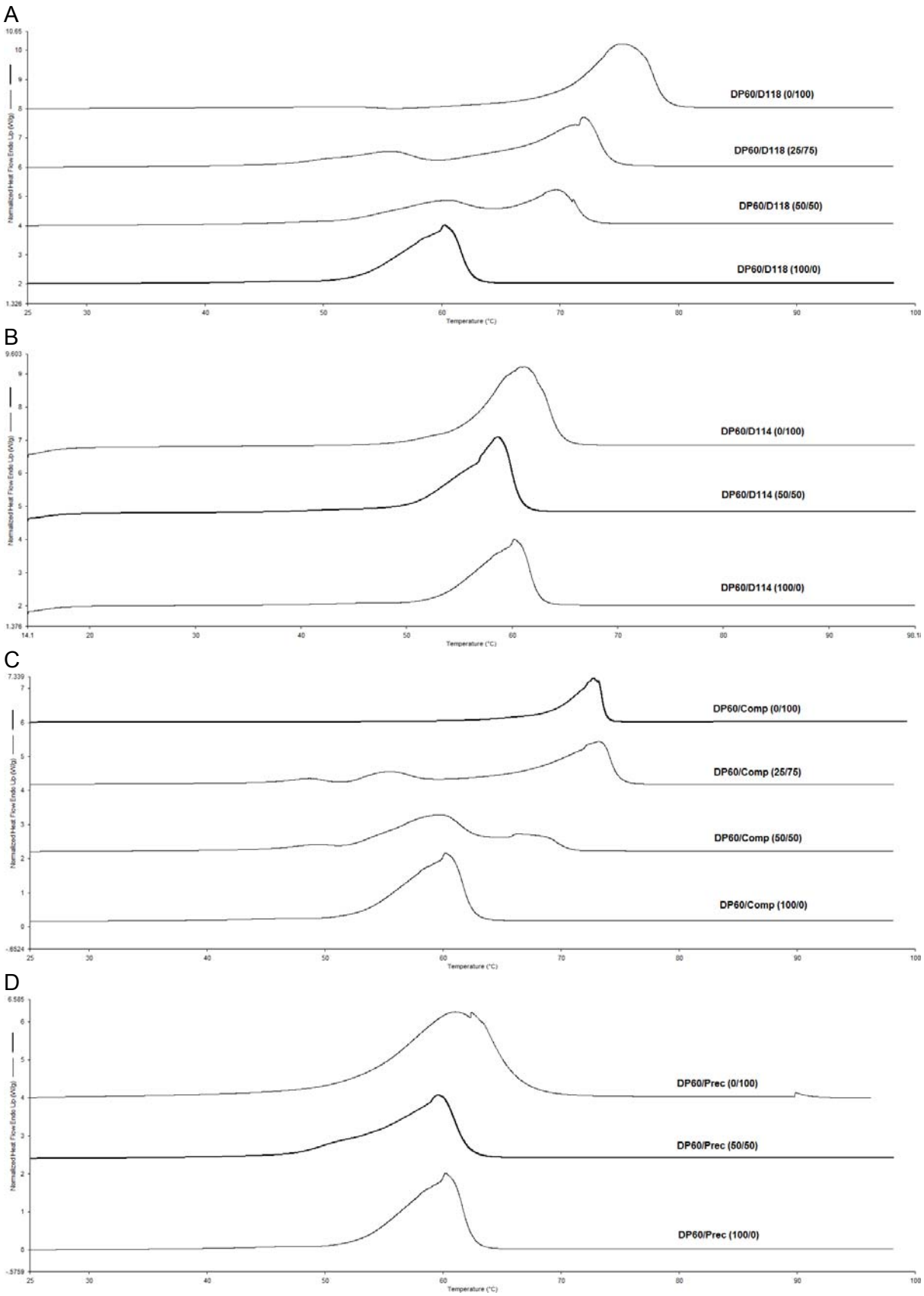

Figure 66 DSC thermograms of 5% OVA-loaded implants using blends of DP60:D118 [A], DP60:D114 [B], DP60: Compritol [C] and DP60: Precirol [D] as matrices

Furthermore, polymorphic changes cannot be ruled out since the melting peaks of the blends presented a lower temperature than the ones of the bulk materials (Figure 66). Therefore, this approach should be assessed with care, especially regarding matrix aging and stability of the formulation after storage since rearrangements of the lipidic microstructure can occur changing the formulation performance (San Vicente et al., 2000; Sato, 2001; Schulze and Winter, 2009).

4.3.2 Effect of processes after extrusion on protein integrity and dissolution

Besides the inclusion of co-excipients as an strategy to modify the dissolution from lipid-based implants, additional processes, such as curing and coating after implant preparation, have also been reported as suitable approaches (Even et al., 2015; Guse et al., 2006b; Jannin and Cuppok, 2013; Kreye and Siepmann, 2011).

4.3.2.1 Curing

Two different temperatures (40 and 50°C), both under the melting temperature of the implants to avoid their deformation, were selected for curing experiments. In the case of D118-based implants, only one melting peak, and with very similar temperature onset between them, were detected for all conditions tested, indicating that curing did not induced the formation of metastable forms with lower melting temperatures (Figure 67). This could be attributed to the use of temperatures were the lipid is not melted. Interestingly, the increase in curing temperature and in curing time led to a narrowing of the melting peak (Figure 67), which indicated the formation of crystal structures with a closer distribution of melting peaks (Reitz and Kleinebudde, 2007).

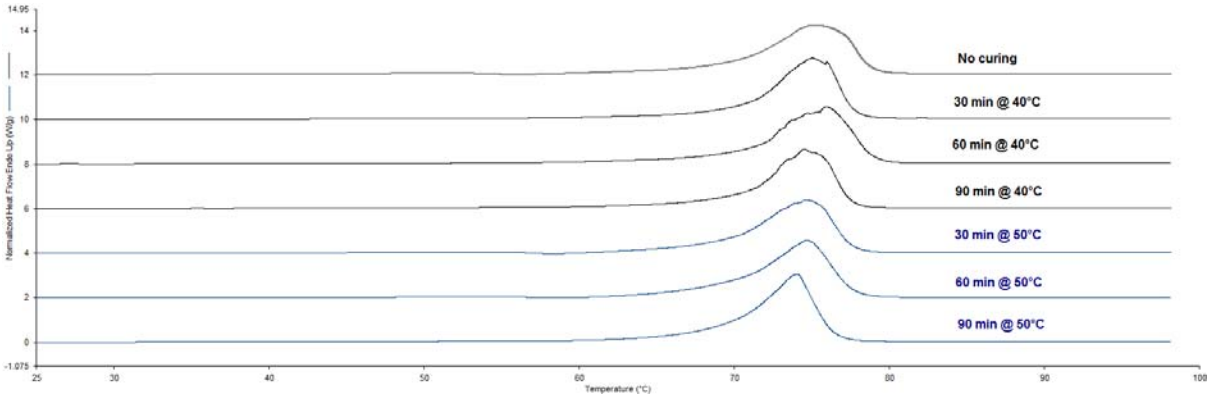

Figure 67 DSC thermograms of D118-based implants after curing at different conditions

These findings are in line with the XRPD patterns observed (Figure 68, left), where the crystalline structure changes with the curing conditions becoming more crystalline. Right after extrusion and prior curing, the XRPD pattern showed a broad spacing characteristic of the α-form, while the thermogram showed the broadest melting peak as an indication of the

mixture of different crystal structures within the matrix (Reitz and Kleinebudde, 2007; Sax and Winter, 2012; Schulze and Winter, 2009). With a progression of the curing conditions, the lipidic matrix converted gradually into its β- and β'-modifications losing its α-one, which are more stable and crystalline (Sato, 2001; Sax and Winter, 2012).

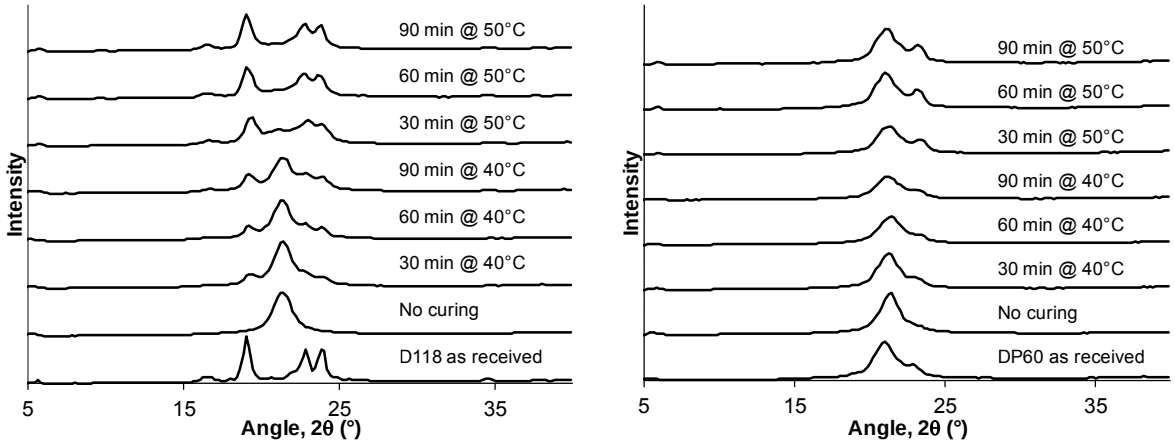

Figure 68 XRPD patterns of D118-based [left] and of DP60-based implants [right] after curing at different conditions

OVA was released faster from the lipids cured at 50°C (Figure 69), which is related to the increase in lipid crystallinity. The presence of more crystallites within the implant microstructure led to a higher anisotropy of the protein distribution and, thus, to a faster release. Moreover, curing at high temperatures might lead to the formation of bigger pores that facilitate the efflux of OVA generating faster dissolution rates (Kreye and Siepmann, 2011). In contrast, implants cured at 40°C had a slightly higher burst release than the non-cured ones, but a slower diffusion rate when the implants were cured for 60 min or more at this temperature (Figure 69). OVA molecules are harder to diffuse out because curing under these conditions created a denser matrix with reduced pores size, and so impaired water mobility (Even et al., 2015; Kreye and Siepmann, 2011).

In the case of DP60-based implants the differences in thermal properties, crystallinity and dissolution were less evident than in the previous case. Thermograms of the cured implants showed a broad melting peak for all the formulations, evidencing the mixture of lipids that composes DP60 (Figure 70). Nonetheless, a slight increase in the melting peak temperature was evidenced for the implants cured at 50°C, being more perceptible for the formulations cured during 90 minutes. As in the case of D118, this could be an indication of the formation of more crystalline structures within the matrix (Reitz and Kleinebudde, 2007).

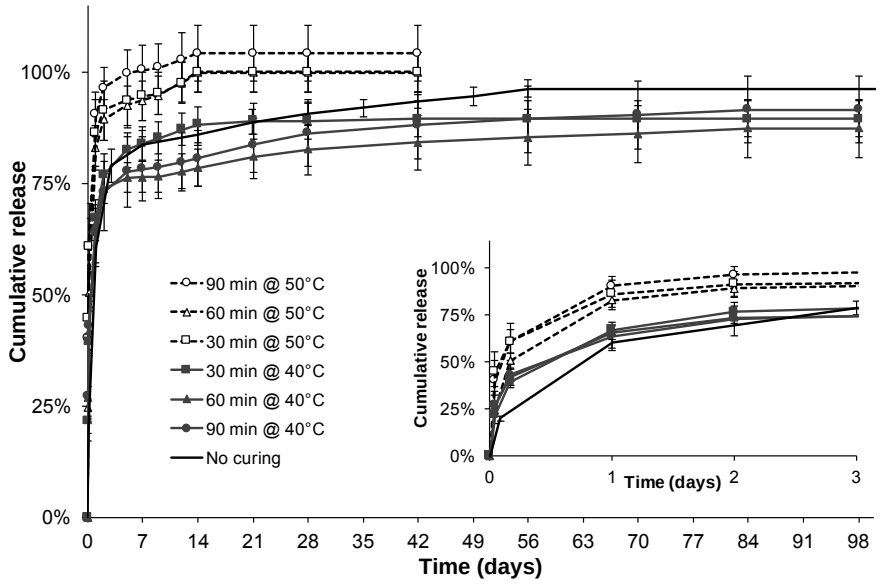

Figure 69 Release profile of 5% OVA-loaded D118-based implants after curing at different conditions

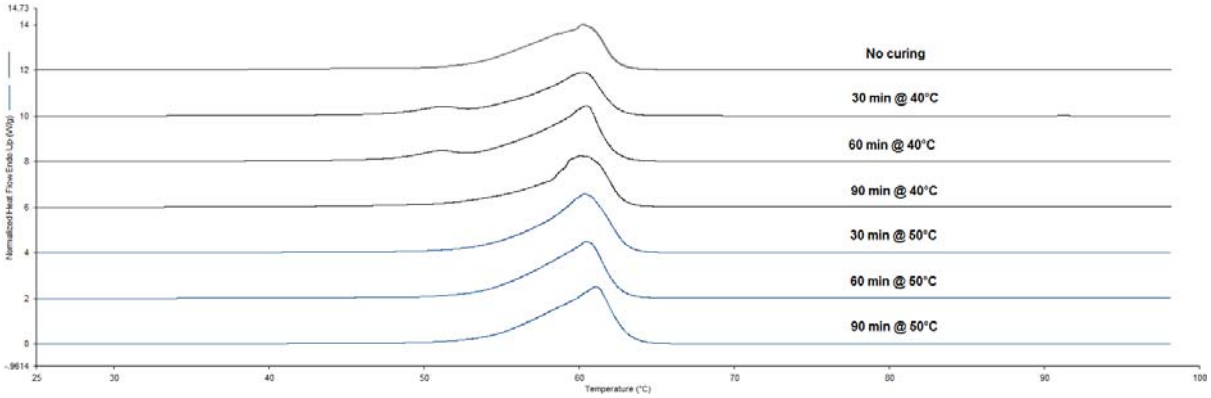

Figure 70 DSC thermograms of DP60-based implants after curing at different conditions

XRPD patterns also showed the formation of a more stable form of the lipid with the progression of curing conditions (Figure 68, right). Without curing, one single reflection was observed, which could be attributed to the α- and β'-forms of the lipid. Under curing, the lipid started to show another reflection corresponding to the more stable crystalline forms β' and β (Sato, 2001). This transformation might correspond to a melt-mediated crystallization that can occur by using curing temperatures close to the melting temperature of the lipid (50°C vs. 58-62°C).

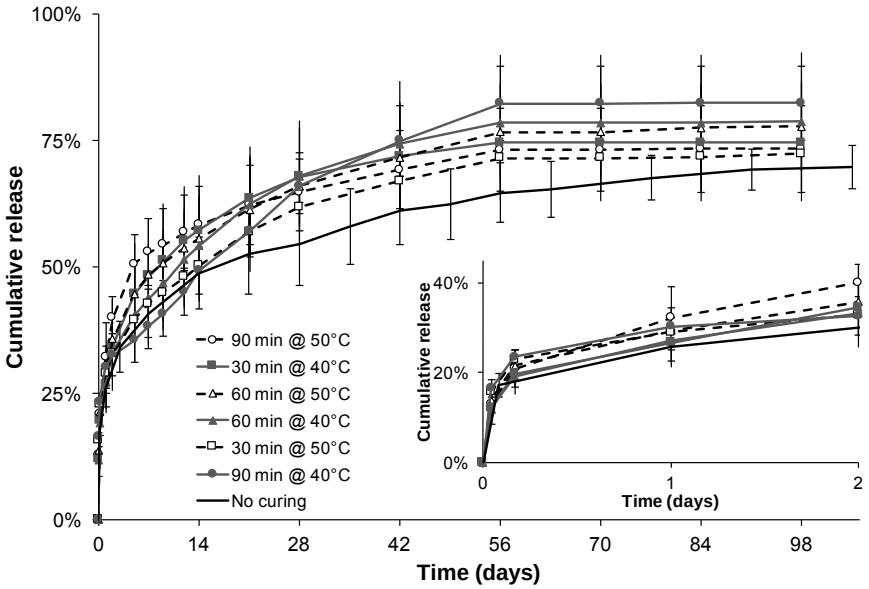

Figure 71 Release profile of 5% OVA-loaded DP60-based implants after curing at different conditions

The dissolution kinetics of the cured DP60-based implants varied less than in the case of the D118-based ones (Figure 71 vs. Figure 69). No change in the burst release was observed, but the diffusion rate during the first month of release was faster for all the cured implants than the non-cured ones (Figure 71). Nonetheless, neither a clear difference nor trend between the curing conditions and OVA release kinetics could have been established in this specific case. It seems that curing at both temperatures created larger channels within the lipidic matrix enabling the faster release of the protein (Kreye and Siepmann, 2011). The use of lower temperatures (i.e. 30°C below the melting temperature) might be suitable to decrease the diffusion rate, if necessary. However, less total cumulative release may be observed in this case, which could be undesirable.

Curing experiments at different temperatures and time intervals, showed crystallinity changes in the matrices, which also had a significant effect on the dissolution profile of OVA. Interestingly, DP60 showed a more stable structure with less polymorphic changes that could avoid unpredictable changes of the prepared implants during manufacturing and storage (Windbergs et al., 2009b).

4.3.2.2 Dip-coating with lipidic materials

Coating of implants can also help to modify the dissolution of OVA, and more specifically for the case of D118, to reduce the diffusion rate obtaining a prolonged release (Guse et al., 2006a; Qian et al., 2002; Raiche and Puleo, 2006). Therefore, lipidic dip-coating of the 10% OVA-loaded D118-based implants was performed. Compritol, Precirol and DP60 were used as coating materials by applying one or two layers of them on the surface of the implants.

These materials were selected for their suitability as hot-melt coating excipients (Jannin and Cuppok, 2013). Thickness of the coating was comparable in all three cases, being slightly bigger for DP60 but more homogenous for Precirol (Figure 72). Both, Compritol and DP60 coatings, presented irregularities and cracks on the surface, caused by rupture of the lipid after it cooled down. This could be caused by poor adhesion forces between the core and the coating material (Achanta et al., 1997). In contrast, the coatings with Precirol were more homogenous and presented higher mechanical stability. Since both lipids, D118 and Precirol, are composed totally or partially by glyceril di- or tristearates, higher compatibility between these might have been achieved. Affinity between the lipids and the creation of physical interactions might have contributed to this (Jannin and Cuppok, 2013).

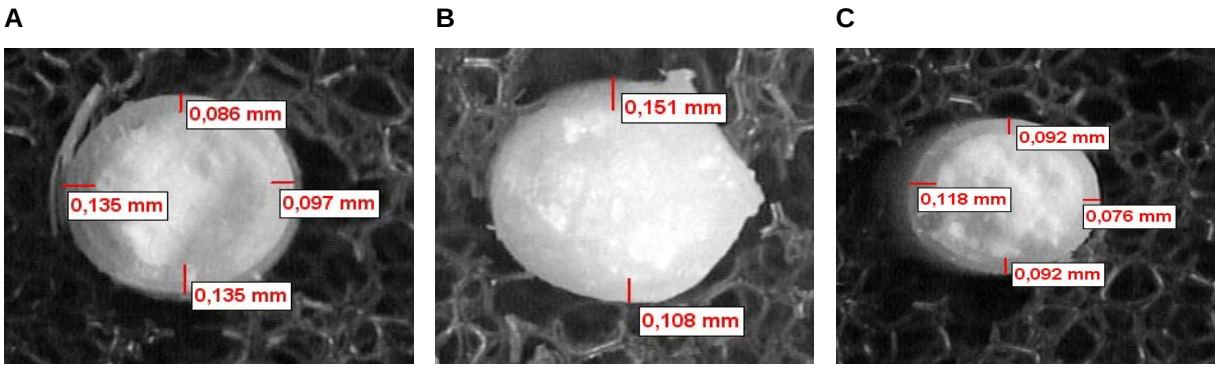

Figure 72 Dip-coated implants with Compritol [A], DP60 [B] and Precirol [C]: 2x dipping with texture analyzer

In agreement with these results, higher variation in OVA dissolution between the coated implants was observed for Compritol and DP60 than for Precirol (Figure 73 and Figure 74 Vs. Figure 75). Moreover, a reduction in the diffusion rate was clearly observed for Compritol and Precirol. However, no clear correlation between the number of layers and the reduction on release rate was observed for the Compritol, whereas for Precirol, there was a clear difference when 1 or 2 layers were applied (Figure 75). If the coating is ruptured, the diffusion of the protein cannot be controlled, and thus greater variations are expected. The use of a more robust process (i.e. spray coating of the molten lipid) could help to optimize this approach, at least for coatings with Precirol (Achanta et al., 1997; Jannin and Cuppok, 2013; Jozwiakowski et al., 1990; Kulah and Kaya, 2011). Nonetheless, achieving the proper coating level might be challenging as well.

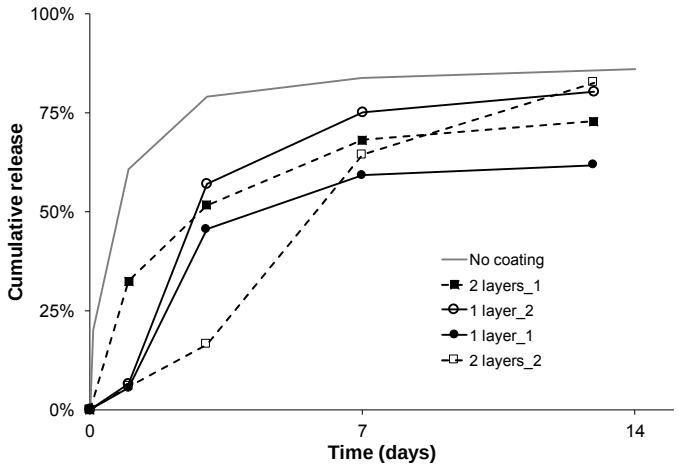

Figure 73 Release profile of 5% OVA-loaded D118-based implants dip coated with 1 [continuous line] or 2 [dashed line] layers of Compritol

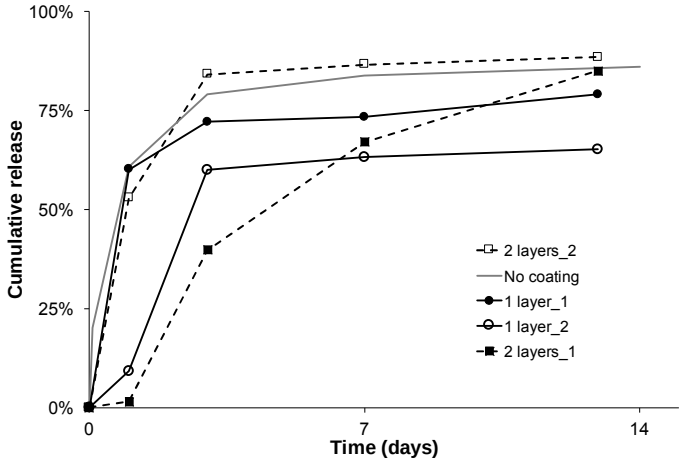

Figure 74 Release profile of 5% OVA-loaded D118-based implants dip coated with 1 [continuous line] or 2 [dashed line] layers of DP60

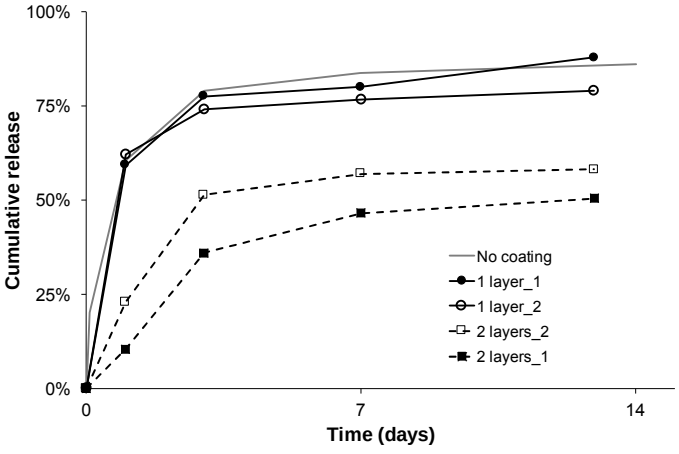

Figure 75 Release profile of 5% OVA-loaded D118-based implants dip coated with 1 [continuous line] or 2 [dashed line] layers of Precirol

4.3.3 Effect of terminal sterilization on lipid-based implants

As already mentioned in chapter 3.4.3, sterility of parenterals should be considered early during product development to stablish the best process that ensures sterility without hindering the performance of the formulation (Burgess et al., 2004; Volland and Wolff, 1994). For lipid-based formulations either aseptic manufacturing (Elkharraz et al., 2006; Kathe et al., 2014; Wong et al., 2008) or terminal sterilization by autoclaving (Kuntsche and Bunjes, 2007; Negi et al., 2014; Wong et al., 2008) have been reported as suitable methods to ensure sterility of the formulations. Gamma-irradiation might be suitable, but the creation of free radicals associated to this process, could generate degradation and/or rearrangements in the lipid structure (Kathe et al., 2014). Nonetheless, since the implants are dry and their water content is expected to be very low, mobility of the molecules is more difficult during the irradiation process; thus, the creation of free radicals might be limited. Therefore, the suitability of gamma-irradiation as terminal sterilization technique was assessed for the D118- and DP60--based implants prepared. As it was done for the PLGA-based implants, the lipidic ones were packaged in sealed blisters, with or without dry ice (HTS and LTS, respectively), and exposed to an irradiation dose of ≥25 kGy, which is enough to guarantee sterility (Montanari et al., 2001). The evaluation of the implants was done at a physicochemical level and not a microbiological one.

The bulk lipid powders were also irradiated under the same conditions to evaluate possible polymorphic changes. Gamma-irradiation decreased slightly the melting temperature for both, D118 and DP60 powders (Figure 76 and Figure 77). In the case of D118, this change was accompanied by small decrease of the enthalpy of fusion as well (Figure 76), whereas in the case of DP60 it was the opposite and the ΔH increased (Figure 77). For both conditions tested the Tm of D118 was comparable, but the ΔH decreased more under HTS conditions than the LTS ones. For DP60, both the ΔH and Tm, were higher under LTS than HTS conditions, indicating that the dry ice might have prevented some mobility of the molecules. The differences between the two lipids could be explained by differences on their rearrangements. Most probably, D118 rearranged again on its β-form, which is the more stable one, but with some loss of crystallinity during this process (Sato, 2001). On the contrary, since DP60 is a mixture of glycerides, the distribution of these components might have changed creating a closer distribution of the different melting peaks caused by the formation of crystal structures (Reitz and Kleinebudde, 2007). In general, these findings indicate that the energy inherent to the gamma irradiation process was able to create small rearrangements within the structure of the lipids, changing their melting and crystallinity degree.

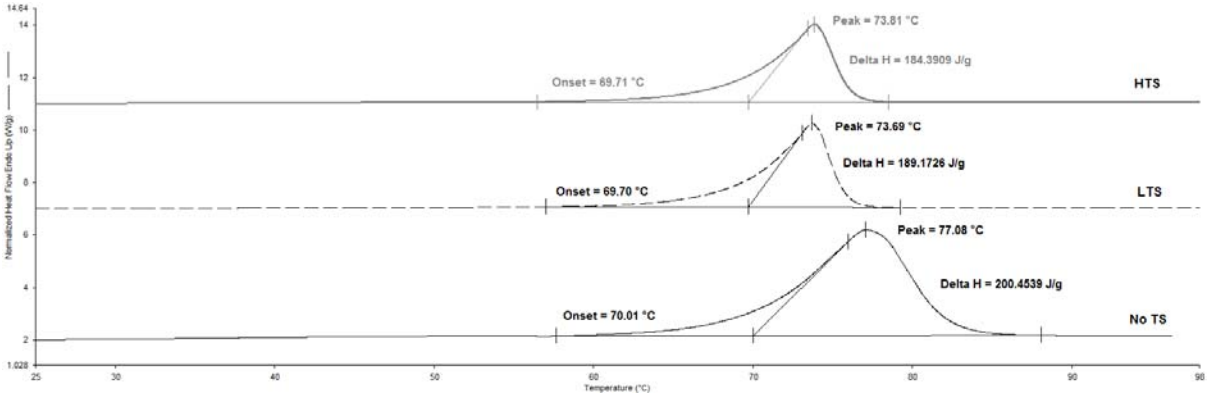

Figure 76 DSC thermograms of D118 (powder) before and after terminal sterilization

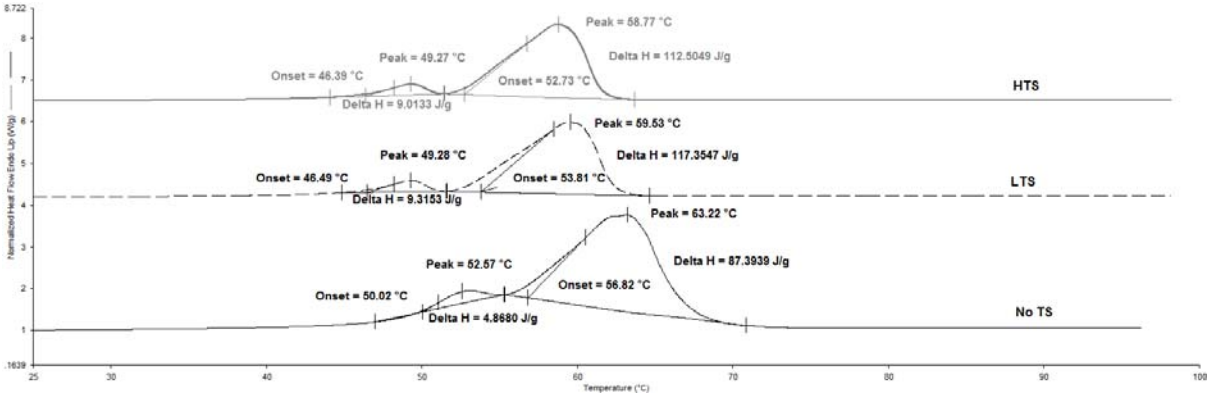

Figure 77 DSC thermograms of DP60 (powder) before and after terminal sterilization

D118-based implants also showed a decrease in crystallinity after irradiation, but the changes in Tm were not the same for the two conditions used: for HTS it decreased, whereas for LTS it increased (Figure 78). Nonetheless, it indicates that a rearrangement of the lipid structure occurred, at least to a certain extent, also in this case. For the DP60-based implants the Tm decreased after irradiation, while the ΔH did not change under LTS but it increased under HTS (Figure 79). Also in this case, the use of cooling agents during irradiation helped to prevent bigger transformations within the lipid matrix by reducing the mobility of the molecules.

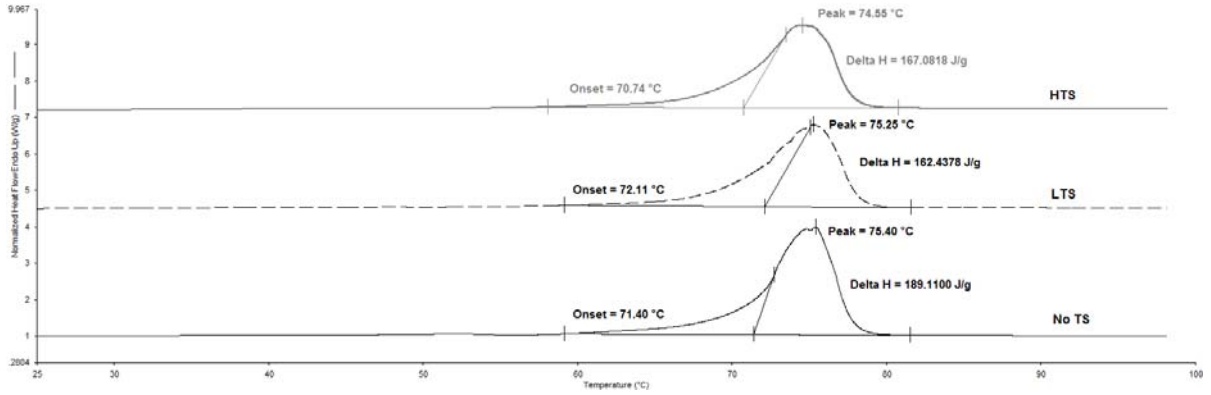

Figure 78 DSC thermograms of D118-based implants before and after terminal sterilization

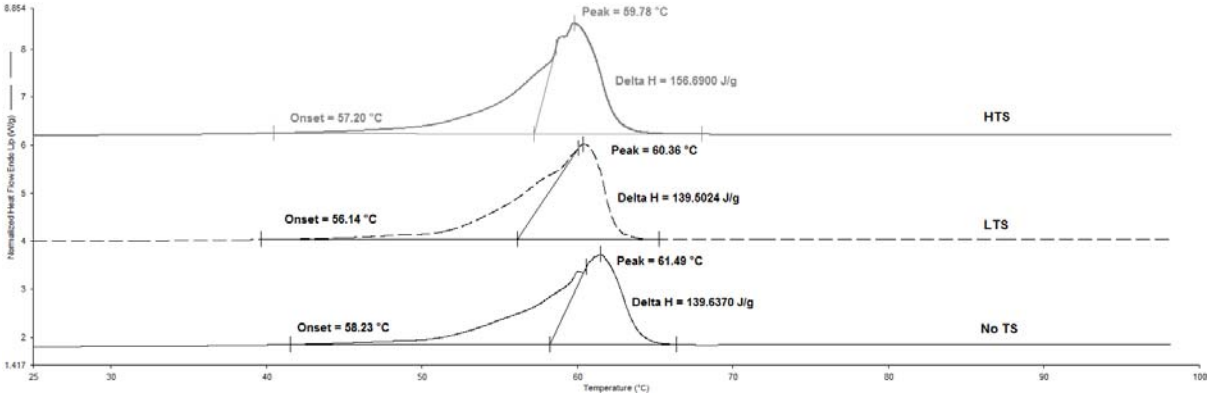

Figure 79 DSC thermograms of DP60-based implants before and after terminal sterilization

Protein hydrophobicity increased after gamma irradiation, being more noticeable for the implants irradiated under HTS than LTS, probably caused by the uncontrolled temperature during sterilization (Figure 80). An increase in OVA's hydrophobicity can be explained by the disruption of the ordered structure of the protein during sterilization that causes exposure of its hydrophobic regions (Moon and Song, 2001). These changes were more visible for the DP60-based implants than for the D118-ones. This could be attributed to the lower melting temperature of DP60 when compared to D118; a higher molecular mobility could be reached if the temperatures during the sterilization process are too high. Furthermore, due to this increased mobility, additional interaction between the lipid and OVA might have occurred, which could have impact the tertiary structure of the protein as well (Rothen-Weinhold et al., 1999).

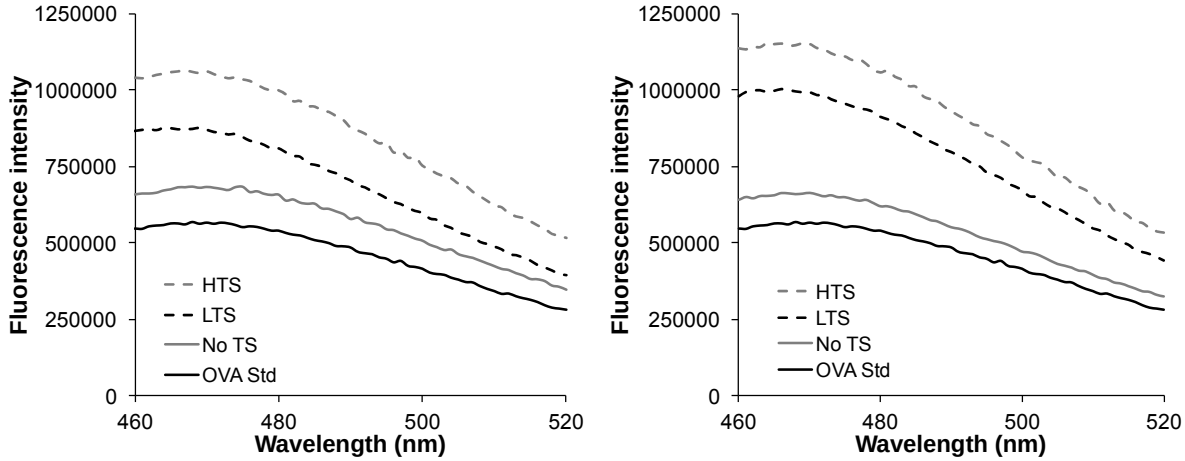

Figure 80 Fluorescence emission spectra of OVA extracted from D118-based [left] and DP60-based [right] implants before and after terminal sterilization

Gamma-irradiation increased the burst release and accelerated the dissolution of OVA from D118-based implants (Figure 81, gray lines), which was unexpected since OVA

hydrophobicity increased (i.e. lower water solubility) and the crystallinity of the lipid matrix decreased (i.e. stronger physical interaction with the protein). Nonetheless, it might be possible that the rearrangements that occurred within the matrix led to the formation of inner and bigger channels, that allowed the influx of water and the efflux of the protein. Moreover, the standard deviation was also increased for these samples, probably because the heterogeneous rearrangements of the lipid matrix along the implant occurred. For the case of DP60-based implants, the non-irradiated samples and the ones irradiated under LTS presented comparable dissolution kinetics (Figure 81, black lines). Although there was an increase in protein's hydrophobicity after irradiation, the thermal properties of these samples were comparable, indicating that no big rearrangements of the lipidic structure occurred; thus, no big differences in the diffusion rate were expected. On the contrary, implants irradiated under HTS conditions showed a decrease in the diffusion rate that could have been caused by the changes in OVA's tertiary structure and possible interactions between the protein and the lipid, as stated before. These two effects contributed to decrease the diffusivity of the protein in the release medium. It is worth to mention that in all cases the remaining fraction of protein was extracted from the implants, indicating that insoluble aggregates were not formed during or after the irradiation process.

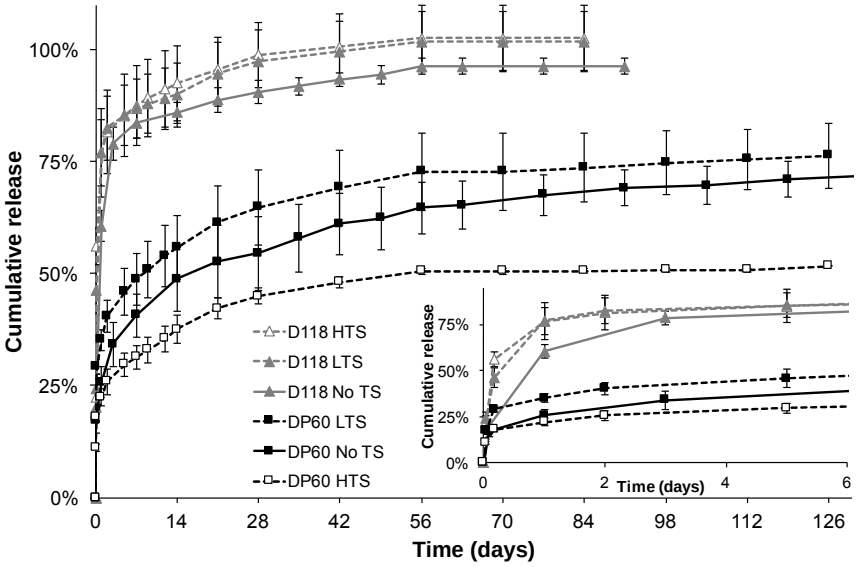

Figure 81 Release profile of 5% OVA-loaded D118-based [gray lines] and DP60-based [black lines] implants before and after terminal sterilization

Implants prepared with blends of DP60 and PEG 4000 or PEG 6000 were also exposed to irradiation. Since PEG is a more hydrophilic molecule than DP60, differences in molecular mobility and/or interaction with the protein may be observed. For the implants containing PEG 4000 as co-excipient, the dissolution was slower after irradiation, specially during the

first two weeks of release, and could be ranked as No TS > LTS > HTS (Figure 82, black lines), which correlated well with the changes in OVA's hydrophobicity (Figure 83, black lines). Thus, in this case the diffusion of the protein was delayed probably by its change in solubility but also by changes in PEG properties. PEG could have undergone radiolytic degradation with changes on its hydrophilicity and mechanical properties impacting the dissolution from implants (Bhatnagar et al., 2016). Interestingly, for the implants containing PEG 6000 the release was faster for the implants irradiated under HTS than the non-irradiated and the ones under LTS conditions, ranked as HTS > No TS > LTS (Figure 82, gray lines). These last ones released the slowest most probably due to the higher increase in protein's hydrophobicity (Figure 83, gray lines) and possible changes within the lipidic structure, which also created higher variation between the triplicate. It is possible that the higher energy presented with the HTS conditions have caused bigger rearrangements of the implant microstructure creating larger pores that allowed diffusion of the PEG and OVA molecules. Furthermore, the hydrophobicity of OVA from the HTS-irradiated implants was slightly lower than the LTS-ones, which could also explain the differences between these two conditions (Figure 83, gray lines).

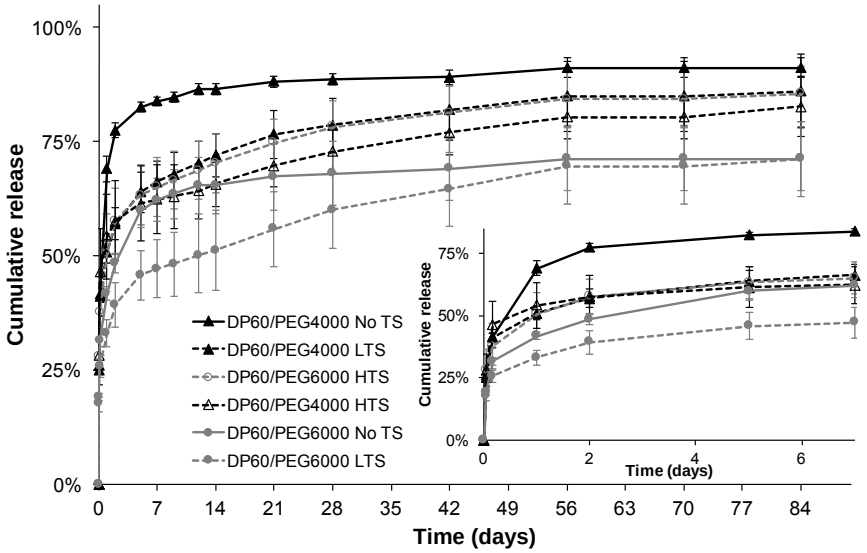

Figure 82 Release profile of 5% OVA-loaded DP60/PEG6000-based [gray lines] and DP60/PEG4000-based [black lines] implants before and after terminal sterilization

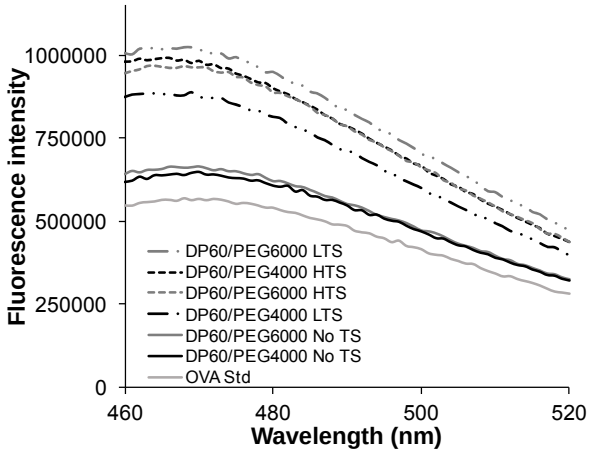

Figure 83 Fluorescence emission spectra of OVA extracted from DP60/PEG6000-based and DP60/PEG4000-based implants before and after terminal sterilization

Gamma-irradiation had an impact on implant characteristics, being more perceptible when non-controlled conditions of temperature were used (i.e. HTS vs. LTS). Although the protein hydrophobicity increased after sterilization, all the protein was recovered after release test indicating that there was no formation of insoluble aggregates. A deeper understanding on the microstructure changes caused by irradiation, together with evaluation of radical formation, might help to define the best sterilization conditions for the lipid-based implants. As in the case of PLGA-based implants (see 3.4.3), the implementation of a low bioburden approach may be suitable to obtain a sterile formulation without impacting the desirable performance.

4.4 Design of experiments to optimize the release of OVA from lipid-based implants

To build quality by design (QbD) during the development of a pharmaceutical product has become an important concept in the pharmaceutical industry (Yu et al., 2014). Regulatory entities (i.e. EMA and FDA) encourage the adoption of QbD concepts with the aim to develop a high-quality product while reducing the costs of unnecessary experiments or product characterization (Shin et al., 2011; Sonam et al., 2014; Yu et al., 2014). An important tool of the QbD to better understand the product and process being developed, is the design of experiments (DoE). This tool not only allows the minimization of resources required to evaluate all the critical parameters, but it also permits to evaluate interactions by seeing how different factors, while being together, affect the responses (i.e. product/quality attributes) (Yu et al., 2014). Different DoE approaches can be applied to the product/process development. One of them is the Taguchi method which reduces the number of experimental runs required to study the relevant parameters, by using orthogonal arrays (e.g. 27 runs instead of 81 runs for evaluation of 4 parameters at 3 levels) (Bolboacă and Jäntschi, 2007). This design has been applied before to other dosage forms to understand the effect of process/materials variables and optimize a formulation (Kumar et al., 2016; Park et al., 2010; Shin et al., 2011; Sonam et al., 2014). Therefore, this methodology was applied to optimize the dissolution kinetics of the lipid-based implants in order to obtain a long and sustained release formulation of OVA.

4.4.1.1 Taguchi design

A Taguchi design with four independent process or formulation variables at three levels was design (Table 10). All the other process parameters such as blending time and technique, extrusion method and implant characterization was kept constant for all the formulations prepared.

Table 10 Levels of independent factors

Independent factors		Units	Levels of factors		
			1	**2**	**3**
A	**Curing temperature**	ºC	40	45	50
B	**Matrix composition**	-	D118	DP60	DP60/D118 (50:50)
C	**Curing time**	*min*	30	60	90
D	**Protein loading**	%	5	7.5	10

An orthogonal array with 27 different formulations (L_{27}; F1 – F27) (Table 11) was selected to evaluate the influence of the selected factors and their levels. All the statistical evaluation, including the design of the orthogonal array, was used using JMP® Pro software, version 11.0.0.

Table 11 L_{27} Orthogonal array of experiments

Trial No./ Formulation	Levels of factors			
	Curing temp (ºC)	Matrix	Curing time (min)	Protein loading (%)
F1	40	D118	30	5
F2	40	D118	60	7.5
F3	40	D118	90	10
F4	40	P60	30	7.5
F5	40	P60	60	10
F6	40	P60	90	5
F7	40	DP60/D118	30	10
F8	40	DP60/D118	60	5
F9	40	DP60/D118	90	7.5
F10	45	D118	30	7.5
F11	45	D118	60	10
F12	45	D118	90	5
F13	45	P60	30	10
F14	45	P60	60	5
F15	45	P60	90	7.5
F16	45	DP60/D118	30	5
F17	45	DP60/D118	60	7.5
F18	45	DP60/D118	90	10
F19	50	D118	30	10
F20	50	D118	60	5
F21	50	D118	90	7.5
F22	50	P60	30	5
F23	50	P60	60	7.5
F24	50	P60	90	10
F25	50	DP60/D118	30	7.5
F26	50	DP60/D118	60	10
F27	50	DP60/D118	90	5

Since the main objective of the DoE was to optimize the dissolution of the implants, the following outcomes were selected as responses:

- Burst release
- Cumulative release after 1 week
- Diffusion rate during the initial rapid diffusion phase
- Area under the curve (AUC) from the first month of release

4.4.1.2 Array response analysis

All the formulations were well processable with the mini-ram extruder and presented good mechanical stability to be handled afterwards. The dissolution profiles of the 27 formulations are presented in three different figures grouped per matrix composition due to the larger number of runs (Figure 84, Figure 85 and Figure 86).

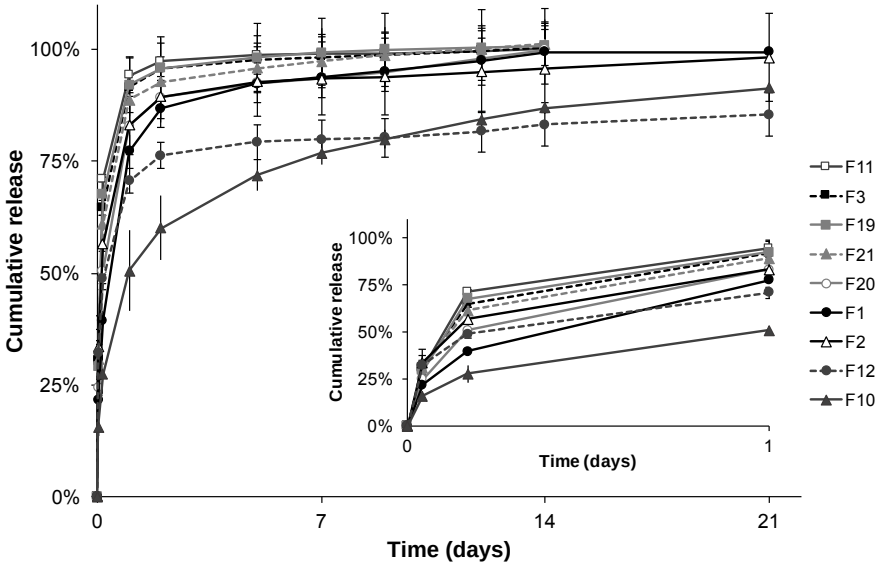

Figure 84 Release profile of D118-based implants part of the L_{27} orthogonal array (refer to Table 11 for formulation characteristics)

Differences in the burst release, dissolution rate and total amount released among all the formulations were observed. Although the interpretation of the results requires the respective statistical evaluation of the Taguchi model, some general conclusions were drawn based on observations of the release profiles. The total dissolution time varied between 14 and 98 days, being the D118-based implants the fastest. F11 was the fastest-releasing formulation whereas F16 was the slowest. The burst release was in overall higher for the D118-based implants (16-32%) (Figure 84), followed by the DP60-based ones (15-22%) (Figure 85) and the DP60/D118-based formulations (14-15%) (Figure 86). In general, the implants loaded with 10% protein were the ones releasing faster due to the bigger pores created that allowed

the faster diffusion of the remaining protein fraction (Kreye et al., 2011b). For the DP60-based implants a clear correlation between protein loading and burst release and diffusion rate was observed (Figure 85). Whereas for the other two matrices this correlation was not clearly evidenced, probably caused by the influence of the other processing factors (i.e. curing).

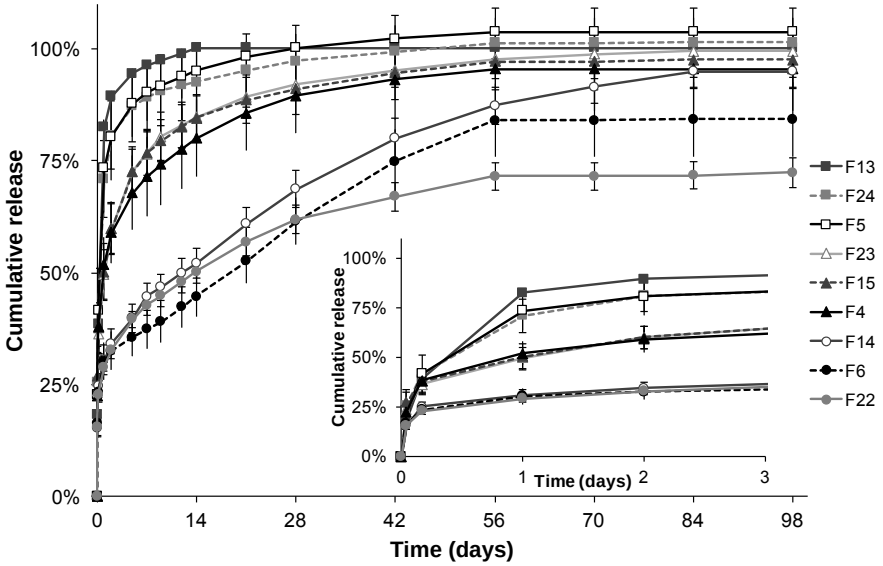

Figure 85 Release profile of DP60-based implants part of the L_{27} orthogonal array (refer to Table 11 for formulation characteristics)

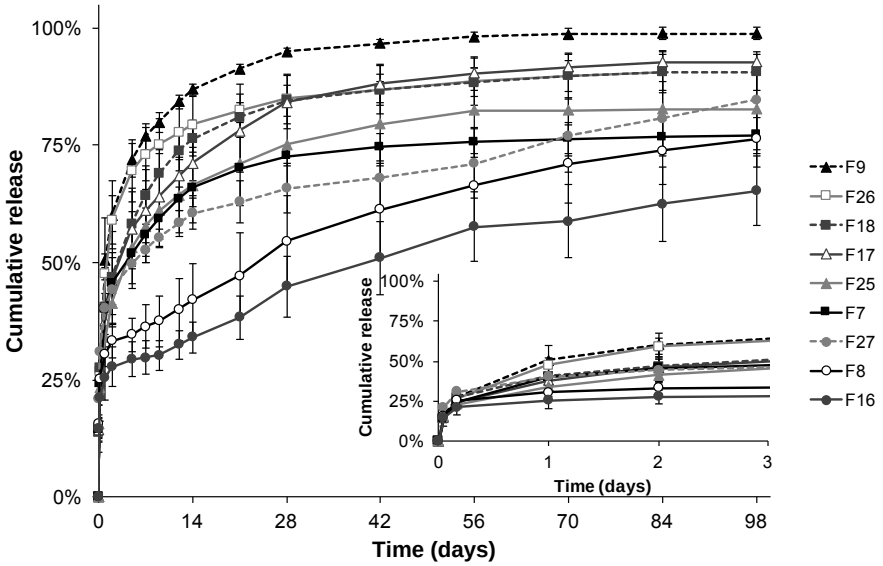

Figure 86 Release profile of DP60/D118-based implants part of the L_{27} orthogonal array (refer to Table 11 for formulation characteristics)

The different responses were analyzed by signal to noise (S/N) ratio to establish the significance of each factor evaluated. The effect of the factors at their different levels on the

responses was evaluated by plotting the main effect plot for S/N ratio (mean S/N ratio vs. each factor at each level) (Figure 87). The effects on the responses are summarized in Table 12. In general, the fastest-releasing formulation with the higher burst release and faster diffusion rate is obtained by loading 10% of OVA into the D118 matrix, and curing these implants at 50°C for 90 min. In contrast, the slowest-releasing formulation with a low burst and slow diffusion rate is obtained by loading 5% of OVA into the DP60/D118 matrix and applying 30 min of curing at 45°C (same as F16).

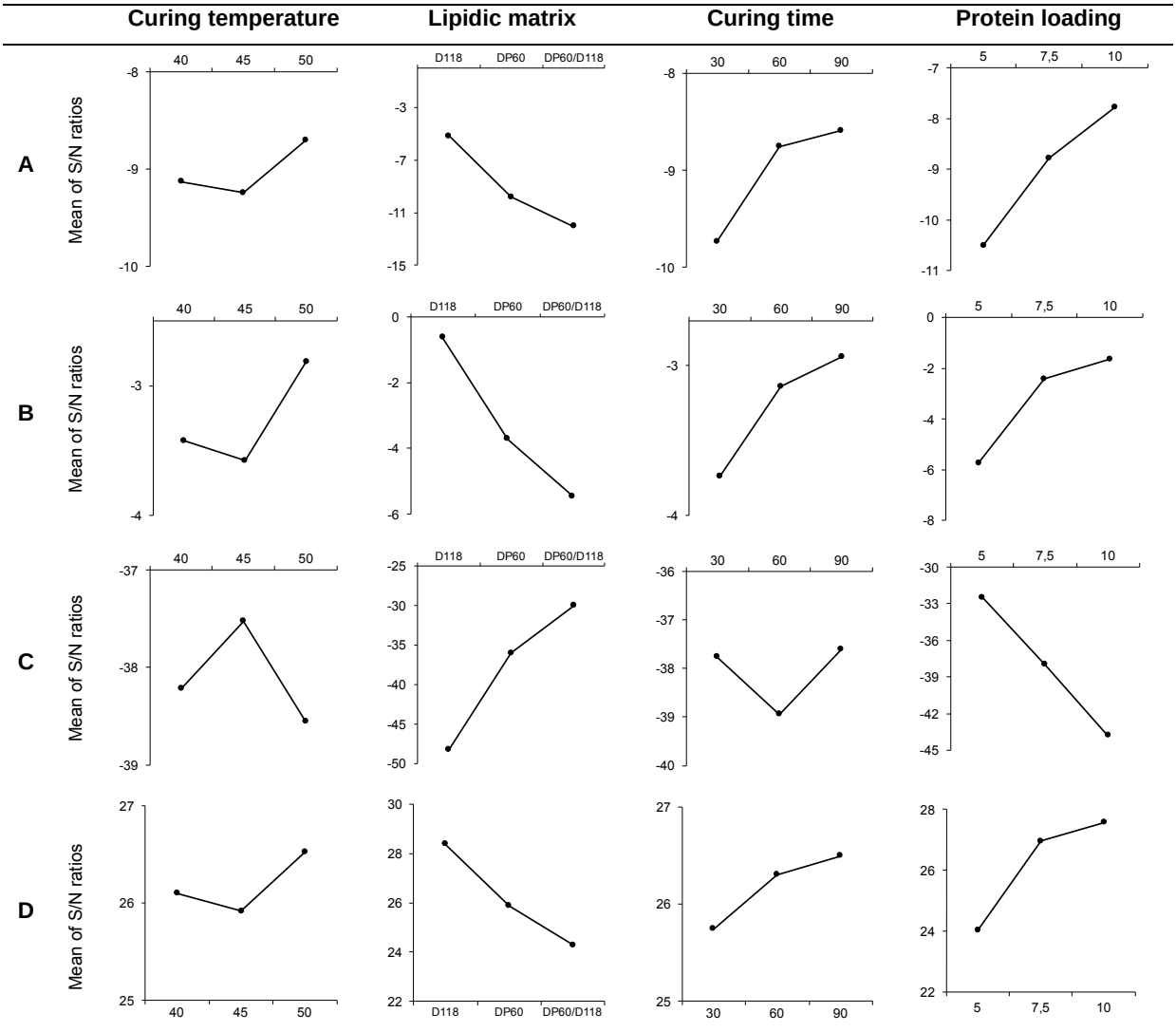

Figure 87 Effect of factors on responses: burst release [A], cumulative release after 7 d [B], diffusion rate [C] and AUC (up to 28 d) [D]

Table 12 Summary of effects of factors on responses

Response	Factors			
	Curing temp. (°C)	Matrix comp.	Curing time (min)	Protein load. (%)
Higher burst release	50	D118	90	10
Lower burst release	45	DP60/D118	30	5
Higher cum. Rel. after 7d	50	D118	90	10
Lower cum. Rel. after 7d	45	DP60/D118	30	5
Faster diffusion rate	50	D118	60	10
Slower diffusion rate	45	DP60/D118	30	5
Larger AUC	50	D118	90	10
Shorter AUC	45	DP60/D118	30	5

The significance of each factor was determined statistically by performing analysis of variance (ANOVA) on S/N ratios of every response (Table 13, Table 14, Table 15 and Table 16). Matrix composition and protein loading were the factors having a greater impact on the responses ($p \leq 0.0002$). Thus, dissolution profile is mainly controlled by these two parameters, and to a lesser extent by curing temperature and curing time.

Table 13 ANOVA table for S/N ratio of the burst release

Source	DF	Sum of Squares	Mean Square	F Ratio	Prob > F
Curing Temperature	2	1.431		0.502	0.614
Matrix composition	2	219.646		77.051	<.0001*
Curing time	2	6.849		2.403	0.119
Protein loading	2	34.070		11.952	0.0005*
Model	8	261.997	32.750	22.977	
Error	18	25.656	1.425		
C. Total	26	287.653			<.0001*

Table 14 ANOVA table for S/N ratio of the cumulative release after 7 d

Source	DF	Sum of Squares	Mean Square	F Ratio	Prob > F
Curing Temperature	2	2.924		0.504	0.612
Matrix composition	2	107.634		18.548	<.0001*
Curing time	2	3.095		0.533	0.596
Protein loading	2	85.064		14.658	0.0002*
Model	8	198.717	24.840	8.561	
Error	18	52.228	2.902		
C. Total	26	250.946			<.0001*

Table 15 ANOVA table for S/N ratio of the diffusion rate

Source	DF	Sum of Squares	Mean Square	F Ratio	Prob > F
Curing Temperature	2	4.942		0.198	0.822
Matrix composition	2	1548.050		62.056	<.0001*
Curing time	2	9.730		0.390	0.683
Protein loading	2	577.662		23.156	<.0001*
Model	8	2140.385	267.548	21.450	
Error	18	224.516	12.473		
C. Total	26	2364.900			<.0001*

Table 16 ANOVA table for S/N ratio of the AUC (up to 28 d)

Source	DF	Sum of Squares	Mean Square	F Ratio	Prob > F
Curing Temperature	2	1.725		0.398	0.678
Matrix composition	2	76.321		17.610	<.0001*
Curing time	2	2.759		0.637	0.541
Protein loading	2	64.664		14.920	0.0002*
Model	8	145.468	18.184	8.391	
Error	18	39.005	2.167		
C. Total	26	184.474			<.0001*

4.4.1.3 Formulation optimization and characterization

Based on the previous evaluation, a long and sustained formulation would be obtained by preparing an DP60/D118-based implant with 5% OVA. Moreover, the optimum factor level was indicated to be A1B3C2D1 considering “nominal is best” responses of S/N ratios. Hence, a formulation of 5% OVA-loading DP60/D118-based implants with further curing for 60 min at 40°C was prepared. Nonetheless, since the curing conditions have a lesser effect on the dissolution, the same formulation but without curing was also prepared for comparison purposes.

The dissolution of these implants showed a prolonged release of OVA during 56 and 126 days for the non-cured and the cured formulations, respectively (Figure 88). Burst release (~16%) and the total cumulative release (≥82%) were comparable for both formulations, indicating that curing did not affect these parameters. The diffusion rate was slightly faster for the non-cured formulation than the cured one. This can be attributed to changes in the pore size. Curing might decrease the size of the channels available for the drug to diffuse out, delaying its release (Even et al., 2015; Kreye and Siepmann, 2011).

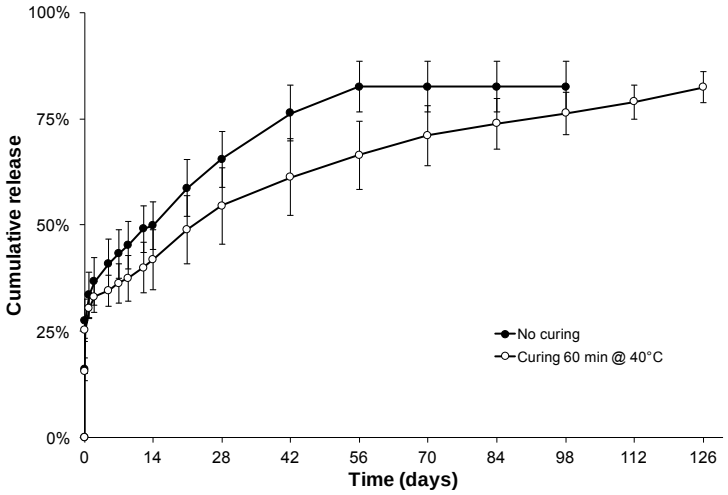

Figure 88 Release profile of DP60/D118-based implants selected as optimized formulations (verification result)

Additionally, the fluorescence spectra of these two formulations showed that both presented higher hydrophobicity than the standard (Figure 89), probably caused by interactions of OVA with the lipid-matrix (Mohl and Winter, 2004). However, these interactions did not affect the complete recovery of the protein after extraction of the remaining fraction. A slightly higher intensity was observed for the cured implants, which might have been caused by the aggregating effect (i.e. formation of hydrophobic structures) that temperature has on OVA (Kawachi et al., 2013).

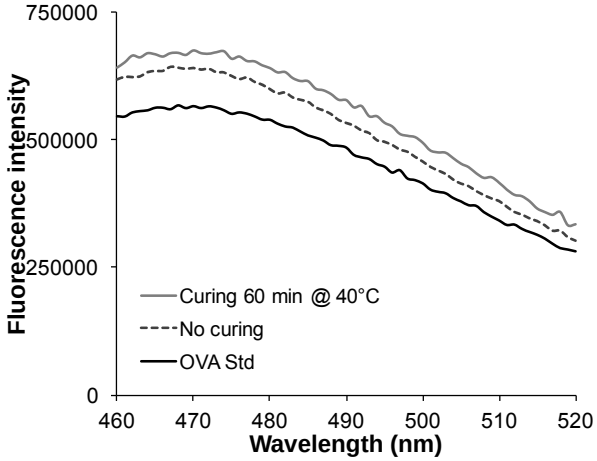

Figure 89 Fluorescence emission spectra of OVA extracted from DP60/D118-based implants selected as optimized formulations

The thermograms of the implants indicated that the two lipids that formed the matrix did not mix into one single phase (Figure 90). In the case on the non-cured implants three melting peaks where observed that correspond to the two peaks characteristic of DP60 and the one

of D118 at a higher temperature. In the case of the cured implants one of the DP60 melting peaks did not appear, but an additional melting peak close to the D118 one was observed, which could be assigned as the β'-metastable form of this lipid (Schulze and Winter, 2009). This indicates that the curing induced polymorphic changes in the matrix which could explain the differences in release observed. These changes should be considered carefully because they could impact the performance of the formulation and/or the protein stability after certain storage time. The use of a different extruder that allows mixing (i.e. twin-screw extruder) could help to improve the miscibility of the matrix solving this issue. However, shear forces might impair the performance of the formulation as well. Therefore, another DoE would be advisable to assess the impact of the new process conditions.

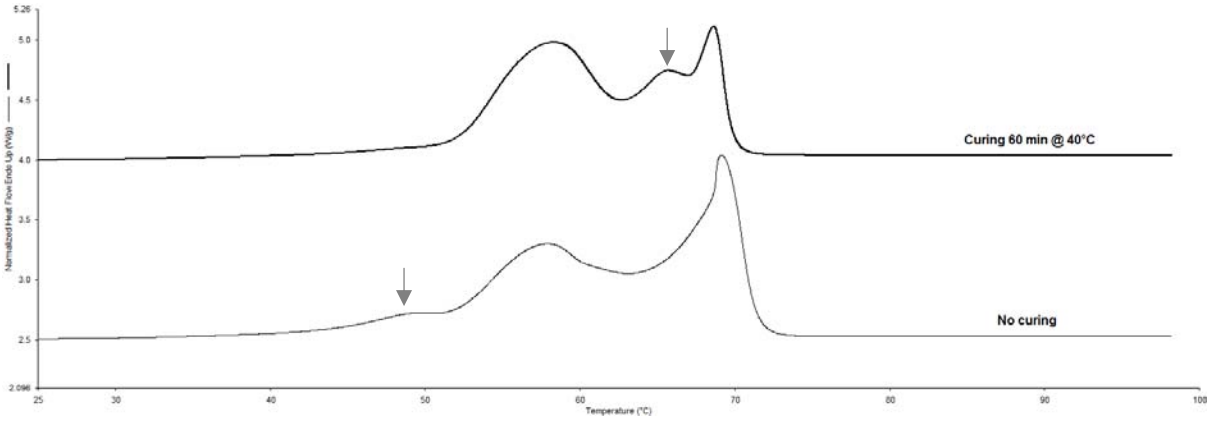

Figure 90 DSC thermograms of DP60/D118-based implants selected as optimized formulations

The Taguchi design applied allowed the identification of critical parameters on the dissolution of OVA-loaded lipid-based implants prepared with the mini-ram extruder. Matrix composition and protein loading were the factors with a greater impact on the responses. An optimized formulation was prepared using the results gathered with this DoE. The implants were able to release constantly OVA for a long period of time.

4.5 Conclusions

The release of OVA was dependent on the crystallinity degree of the lipidic matrix used. The hot-melt extrusion process influenced the thermal properties of all the matrices, indicating a recrystallization of the stable β-form from the α-form after melting occurred during the production process. With the use of a more amorphous matrix, like DP60, the release of OVA was prolonged because of possible physical interactions between the lipid and the protein. In contrast, more crystalline and homogenous matrices, like D114 and D118, presented a fast protein release probably because the presence of crystallites within the matrix led to a higher anisotropy of OVA distributions and, thus, rapid dissolution. An increase in protein loading led to faster release in all the matrices evaluated, which might be attributed to a higher burst release that causes an increase in implant porosity. When a smaller protein was loaded into these lipidic materials, longer releases times were observed for the D118- and DP60-based implants, even though their mechanical properties were comparable. The differences in the molecular weight of the proteins could explain this observation. With a smaller protein, smaller pores are formed inside the matrix, which can decrease the diffusion of water into the implant, and hence, slower the diffusion rate of the protein.

The inclusion of PLA (20%) into the D118-based implants prolonged the release of OVA from 1 to 4 weeks. Because this polymer has a long degradation time, no acidic microclimate was formed within the implant, so the protein integrity was not affected; the diffusivity of OVA was decreased thanks to the impermeable barrier formed by the polymer. In contrast, the use of PEG as co-excipient accelerated the release of OVA from DP60-based implants, with a dependence on its molecular weight: higher diffusion rates during the first 21 days of release were obtained when lower molecular weight PEG was used. In this case, PEG created pores in the matrix by dissolving rapidly in the release medium, allowing the protein to diffuse out. The release from DP60-based implants was also faster when binary lipid blends were used. The speed was related to the fatty acid chain length of the second lipid (i.e. lipophilicity): by being shorter the release was faster. Nonetheless, thermal characterization of these blends indicated that the lipids did not mixed at a molecular level, presenting some phase separation. In this case, it would be recommended to use an extruder that compounds the materials while they are in their molten state. This could avoid changes on the lipidic microstructure after storage.

Curing at different temperatures and time intervals, showed crystallinity changes in the matrices, which also had a significant effect on the dissolution profile of OVA. All the cured DP60-based implants and the D118-ones cured at 50°C presented a faster dissolution. This could be attributed to the creation of larger pores or channels that increased the diffusivity of

OVA. In the case of the D118-based implants cured at 40°C, the protein was diffuse out slower than the non-cured ones probably because a denser matrix was created by partial melting of the lipid. Interestingly, DP60 showed a more stable structure with less polymorphic modifications that could avoid unpredictable changes of the prepared implants during manufacturing and storage. In general dip coating with other lipid materials, especially with Precirol, decreased the burst release of D118-based implants. However, irregularities and cracks of the coating led to big variations between replicates. Thus, this process has still room for improvement.

Terminal sterilization with gamma-irradiation influenced the characteristics of the implants by increasing the hydrophobicity of the protein, by altering the release kinetics of the protein and inducing rearrangements of the lipidic microstructure. Using a cooling agent during the sterilization process decreased these changes, since it reduced the mobility of the molecules during the irradiation. Additional characterization of the sterile implants after storage and the evaluation of a low bioburden process should be considered to optimize this step.

Matrix composition and protein loading were the most critical factors on the dissolution of OVA as indicated by the Taguchi DoE. Curing conditions had also an impact, but they were not as significant as the former parameters. This DoE guided the preparation of an optimized implant formulation, which released OVA constantly for over 18 weeks.

5. Summary

Different drug delivery systems have been developed for peptides and proteins, with special interest on those that allow sustained parenteral release; they can prolong protein circulation, resulting in better therapeutic results and higher patient compliance. However, many of the manufacturing methods used involve conditions that can be detrimental for these molecules, such as the use of organic solvents, pH gradients, reduced pressure or heat. Besides, obtaining the desired formulation performance might be difficult since the dissolution profile might be far from optimal, or because the integrity of these bio-macromolecules cannot be preserved within the matrix. Thus, the development of these systems has followed a complex and challenging route, which have resulted in long development periods and few commercialized products. Therefore, gathering additional understanding of these systems and defining key parameters that impact the performance of them, is important to accelerate and assist the development of parenteral sustained release systems.

This work focused on the development of biodegradable implants for protein delivery, using ovalbumin (OVA) as acid-labile model protein. Hot melt extrusion (HME) was selected as the manufacturing method, since it does not involve the use of solvents and the protein can be incorporated on its more stable dry state, avoiding the creation of interfaces that compromise protein stability. Nonetheless, the use of high temperatures and presence of shear forces might impact protein stability. Therefore, the feasibility of HME to prepare OVA-loaded implants was investigated. With this purpose, a mini-ram extruder (syringe-die device) was used as a rapid screening tool. Moreover, two types of biodegradable matrices (PLGA- and lipid-based) were used to assess differences on formulation performances, with special emphasis on dissolution and protein stability.

OVA was stable during extrusion as indicated by SEC-HPLC, FTIR, CD and fluorescence spectroscopy. It showed comparable behaviors when analyzed as received and after extraction from the freshly prepared implants. This was observed for the two types of matrices used, indicating that they might have a protective effect on the protein. As they melt or soften during the process, they may act as a “protective cushion” against heat and shear forces.

In the case of PLGA-based implants, OVA release was characterized by a low burst and a slow release up to day 21 which plateaued thereafter, resulting in incomplete release for all evaluated protein loadings. The percolation threshold of this matrix was reached at loadings ≥25%, but cumulative releases did not reach 100% either. Release incompleteness was accompanied by the formation of an insoluble residual mass. Characterization of this mass indicated that it consisted of non-covalent protein aggregates and polymer, where ovalbumin was ionically bound as the pH inside the degrading matrix felt below the pI of the protein. Exposure to the acidic microclimate created by the degradation process of the matrix induced structural changes in OVA by increasing its hydrophobicity and its β-sheet content. Furthermore, the autocatalytic rate of hydrolysis of PLGA was decreased in the presence of OVA since the protein has certain buffering capacity. These changes increased the likeliness of protein-protein ad protein-polymer/oligomer interactions.

To create a viscous environment within the implant, PVP and Poloxamer were used as protein co-excipients. For this, these compounds were dissolved together with the protein and freeze-dried prior blending with the polymer and extrusion. The release of OVA during the first days was increased, indicating that these excipients effectively decreased the adsorption of the protein on the PLGA. Nonetheless, they were not able to control the acidic inner pH and thus, OVA aggregation was not prevented and release incompleteness was still observed. Furthermore, there were changes in OVA secondary structure caused by the freeze-drying process and the interaction of the co-excipients and the protein when they were in solution. The optimization of the freeze-drying conditions and co-excipient: protein ratio could improve the stability of the protein. However, strategies to control the acidic microclimate may still be required to obtain an optimal formulation.

PEGs of various molecular weights were used as “pore formers” (10% loading). At lower PEG’s molecular weight, higher OVA cumulative release was obtained. This was attributed to the differences on PEG hydrophilicity, which is higher at lower molecular weights. However, the release plateaued after 21 days in all the cases, most probably caused by pore closure of the matrix after PEG had diffused out rapidly during the first weeks, as well as by the uncontrolled acidic microclimate. Sugars and inorganic salts were also evaluated as pore forming agents (at 10% loading). Unfortunately, incomplete release was still observed; they were not able to control the acidic pH and induced OVA aggregation by increasing the ionic strength within the matrix. Hence, they were unsuitable to improve the release completeness of OVA from PLGA-based implants

Since the acidic microclimate was found to be the primary trigger for the incomplete release of OVA, pH modifiers were incorporated within the matrix. The use of $MgCO_3$ and $Mg(OH)_2$ (3.5% loading) increased the released fraction of OVA in a 20% and 10% respectively. They also delayed by one week the degradation onset of PLGA thanks to their neutralization effect during the first weeks of dissolution. Nevertheless, release incompleteness was still observed since this effect did not last long and the pH was not kept above OVA's pI. Higher amounts of these co-excipients should be used to achieve a long-lasting effect. However, this increase may result in an increase in the inner ionic strength and the induction of OVA aggregation, which is unfavorable. Changing the polymer matrix to a slower-degrading one, where the pH drops slower, could work as well, but care should be taken to avoid greater increase in hydrophobicity that might hinder the protein.

With the use of shellac, a well-known enteric and biocompatible polymer, as protective co-excipient (1:5 and 1:10 protein: shellac ratio), a distinct late release phase occurred and release completeness was increased to more than 75% (cumulative release). Shellac seemed to protect the protein against the acidic microclimate due to its low solubility at low pH. The so protected OVA was then released once the pH increased, due to the declining PLGA-oligomer formation. The result was a triphasic release profile, consisting of an initial burst, a slow diffusion phase over about 7 weeks, and an erosion-controlled dissolution phase over the next three weeks. An acid-labile protein like OVA was thus effectively protected from an interaction with PLGA and its degradation products, resulting in a controlled delivery of more than 90% of the original payload. One of these formulations (1:5 OVA: shellac ratio) was up-scaled from the mini-ram extruder to a twin-screw extruder using a scale-up size factor of 15. No substantial differences on OVA integrity between both extrusion methods were detected. The dissolution for the up-scaled formulation showed also a triphasic release profile, but with a lower burst release (10% vs. 30%), probably caused by a densification of the matrix after extrusion. The dissolution of the protein during the erosion-controlled phase of release was slightly slower for the up-scaled formulation and lasted longer (8 vs. 3 weeks) reaching also more than 75% of cumulative release. These differences were attributed to the lower burst release and less pore formation, which slowed down the protein's diffusion. In both cases an insoluble mass remained after the release. However, it was identified as undissolved shellac together with the small portion of unreleased protein. A further characterization of the degradation properties of these implants will be interesting to assess their suitability as a depo formulation intended for multiple applications.

Storage stability of the up-scaled formulation indicated a change in thermal properties (decrease in Tg) and dissolution profile over the time when the implants were stored at ≥25°C, being more drastic for storage temperatures above the formulation's Tg (37°C) since mobility of the polymer chains and re-arrangements into a less rigid structure occurred. No substantial changes in OVA's hydrophobicity or formation of additional aggregates were observed when the implants were stored at ≤25°C. Protein conformational changes and increase of interactions between the matrix and the protein were induced by higher storage temperatures. The dissolution profile was comparable for all the evaluated implants prior and after storage during the burst release and lag phase. Differences were observed during the erosion phase, which could be attributed to the decrease on Tg after storage, with a faster release upon storage for longer time. In conclusion, the implants should be stored at refrigerated conditions to guarantee their proper performance and avoid undesirable changes.

Compared with the case of PLGA, OVA was generally more stable both within the lipid-based matrix and during its release from it, since no acidic environment was created (pH was always ≥ 6.8). The extrusion process did not alter the polymorphism of D114 or D118, but it induced a reordering of the lipidic chains in the case of DP60. However, this reordering was always observed, indicating that this lipid adopted a more stable conformation after extrusion. The release of OVA from the lipid-based implants was mainly driven by diffusional processes: influx of water that dissolved the protein allowing its efflux. It was also dependent on the crystallinity degree of the lipidic matrix used: the release was slower and longer when a more amorphous and heterogeneous lipid, like DP60, was used. In contrast, the presence of crystallites within the structure of more crystalline materials, like D114 and D118, led to a higher anisotropy of the protein distribution yielding to a faster release. Incomplete release from the DP60 matrix was observed when OVA was loaded at 5%, but without the formation of insoluble aggregates. This behavior was attributed to possible stronger physical interactions between the protein and the matrix. By increasing the protein loading, faster and more complete release was observed, which can be ascribed to the formation of more and/or bigger pores at higher protein loadings. Loading lysozyme, a smaller protein, instead of OVA resulted in a more prolonged release with similar time-frame for D118 and DP60. This was probably caused by the creation of smaller and less interconnected pores, and a stronger physical interaction between the matrix and the protein. A deeper investigation on these interactions and the distribution of the protein within the matrix might be helpful to determine their possible impact on microstructural rearrangement upon storage.

The use of PLA as a co-excipient on the D118-lipid matrix was a suitable approach to prolong the release of OVA from 1 week to 1 month without the detrimental effects that the polymeric matrix could have on the protein. In contrast, incorporation of PEG in the DP60-based matrix accelerated the diffusion rate of the protein during the first weeks of release. This effect was correlated with PEG's molecular weight: the lower it was, the faster the release obtained. The release from DP60-based implants was also faster when binary lipid blends were used. The rate was related to the fatty acid chain length of the secondary lipid: by being shorter the release was faster. This could be ascribed to the decrease in lipid wettability with the increase on its chain length, since diffusivity of the protein depends on the influx of water. Thermal characterization of these blends indicated that the lipids did not mixed at a molecular level, presenting some phase separation. In this case, it would be recommended to use an extruder that compounds the materials while they are in their molten state. This could avoid changes on the lipidic microstructure after storage. In general, the dissolution of OVA was successfully tuned by the inclusion of more hydrophobic or more hydrophilic excipients, leading to different dissolution speeds with times ranging from 2 to 15 weeks. The versatility of these systems without the inclusion of many components makes them an attractive option for protein delivery with various applications.

Crystallinity changes in the lipid matrices were observed after curing under different conditions; these changes also had a significant effect on the dissolution profile of OVA. All the cured DP60-based implants as well as the D118-ones cured at 50°C presented a faster dissolution, ascribed to the creation of larger channels that increased the diffusivity of OVA. In contrast, slower diffusion was observed for the D118-based implants cured at 40°C. In this case, the partial melting of the lipid might have created a denser matrix. In general, the DP60 matrix showed less polymorphic changes, probably due to its more heterogeneous and amorphous character. This could represent a more stable formulation without unpredictable variations upon storage.

A sustained and prolonged OVA release formulation with optimized dissolution was obtained after the application of a Design of Experiments (DoE). The used Taguchi method allowed to study four factors at three different levels, with a reduction of experimental runs from 81 to 27, thanks to the use of an orthogonal array. It was found that the release of OVA was significantly influenced by the matrix composition and protein loading, and to a lesser extent by the curing conditions (temperature and time). Based on the results, a formulation with 5% protein loading, DP60/D118 (50:50) as matrix and curing at 40°C during 60 minutes was found to be the optimal one with a constant release over 28 weeks at a rate of ~2.8%/week.

DoE is a valuable tool that allows the evaluation of various formulation and process parameters without incurring on unnecessary experiments.

Gamma-irradiation affected the performance of both prepared formulations, PLGA: shellac- and lipid-based, and it proved to be unsuitable for the OVA-loaded implants. Increase in protein hydrophobicity, changes in OVA dissolution and induction of rearrangements within the biodegradable matrix were caused by the sterilization process. The use of a cooling agent during the irradiation decreased the magnitude of these changes, because molecule mobility was reduced, but it did not avoid them. Further evaluation of the polymers' molecular weight distribution, protein and matrix distribution and free radical formation would be ideal to fully understand the effect of irradiation on the implants and to assess whether the incorporation of other co-excipients (e.g. antioxidants) could maintain the physicochemical characteristics of the formulation after irradiation. A suitable alternative may be the use of a low-bioburden sterilization process, which could produce sterile implants that maintain their physicochemical properties after irradiation at a lower dose.

In conclusion, HME was a suitable process for the preparation of biodegradable implants with sustained and prolonged release of OVA. Different types of matrices were evaluated, obtaining different release patterns and various releasing times. Protein stability and release completeness were improved after understanding its degradation mechanism and the corresponding key formulation parameters. The ability to obtain tailored properties out of the same dosage form, makes biodegradable implants an interesting and promising candidate for protein delivery.

6. Zusammenfassung

Verschiedene Systeme für die kontrollierte Freisetzung von Peptid- und Proteinwirkstoffen aus Arzneimittelpräparaten sind entwickelt worden. Der Fokus wurde auf diejenigen gesetzt, die eine anhaltende parenterale Freisetzung ermöglichen, sie können die Proteinfreisetzung verlängern. Dies führt zu einer Verbesserung der therapeutischen Ergebnisse, sowie der Compliance der Patienten. Viele von den aktuellen Herstellungsmethoden werden unter Bedingungen durchgeführt, die schädlich für solche Moleküle sein können, z. B. die Anwendung von organischen Lösemitteln, pH-Gradienten, Vakuum und/oder Hitze. Auch die Herstellung der Formulierung mit den gewünschten Freisetzungsparametern kann schwierig sein, weil das gewünschte Freisetzungsprofil nicht optimal ist, oder weil die Integrität dieser Biomakromoleküle in der Matrix nicht haltbar ist. Die Entwicklung dieser Systeme ist eine komplexe und herausfordernde Aufgabe mit langen Entwicklungszeiten und wenigen kommerzialisierten Produkten als Schlussfolge. Sowohl das Sammeln von neuen Erkenntnissen über diese Systeme, als auch die Feststellung die wichtigsten Parameter, die das Verhalten der Präparate beeinflussen, ist daher von Bedeutung um die Entwicklung von Präparaten zur Parenteral-Wirkstofffreisetzung zu unterstützen und zu beschleunigen.

Diese Arbeit beschäftigte sich mit der Entwicklung von bioabbaubaren Implantaten zur Proteinwirkstofffreisetzung. Es wurde Ovalbumin (OVA) als Säure-labiles Modellprotein verwendet. Die Herstellungsmethode der Wahl war Schmelzextrusion (Hot melt extrusion, HME), da organische Lösemittel dabei nicht benötigt werden und das Protein in seinem stabilsten, trockenen Zustand hinzugefügt werden kann. Dabei wird auch die Erzeugung von weiteren Grenzflächen vermieden, die die Proteinstabilität gefährden können. Nichtsdestotrotz, die Verwendung von hohen Temperaturen und die dazugehörigen Scherkräfte können eine negative Wirkung auf die Proteinstruktur haben. Daher wurde untersucht, ob OVA enthaltende Implantate mit Hilfe der HME hergestellt werden können.
Um dies zu untersuchen wurde ein Mini-Ram Extruder (Syringe-die-Gerät) als Screening-Werkzeug genutzt. Zum Vergleich wurden zwei verschiedene bioabbaubaren Matrix-Bildner (PLGA- und Lipide-basierte) ausgewählt, um die Freisetzung und Proteinstabilität zu untersuchen.

Laut SEC-HPLC-, FTIR-, CD-, und Fluoreszenzspektroskopie war das OVA während der Extrusion stabil. Vergleichbare Ergebnissen wurden beim neu vom Lieferant erhaltenen OVA und dem OVA ermittelt, dass aus den hergestellten Implantaten extrahiert wurde.

Dieses Ergebnis ist bei beiden Matrizen beobachtet worden, was ein Hinweis auf den Schutzeffekt auf das Protein sein kann. Wenn sie während das Prozess schmelzen oder weich werden, können sie als „Schutzkissen“ gegen Hitze oder Schubkräfte fungieren.

Bei PLGA-basierten Implantaten zeigte die OVA-Freisetzung eine anfängliche kurze schnelle Freisetzung (burst release) auf die eine langsame Freisetzung folgte, die nach 21 Tagen in einem Plateau endete. Keine der untersuchten Formulierungen zeigte eine 100%ige Freisetzung. Die Perkolationsschwelle dieser Matrizen wurde bei Ladungen von ≥25% erreicht, selbst die kumulative Freisetzung erzielte keine 100%. Die unvollständige Freisetzung ging mit der Absetzung von einem unlöslichen Niederschlag einher. Die Charakterisierung von diesem Feststoff zeigte, dass es aus nicht-kovalenten Proteinaggregaten und Polymer bestand, in dem Ovalbumin ionisch gebunden wurde, als der pH in der abbaubauenden Matrix unter den isoelektrischen Punkt des Proteins fiel. Der Kontakt zu dem sauren Mikroklima, das der Abbauprozess der Matrix erzeugt hat, kann strukturelle Änderungen in der OVA-Struktur verursachen, z.B. die Erhöhung der hydrophoben Eigenschaften und der β-Faltblatt-Anteile. Außerdem ist die autokatalysierte Hydrolysegeschwindigkeit des PLGAs bei der Anwesenheit von OVA gesunken, da das Protein gewisse Puffer-Eigenschaften besitzt. Diese Änderungen erhöhen die Wahrscheinlichkeit von Protein-Protein und Protein-Polymer/Oligomer Wechselwirkungen.

Um eine viskose Umgebung innerhalb der Implantate zu generieren, wurden PVP und Poloxamer als Hilfsstoff angewendet. Diese Zusatzstoffe wurden zusammen mit dem Protein in Lösung gebracht und dann gefriergetrocknet, bevor sie dann mit dem Polymer gemischt wurden um die Extrusion durchzuführen. Die Freisetzung von OVA war während der ersten Tage erhöht. Dies weist darauf hin, dass diese Träger gewissermaßen die Adsorption des Proteins auf dem PLGA herabsetzen. Trotzdem waren sie nicht in der Lage, das Ansäuern des inneren pHs zu kontrollieren um die Aggregation von OVA zu vermeiden, sodass auch in diesem Fall keine vollständige Freisetzung beobachtet wurde. Außerdem gab es Änderungen in der Sekundärstruktur des OVAs, die sowohl von dem Gefriertrocknungsprozess als auch von der Wechselwirkung mit dem gelösten Träger verursacht worden sind. Die Optimierung der Prozessparameter bei der Gefriertrocknung und des Protein/Träger-Verhältnisses können die Proteinstabilität verbessern. Strategien um das saure Mikroklima zu kontrollieren sind allerdings immer noch notwendig, damit eine optimale Formulierung hergestellt werden kann.

PEG mit verschiedenen Molmassen wurde als „Poren-Bilder“ (10%-Ladung) genutzt. Je kleiner die Molmasse des PEGs war, desto höher war die erhaltene Kumulative-Freisetzung des OVAs. Dies ist eine Konsequenz der unterschiedlichen hydrophoben Eigenschaften des PEGs, die größer werden, wenn das Molgewichte steigt. Nichtsdestotrotz hat die Freisetzung nach 21 Tagen in jedem Fall ihr Maximum erreicht. Die Gründe dafür liegen höchstwahrscheinlich an dem Poren-Verschluss der Grundmasse, nach dem PEG während der ersten Wochen rausdiffundierte, sowie an dem unkontrollierten sauren Mikroklima. Zucker und anorganische Salze wurden auch als „Poren-Bilder“ getestet (10%-Ladung). Leider ist die unvollständige Freisetzung immer noch beobachtet worden. Diese Zusätze waren nicht in der Lage den sauren pH zu puffern und haben die OVA-Aggregation aufgrund der erhöhten Ionenstärke in der Matrix gefördert. Von daher waren sie nicht geeignet, die Freisetzungsvollständigkeit von OVA aus PLGA-basierte Implantaten zu verbessern.

Es wurde festgestellt, dass das saure Mikroklima der Hauptgrund zur unvollständigen Freisetzung von OVA war. Deswegen wurden pH-modifizierende Reagenzien zu dem System hinzugefügt. Die Verwendung von $MgCO_3$ und $Mg(OH)_2$ (3,5%-Ladung) hat die Freisetzung von OVA jeweils um 20% und um 10% erhöht. Diese Zusätze haben durch den neutralisierenden Effekt innerhalb der ersten Wochen den Beginn der Zersetzung des PLGAs hinausgezögert. Dabei ist die unvollständige Freisetzung wieder beobachtet worden, da dieser Effekt nicht lange genug aufrechterhalten und der pH nicht über dem isoelektrischen Punkt des OVAs gehalten wurde. Höhere Mengen dieser Additive müssen hinzugefügt werden um einen dauerhaften Effekt zu bewirken. Andererseits könnte diese Erhöhung eine Steigung der Ionenstärke verursachen und damit die Aggregation des OVA, was ungünstig wäre. Die Veränderung der Polymermatrix zu einem langsamer abbauenden PLGA, bei dem der pH langsamer absinkt, könnte auch zu einer Verbesserung führen, jedoch muss eine zu große Erhöhung der hydrophoben Eigenschaften vermieden werden, da es das Protein negativ beeinflussen kann.

Durch die Verwendung von Schellack, einem bekannten magensaftresistenten und biokompatiblen Polymer als Schutz-Hilfsstoff (1:5 und 1:10 Protein:Schellack Verhältnis), fand eine verspätete Freisetzung mit einer kumulativen Freisetzung von 75% statt. Schellack scheint das Protein gegen das saure Mikroklima dank seiner niedrigen Löslichkeit bei niedrigen pH-Werten zu schützen. Das so geschützte OVA wird dann freigesetzt, wenn der pH durch die abnehmende PLGA-Oligomer Bildung wieder erhöht wird. Das Ergebnis war ein drei-Phasen Freisetzungsprofil, bestehend aus einer anfänglichen schnellen Freisetzung, einer langsamen Diffusion-kontrollierten Phase, die länger als 7 Wochen war und einer Erosions-kontrollierten Freisetzungsphase in den folgenden drei Wochen. Ein

Säure-labiles Protein wie OVA kann somit erfolgreich gegen die Wechselwirkungen mit PLGA und seinen Abbauprodukten geschützt werden, damit eine kontrollierte Freisetzung von mehr als 90% der ursprünglichen Ladung erreicht wird. Eine von diesen Formulierungen wurde mit einem Doppelschneckenextruder in einem 15-fach größeren Maßstab hergestellt. Zwischen beiden Methoden sind keine erkennbaren Unterschiede in der OVA-Integrität beobachtet worden. Die Freisetzungsuntersuchungen für die im Produktionsmaßstab erzeugten Extrudates haben das gleiche drei-Phasen Profil ergeben, allerdings mit einer kleineren Anfangsfreisetzung (10% statt 30%), wahrscheinlich wegen einer Verdichtung der Matrix nach der Extrusion. Die Proteinfreisetzung während der Abbau-kontrollierten Phase ist bei den Implantaten, die im vergrößerten Produktionsmaßstab hergestellt wurden, etwas langsamer und dauerte länger (8 statt 3 Wochen). Die kumulative Freisetzung betrug zudem mehr als 75%. Diese Unterschiede können durch die kleinere anfängliche Freisetzung und die geringere Poren-Erzeugung erklärt werden, wodurch die Protein-Diffusion langsamer wird. In beiden Fälle ist eine unlösliche Masse nach dem Versuchen zurückgeblieben. Sie bestand aus ungelöstem Schellack und einer kleinen Menge nicht-freigesetzten Proteins. Eine weiterführende Charakterisierung solcher Implantate könnte interessant sein, um seine Eignung zur Herstellung von Depotformulierungen mit mehrfacher Freisetzung zu prüfen.

Versuche bezüglich der Lagerungsstabilität bei der vergrößerten Formulierung haben Änderungen gezeigt, sowohl in den thermischen Eigenschaften (Minderung des Tgs), als auch in dem Freisetzungsprofil, wenn die Implantate bei ≥25°C gelagert wurden. Bei Lagerungstemperaturen über der Formulierungs-Tg (37°C) waren eindeutiger, da die Mobilität von den Polymerketten gefördert wurde. Wenn die Implantate bei ≤25°C gelagert worden sind, konnten weder entscheidende Änderungen in den hydrophoben Eigenschaften des OVAs, noch die Entstehung von weiteren Aggregaten festgestellt werden. Bei höheren Lagertemperaturen sind sowohl konformative Veränderungen beim OVA als auch stärkere Protein-Matrix Wechselwirkungen zu erwarten. Die Freisetzungsprofile der untersuchten Implantate waren vor und nach der Lagerung, sowohl für die anfängliche Freisetzungsphase, als auch während die Verzögerungsphase, vergleichbar. In der Erosions-Phase wurden Unterschiede gesehen, die durch die Minderung des Tgs nach der Lagerung erklärt werden können und dadurch eine schnelleren Freisetzung nach langen Lagerungszeiten verursachten. Die Implantate müssen daher gekühlt gelagert werden, um eine optimale Funktion zu garantieren und um ungewünschte Änderungen zu vermeiden.

Im Vergleich zu den Formulierungen mit PLGA ist OVA in einer Lipid-Matrix generell stabiler, sowohl in der Lagerungsform als auch beim Rausdiffundieren, da keine saure Umgebung

entsteht (pH-Werte sind immer ≥ 6.8). Das Extrusionverfahren hatte keinen Einfluss auf den Polymorphismus von D114 oder D118, obwohl es gewisse strukturelle Änderungen in DP60 verursacht hat. Diese Änderungen sind immer wieder beobachtet worden; sie weisen darauf hin, dass diese Lipide eine stabilere Konformation nach der Extrusion erreichen. Die Freisetzung von OVA aus lipidischen Implantaten ist hauptsächlich von Diffusionsprozessen kontrolliert, das Wasser diffundiert rein und das gelöste Protein diffundiert raus. Es war auch von der Kristallinität der verwendeten lipid-Matrix abhängig. Die Freisetzung war langsamer und länger, wenn ein amorpheres und heterogeneres Lipid (wie DP60) verwendet wurde. Dem gegenüber führte die Anwesenheit von Kristalliten innerhalb der Matrix durch kristallines D114 oder D118 zu einer höheren Anisotropie in der Proteinverteilung und damit zu einer schnelleren Freisetzung. Eine unvollständige Freisetzung aus einer PD60-Matrix mit einer OVA-Ladung von 5% wurde beobachtet, allerdings ohne die Bildung eines unlöslichen Aggregates. Dieses Verhalten könnte durch die stärkeren Wechselwirkungen zwischen OVA und der Matrix erklärt werden. Die Freisetzung bei höheren Proteinbeladungen war schneller und ausgeprägter, wahrscheinlich durch die Bildung von mehreren und größeren Poren. Die Beladung von Lysozyme, einem kleineren Protein als OVA zeigte in einem vergleichbaren Zeitfenstern längere Freisetzungszeiten mit D118 und DP60. Grund dafür könnte die Bildung von wenigen, kleineren, schlecht verbundenen Poren und eine stärkere Wechselwirkung mit der Matrix sein. Eine weiterführende Untersuchung dieser Wechselwirkungen zusammen mit der Proteinverteilung in der Matrix könnte hilfreich sein, um die möglichen Einflüsse von mikrostrukturellen Umlagerungen nach der Lagerung zu verstehen.

Die Verwendung von PLA als Träger in der D118-lipid-Matrix war eine zielführende Lösung, um die OVA-Freisetzung von 1 Woche bis zu 1 Monat zu verlängern, ohne die schädlichen Wirkungen der Matrix auf das Protein zu erhalten. Der Zusatz von PEG in die DP60-Matrix hat die Diffusionsgeschwindigkeit von OVA während der ersten Wochen der Freisetzung beschleunigt. Dieser Effekt war von der Molmasse des PEGs abhängig, je kleiner sie war, desto schneller fand die Freisetzung statt. Die Freisetzung aus DP60-basierten Implantaten war schneller, wenn binäre lipidische Mischungen verwendet worden sind. Die Geschwindigkeit war von der Kettenlänge der Fettsäuren der zweiten Lipide abhängig, je kürzer die Ketten, desto schneller die Freisetzung. Es könnte die Folge einer Erhöhung der hydrophoben Eigenschaften der Lipide mit deren Kettenlänge sein, da die Proteindiffusion vom Eindringen des Wassers abhängig ist. Die thermische Charakterisierung solcher Mischungen hat gezeigt, dass sich die Lipide auf der molekularen Ebene nicht miteinander mischen und eine Phasentrennung stattgefunden hat. In diesem Fall kann es empfehlenswert sein einen Extruder zu nutzen, der beide Materialien in geschmolzenem

Zustand aufarbeiten kann. Das könnte die Änderungen der lipidischen Mikrostruktur während der Lagerung vermeiden. Die Freisetzung von OVA könnte durch die Zugabe von hydrophoben oder hydrophilen Trägern erfolgreich eingestellt werden. Dies führt zu einstellbaren Freisetzungsgeschwindigkeiten mit Zeiten von 2 bis 15 Wochen. Die Vielseitigkeit dieser Systeme, ohne Zugabe von mehreren Komponenten, macht dieses Verfahren vielversprechend für verschiedene Proteinfreisetzungsanwendungen.

Nach Wärme-Aufarbeitung unter verschiedenen Bedingungen wurden Veränderungen in der Kristallinität der Lipide-Matrizen beobachtet. Solche Änderungen hatten auch einen wichtigen Einfluss auf die OVA-Freisetzungsprofile. Alle Wärme-aufgearbeiteten (bei 50°C) Implantate, sowohl die DP60-, als auch die D118-basierten, haben schnellere Freisetzungen gezeigt, wahrscheinlich wegen der Bildung von längeren Kanälen, die die Diffusität von OVA fördern. Im Gegensatz dazu, eine langsamere Diffusion wurde bei den D118-Implantaten beobachtet, die bei 40°C Wärme-aufgearbeitet worden sind. Grund dafür könnte das partielle Schmelzen sein, das eine Verdichtung der Matrix hervorruft. Im Allgemeinen, die DP60-Matrix zeigte weniger polymorphische Änderungen, vielleicht wegen seinen heterogenen und amorphen Eigenschaften. Das könnte zu einer stabileren Formulierung führen, ohne unvorhersehbare Änderungen währen der Lagerung.

Ein optimiertes und verlängertes OVA-Freisetzungsprofil wurde durch die Anwendung von „Design of Experiments“ (DoE) erhalten. Mit Hilfe der Taguchi Methode, konnten vier Faktoren auf drei Ebenen untersucht werden. Dies mit einer Verminderung von 81 auf 27 Versuche, Dank der Verwendung eines orthogonalen Arrays. Es wurde gefunden, dass die Freisetzung vom OVA von der Matrix-Zusammensetzung und der Proteinbeladung stark beeinflusst war, aber weniger von den Wärme-Bedingungen bezüglich Temperatur und Zeit. Auf diesen Ergebnissen basierend wurde eine Formulierung mit 5%-Proteinbeladung, aus DP60/D118 (50:50) und Wärme-Aufarbeitung von 60 Minuten bei 40°C als optimal bezeichnet, mit einer dauerhaften Freisetzung von 28 Wochen und eine Geschwindigkeit von 2,8% pro Woche. DoE ist ein außerordentlich wertvolles Instrument, das die Evaluierung von Bedingungen und Prozessparametern ermöglicht, ohne unnötige Experimente mache zu müssen.

Gamma-Strahlung hatte einen negativen Einfluss auf die Eigenschaften von beiden Formulierungen, PLGA/Schellack und Lipide-basierte, und schien für OVA-beladene Implantate ungeeignet zu sein. Erhöhung der hydrophoben Proteineigenschaften, Änderungen in OVA-Löslichkeit und Umlagerungen in der Polymer-Matrix sind bei dem Sterilisationsprozess erzeugt worden. Die Verwendung eines Kühlungsmittels während des

Strahlens konnte die Intensität dieser Effekte mindern, weil die Bewegung der Moleküle reduziert wurde, obwohl es nicht vollkommen vermieden werden konnte. Weitere Untersuchungen über die Mol-Gewicht-Verteilung der Polymere, Proteinverteilung in der Matrix und Bildung von freien Radikalen wären nötig, um den Einfluss der Strahlung auf die Implantate zu verstehen. Damit kann man Strategien entwickeln – zum Beispiel, die Zugabe von Additiven mit Antioxidierungseigenschaften – um die physikochemischen Eigenschaften der Formulierung nach der Bestrahlung zu erhalten. Eine mögliche Lösung wäre die Anwendung von „low-bioburden“ Sterilisationsprozessen, die sterile Implantate mit haltbaren physikochemischen Eigenschaften produzieren könnten, nach Bestrahlung bei kleineren Dosen.

Zum Schluss, HME war ein geeignetes Verfahren zur Herstellung von bioabbaubaren Implantaten mit ausdauernder und dauerhafter Freisetzung von OVA. Verschiedene Sorten von Matrizen wurden untersucht und die verschiedenen Freisetzungsparameter bei verschiedenen Zeiten wurden gemessen. Sowohl Proteinstabilität, als auch die Freisetzungsvollständigkeit wurden verbessert, nachdem die Zersetzungsmechanismen und die entsprechenden Bedingungen verstanden wurden. Die Möglichkeit maßgeschneiderte Eigenschaften aus der gleichen Darreichungsfrom zu erzielen, macht bioabbaubare Implantate interessante und vielversprechende Kandidaten für die Proteinwirkstofffreisetzung.

7. References

Abdul-Fattah, A.M., Kalonia, D.S., Pikal, M.J., 2007. The challenge of drying method selection for protein pharmaceuticals: Product quality implications. J. Pharm. Sci.

Aburahma, M.H., Badr-eldin, S.M., 2014. Compritol 888 ATO: a multifunctional lipid excipient in drug delivery systems and nanopharmaceuticals. Expert Opin. Drug Deliv. 1–19.

Achanta, A.S., Adusumilli, P.S., James, K.W., Rhodes, C.T., 1997. Development of hot melt coating methods. Drug Dev. Ind. Pharm. 23, 441–449.

Agarwal, P., Rupenthal, I.D., 2013. Injectable implants for the sustained release of protein and peptide drugs. Drug Discov. Today 18, 337–49.

AGC Chemicals Europe, 2002. The moulding of PTFE granular powders [WWW Document]. Tech. Serv. Note F2. URL http://www.agcchem.com/newsroom/finish/13-fluon-ptfe-resins/42-processing-note-f2-extrusion-of-ptfe-granular-powders (accessed 2.1.17).

Ahmed, A.R., Bodmeier, R., 2009. Preparation of preformed porous PLGA microparticles and antisense oligonucleotides loading. Eur. J. Pharm. Biopharm. 71, 264–270.

Allen, T.M., Cullis, P.R., 2013. Liposomal drug delivery systems: From concept to clinical applications. Adv. Drug Deliv. Rev. 65, 36–48.

Almeida, A.J., Souto, E., 2007. Solid lipid nanoparticles as a drug delivery system for peptides and proteins. Adv. Drug Deliv. Rev. 59, 478–490.

Andhariya, J. V., Burgess, D.J., 2016. Recent advances in testing of microsphere drug delivery systems. Expert Opin. Drug Deliv. 5247, 1–16.

Arbit, E., Auffret, T., Bedu-Addo, F.K., Boyd, B., Bridges, P., Bummer, P.M., Clark, A.R., Farr, S.J., Gatlin, L.A., Gomez-Orellana, I., Hasselbacher, C., Hastedt, J.E., Hoffmann, H., Koppenol, S., Linn, L.S., Majuru, S., McGoff, P., McNally, E.J., Mire-Sluis, A., Nashabeh, W., Pisch-Heberle, S., Scher, D.S., Shalaev, E.Y., Shire, S.J., Speaker, S.M., Stevenson, C.L., Teagarden, D.L., Wang, W., Wright, J., 2013. Protein formulation and delivery, 2nd ed, Journal of Controlled Release. Informa Healthcare, USA, New York.

Banga, A.K., 2006. Therapeutic Peptides and Proteins Peptides: Formulation, Processing and Delivery Systems, Second edi. ed. CRC Taylor & Francis Group, Boca Raton, FL.

Banga, A.K., Chien, Y., 1988. Systemic delivery of therapeutic peptides and proteins. Int. J. Pharm. 48, 15–50.

Bawa, R., A. Siegel, R., Marasca, B., Karel, M., Langer, R., 1985. An explanation for the controlled release of macromolecules from polymers. J. Control. Release 1, 259–267.

Bhatnagar, D., Dube, K., Damodaran, V.B., Subramanian, G., Aston, K., Halperin, F., Mao,

M., Pricer, K., Murthy, S., Kohn, J., 2016. Effects of Terminal Sterilization on PEG-based Bioresorbable Polymers Used in Biomedical Applications. Macromol. Mater. Eng. 1–14.

Bodmer, D., Kissel, T., Traechslin, E., 1992. Factors influencing the release of peptides and proteins from biodegradable parenteral depot systems. J. Control. Release 21, 129–137.

Bolboacă, S.D., Jäntschi, L., 2007. Design of experiments: Useful orthogonal arrays for number of experiments from 4 to 16. Entropy 9, 198–232.

Bourges, J.L., Bloquel, C., Thomas, a, Froussart, F., Bochot, a, Azan, F., Gurny, R., BenEzra, D., Behar-Cohen, F., 2006. Intraocular implants for extended drug delivery: therapeutic applications. Adv. Drug Deliv. Rev. 58, 1182–202.

Breitenbach, J., 2002. Melt extrusion: from process to drug delivery technology. Eur J Pharm Biopharm 54, 107–117.

Burgess, D., Crommelin, D., Hussain, A., Chen, M., 2004. Assuring quality and performance of sustained and controlled release parenterals: EUFEPS workshop report. AAPS PharmSci 6, 1–12.

Burgess, D., Hussain, A., Ingallinera, T., Chen, M., 2002. Assuring quality and performance of sustained and controlled release parenterals: workshop report. AAPS PharmSci 4.

Byrne, R.A., Joner, M., Alfonso, F., Kastrati, A., 2014. Drug-coated balloon therapy in coronary and peripheral artery disease. Nat Rev Cardiol 11, 13–23.

Capelle, M.A.H., Gurny, R., Arvinte, T., 2007. High throughput screening of protein formulation stability: Practical considerations. Eur. J. Pharm. Biopharm. 65, 131–148.

Capelle, M.A.H., Gurny, R., Arvinte, T., 2009. A high throughput protein formulation platform: Case study of salmon calcitonin. Pharm. Res. 26, 118–128.

Cardamone, M., Puri, N.K., 1992. Spectrofluorimetric assessment of the surface hydrophobicity of proteins. Biochem. J. 282, 589–593.

Carelli, V., Di Colo, G., Guerrini, C., Nannipieri, E., 1989. Drug release from silicone elastomer through controlled polymer cracking: an extension to macromolecular drugs. Int. J. Pharm. 50, 181–188.

Carrascosa, C., Espejo, L., Torrado, S., Torrado, J.J., 2003. Effect of c-Sterilization Process on PLGA Microspheres Loaded with Insulin-Like Growth Factor - I (IGF-I). J. Biomater. Appl. 18, 95–108.

Chaudhuri, T.K., Das, K.P., Sinha, N.K., 1993. Surface hydrophobicity of a low molecular weight basic trypsin subtilisin inhibitor from marine turtle eggwhite. J. Biochem. 113, 729–733.

Cheyne, A., 2016. Flow behaviour of Starch-based solids [WWW Document]. Proj. Synopses Dep. Chem. Eng. Biotechnol. URL

http://www.ceb.cam.ac.uk/research/groups/rg-p4g/research/previous-work (accessed 1.31.17).

Chirino, A.J., Mire-Sluis, A., 2004. Characterizing biological products and assessing comparability following manufacturing changes. Nat Biotech 22, 1383–1391.

Chokshi, R., Zia, H., 2004. Hot-Melt Extrusion technique: A Review. Iran. J. Pharm. Res. 3, 3–16.

Cohen, J., Siegel, R.A., Langer, R., 1984. Sintering technique for the preparation of polymer matrixes for the controlled release of macromolecules 73, 1034–1037.

Crotts, G., Park, T., 1997. Stability and release of bovine serum albumin encapsulated within poly (D, L-lactide-co-glycolide) microparticles. J. Control. Release 44, 123–134.

Crotts, G., Saha, H., Gwan, T., 1997. controlled release Adsorption determines in-vitro protein release rate from biodegradable microspheres : quantitative analysis of surface area during degradation 47, 101–111.

Crowe, J.H., Carpenter, J.F., Crowe, L.M., Anchordoguy, T.J., 1990. Are freezing and dehydration similar stress vectors? A comparison of modes of interaction of stabilizing solutes with biomolecules. Cryobiology 27, 219–231.

Crowley, M.M., Zhang, F., Repka, M. a, Thumma, S., Upadhye, S.B., Battu, S.K., McGinity, J.W., Martin, C., 2007. Pharmaceutical applications of hot-melt extrusion: part I. Drug Dev. Ind. Pharm. 33, 909–926.

Dash, A., Cudworth II, G., 1998. Therapeutic applications of implantable drug delivery systems. J. Pharmacol. Toxicol. Methods 40, 1–12.

Davis, B.K., 1974. Diffusion of polymer gel implants. Proc. Natl. Acad. Sci. U. S. A. 71, 3120–3.

Del Valle, E.M.M., Galán, M.A., Carbonell, R.G., 2009. Drug delivery technologies: The way forward in the new decade. Ind. Eng. Chem. Res. 48, 2475–2486.

Determan, A.S., Wilson, J.H., Kipper, M.J., Wannemuehler, M.J., Narasimhan, B., 2006. Protein stability in the presence of polymer degradation products: consequences for controlled release formulations. Biomaterials 27, 3312–3320.

Di Sabatino, M., Albertini, B., Kett, V.L., Passerini, N., 2012. Spray congealed lipid microparticles with high protein loading: preparation and solid state characterisation. Eur. J. Pharm. Sci. 46, 346–56.

Donovan, J.W., Mapes, C.J., 1976. A differential scanning calorimetric study of conversion of ovalbumin to S-ovalbumin in eggs. J. Sci. Food Agric. 27, 197–204.

Dorati, R., Genta, I., Montanari, L., Cilurzo, F., Buttafava, A., Faucitano, A., Conti, B., 2005. The effect of γ-irradiation on PLGA/PEG microspheres containing ovalbumin. J. Control. Release 107, 78–90.

Dorta, M., Santoveña, A., Llabrés, M., Fariña, J., 2002. Potential applications of PLGA film-

implants in modulating in vitro drugs release. Int. J. Pharm. 248, 149–156.

Eckhardt, B.M., Oeswein, J.Q., Bewley, T. a, 1991. Effect of freezing on aggregation of human growth hormone. Pharm. Res.

Elkharraz, K., Faisant, N., Guse, C., Siepmann, F., Arica-Yegin, B., Oger, J.M., Gust, R., Goepferich, a, Benoit, J.P., Siepmann, J., 2006. Paclitaxel-loaded microparticles and implants for the treatment of brain cancer: preparation and physicochemical characterization. Int. J. Pharm. 314, 127–36.

Even, M.-P., Young, K., Winter, G., Hook, S., Engert, J., 2014. In vivo investigation of twin-screw extruded lipid implants for vaccine delivery. Eur. J. Pharm. Biopharm.

Even, M.P., Bobbala, S., Kooi, K.L., Hook, S., Winter, G., Engert, J., 2015. Impact of implant composition of twin-screw extruded lipid implants on the release behavior. Int. J. Pharm. 493, 102–110.

Farruggia, B., Garcia, G., Angelo, C.D., Pic, G., 2000. Destabilization of human serum albumin by polyethylene glycols studied by thermodynamical equilibrium and kinetic approaches 30.

Fenton, S.S., Fahey, R.C., 1986. Analysis of biological thiols: determination of thiol components of disulfides and thioesters. Anal. Biochem. 154, 34–42.

Fernández-Carballido, a, Herrero-Vanrell, R., Molina-Martínez, I.T., Pastoriza, P., 2004. Biodegradable ibuprofen-loaded PLGA microspheres for intraarticular administration. Effect of Labrafil addition on release in vitro. Int. J. Pharm. 279, 33–41.

Folkman, J., Long, D.M., 1964. The use of silicone rubber as a carrier for prolonged drug therapy. J. Surg. Res. 4, 139–142.

Frank, A., Rath, S.K., Venkatraman, S.S., 2005. Controlled release from bioerodible polymers: Effect of drug type and polymer composition. J. Control. Release 102, 333–344.

Franks, F., Hatley, R.H.M., Friedman, H.L., 1988. The thermodynamics of protein stability. Cold destabilization as a general phenomenon. Biophys. Chem. 31, 307–315.

Frokjaer, S., Otzen, D.E., 2005. Protein drug stability: a formulation challenge. Nat. Rev. Drug Discov. 4, 298–306.

Furp, B.J.A., Hutchinsonb, F.G., 1992. A biodegradable delivery system for peptides : preclinical experience with the gonadotrophin-releasing hormone agonist 21, 117–127.

Gabellieri, E., Strambini, G.B., 2006. ANS fluorescence detects widespread perturbations of protein tertiary structure in ice. Biophys. J. 90, 3239–3245.

Gekko, K., Ohmae, E., Kameyama, K., Takagi, T., 1998. Acetonitrile-protein interactions: Amino acid solubility and preferential solvation. Biochim. Biophys. Acta - Protein Struct. Mol. Enzymol. 1387, 195–205.

Gèze, a, Venier-Julienne, M.C., Cottin, J., Faisant, N., Benoit, J.P., 2001. PLGA

microsphere bioburden evaluation for radiosterilization dose selection. J. Microencapsul. 18, 627–36.

Ghalanbor, Z., Körber, M., Bodmeier, R., 2010. Improved lysozyme stability and release properties of poly (lactide-co-glycolide) implants prepared by hot-melt extrusion. Pharm. Res. 27, 371–379.

Ghalanbor, Z., Körber, M., Bodmeier, R., 2012. Protein release from poly(lactide-co-glycolide) implants prepared by hot-melt extrusion: thioester formation as a reason for incomplete release. Int. J. Pharm. 438, 302–306.

Ghalanbor, Z., Körber, M., Bodmeier, R., 2013. Interdependency of protein-release completeness and polymer degradation in PLGA-based implants. Eur. J. Pharm. Biopharm. 85, 624–630.

Giteau, a, Venier-Julienne, M.C., Aubert-Pouëssel, a, Benoit, J.P., 2008. How to achieve sustained and complete protein release from PLGA-based microparticles? Int. J. Pharm. 350, 14–26.

Gombotz, W.R., Pettit, D.K., 1995. Biodegradable polymers for protein and peptide drug delivery. Bioconjug. Chem. 6, 332–51.

Grimaldi, N., Andrade, F., Segovia, N., Ferrer-Tasies, L., Sala, S., Veciana, J., Ventosa, N., 2016. Lipid-based nanovesicles for nanomedicine. Chem. Soc. Rev. 45, 6520–6545.

Güres, S., Kleinebudde, P., 2011. Dissolution from solid lipid extrudates containing release modifiers. Int. J. Pharm. 412, 77–84.

Guse, C., Koennings, S., Blunk, T., Siepmann, J., Goepferich, a, 2006a. Programmable implants--from pulsatile to controlled release. Int. J. Pharm. 314, 161–9.

Guse, C., Koennings, S., Kreye, F., Siepmann, F., Goepferich, a, Siepmann, J., 2006b. Drug release from lipid-based implants: elucidation of the underlying mass transport mechanisms. Int. J. Pharm. 314, 137–44.

Guse, C., Koennings, S., Maschke, a, Hacker, M., Becker, C., Schreiner, S., Blunk, T., Spruss, T., Goepferich, a, 2006c. Biocompatibility and erosion behavior of implants made of triglycerides and blends with cholesterol and phospholipids. Int. J. Pharm. 314, 153–60.

Hagolle, N., Relkin, P., Dalgleish, D.G., Launay, B., 1997. Transition temperatures of heat-induced structural changes in ovalbumin solutions at acid and neutral pH. Food Hydrocoll. 11, 311–317.

Harris, R.J., Shire, S.J., Winter, C., 2004. Commercial Manufacturing Scale Formulation and Analytical Characterization of Therapeutic Recombinant Antibodies. Drug Dev. Res. 61, 137–154.

Hawe, A., Sutter, M., Jiskoot, W., 2008. Extrinsic fluorescent dyes as tools for protein characterization. Pharm. Res. 25, 1487–1499.

Heller, J., 1993. Polymers for controlled parenteral delivery of peptides and proteins. Adv. Drug Deliv. Rev. 10, 163–204.

Heller, J., Barr, J., 2004. Poly(ortho esters)--from concept to reality. Biomacromolecules 5, 1625–32.

Heller, J., Barr, J., Ng, S.Y., Schwach, K., Gurny, R., 2002. Poly(ortho esters): synthesis, characterization, properties and uses. Adv. Drug Deliv. Rev. 54, 1015–1039.

Herrmann, S., Mohl, S., Siepmann, F., Siepmann, J., Winter, G., 2007a. New insight into the role of polyethylene glycol acting as protein release modifier in lipidic implants. Pharm. Res. 24, 1527–1537.

Herrmann, S., Winter, G., Mohl, S., Siepmann, F., Siepmann, J., 2007b. Mechanisms controlling protein release from lipidic implants: effects of PEG addition. J. Control. Release 118, 161–8.

Ho, E. a, Vassileva, V., Allen, C., Piquette-Miller, M., 2005. In vitro and in vivo characterization of a novel biocompatible polymer-lipid implant system for the sustained delivery of paclitaxel. J. Control. Release 104, 181–91.

Hoffman, A.S., 2008. The origins and evolution of “controlled” drug delivery systems. J. Control. Release 132, 153–163.

Hoth, M., Merkle, H.P., 1991. Formulation of Silicone Matrix Systems for Long-Term Constant Release of Peptides. Drug Dev. Ind. Pharm. 17, 985–999.

Houchin, M.L., Topp, E.M., 2008. Chemical Degradation of Peptides and Proteins in PLGA: A Review of Reactions and Mechanisms. J. Pharm. Sci. 97, 2395–2404.

Hu, H.Y., Du, H.N., 2000. alfa-to-beta structural transformation of ovalbumin: Heat and pH effects. J. Protein Chem. 19, 177–183.

Huntington, J. a, Patston, P. a, Gettins, P.G., 1995. S-ovalbumin, an ovalbumin conformer with properties analogous to those of loop-inserted serpins. Protein Sci. 4, 613–621.

Huntington, J. a, Stein, P.E., 2001. Structure and properties of ovalbumin. J. Chromatogr. B. Biomed. Sci. Appl. 756, 189–98.

Ianeselli, L., Zhang, F., 2010. Protein - Protein Interactions in Ovalbumin Solutions Studied by Small-Angle Scattering: Effect of Ionic Strength and the Chemical Nature of Cations. J. Phys. Chem. B 114, 3776–3783.

Ibraheem, D., Elaissari, a, Fessi, H., 2014. Administration strategies for proteins and peptides. Int. J. Pharm. 477, 578–589.

IJntema, K., Heuvelsland, W.J.M., Dirix, C.A.M.C., Sam, A.P., 1994. Hydroxyapatite microcarriers for biocontrolled release of protein drugs. Int. J. Pharm. 112, 215–224.

Ishimaru, T., Ito, K., Tanaka, M., Tanaka, S., Matsudomi, N., 2014. The Role of the Disulfide Bridge in the Stability and Structural Integrity of Ovalbumin Evaluated by Site-Directed Mutagenesis. Biosci. Biotechnol. Biochem. 75, 544–549.

Jain, R. a, 2000. The manufacturing techniques of various drug loaded biodegradable poly(lactide-co-glycolide) (PLGA) devices. Biomaterials 21, 2475–90.

Jannin, V., Cuppok, Y., 2013. Hot-melt coating with lipid excipients. Int. J. Pharm. 457, 480–487.

Jiang, W., Schwendeman, S.P., 2001. Stabilization and controlled release of bovine serum albumin encapsulated in poly(D,L-lactide) and poly(ethylene glycol) microsphere blends. Pharm. Res. 18, 878–885.

Jones, L.S., Peek, L.J., Power, J., Markham, A., Yazzie, B., Middaugh, C.R., 2005. Effects of adsorption to aluminum salt adjuvants on the structure and stability of model protein antigens. J. Biol. Chem. 280, 13406–13414.

Jorgensen, L., Moeller, E.H., van de Weert, M., Nielsen, H.M., Frokjaer, S., 2006. Preparing and evaluating delivery systems for proteins. Eur. J. Pharm. Sci. 29, 174–82.

Jozwiakowski, M.J., Jones, D.M., Franz, R.M., 1990. Characterization of a Hot-Melt Fluid Bed Coating Process for Fine Granules. Pharm. Res. An Off. J. Am. Assoc. Pharm. Sci.

Kang, F., Singh, J., 2001. Effect of Additives on the Release of a Model Protein from PLGA Microspheres. AAPS PharmSciTech 2, 1–7.

Kang, J., Schwendeman, S., 2007. Pore Closing and Opening in Biodegradable Polymers and Their Effect on the Controlled Release of Proteins. Mol. Pharm. 699–713.

Kang, J., Schwendeman, S.P., 2002. Comparison of the effects of Mg(OH)2 and sucrose on the stability of bovine serum albumin encapsulated in injectable poly(D,L-lactide-co-glycolide) implants. Biomaterials 23, 239–245.

Karimi, A., de Boer, S.W., van den Heuvel, D.A.F., Fioole, B., Vroegindeweij, D., Heyligers, J.M.M., Lohle, P.N.M., Elgersma, O., Nolthenius, R.P.T., Vos, J.A., de Vries, J.P.P.M., 2013. Randomized trial of Legflow((R)) paclitaxel eluting balloon and stenting versus standard percutaneous transluminal angioplasty and stenting for the treatment of intermediate and long lesions of the superficial femoral artery (RAPID trial): study protocol. Trials 14, 87.

Kathe, N., Henriksen, B., Chauhan, H., 2014. Physicochemical characterization techniques for solid lipid nanoparticles: principles and limitations. Drug Dev. Ind. Pharm. 40, 1565–1575.

Kato, A., Nakai, S., 1980. Hydrophobicity determined by a fluorescence probe method and its correlation with surface properties of proteins. Biochim. Biophys. Acta - Protein Struct. 624, 13–20.

Kawachi, Y., Kameyama, R., Handa, A., Takahashi, N., Tanaka, N., 2013. Role of the N-terminal amphiphilic region of ovalbumin during heat-induced aggregation and gelation. J. Agric. Food Chem. 61, 8668–75.

Kikuchi, A., Okano, T., 2002. Pulsatile drug release control using hydrogels. Adv. Drug Deliv.

Rev. 54, 53–77.

Kim, J.M., Seo, K.S., Jeong, Y.K., Hai, B.L., Kim, Y.S., Khang, G., 2005. Co-effect of aqueous solubility of drugs and glycolide monomer on in vitro release rates from poly(D,L-lactide-co-glycolide) discs and polymer degradation. J. Biomater. Sci. Polym. Ed. 16, 991–1007.

Kleiner, L.W., Wright, J.C., Wang, Y., 2014. Evolution of implantable and insertable drug delivery systems. J. Control. Release 181, 1–10.

Koennings, S., Sapin, a, Blunk, T., Menei, P., Goepferich, a, 2007. Towards controlled release of BDNF--manufacturing strategies for protein-loaded lipid implants and biocompatibility evaluation in the brain. J. Control. Release 119, 163–72.

Kong, J., Yu, S., 2007. Fourier transform infrared spectroscopic analysis of protein secondary structures. Acta Biochim. Biophys. Sin. (Shanghai). 39, 549–559.

Körber, M., 2010. PLGA erosion: solubility- or diffusion-controlled? Pharm. Res. 27, 2414–2420.

Körber, M., Bodmeier, R., 2008. Development of an in situ forming PLGA drug delivery system I. Characterization of a non-aqueous protein precipitation. Eur. J. Pharm. Sci. 35, 283–292.

Koseki, T., Kitabatake, N., Doi, E., 1988. Conformational changes in ovalbumin at acid pH. J. Biochem. 103, 425–430.

Kreye, F., Hamm, G., Karrout, Y., Legouffe, R., Bonnel, D., Siepmann, F., Siepmann, J., 2012. MALDI-TOF MS imaging of controlled release implants. J. Control. Release 161, 98–108.

Kreye, F., Siepmann, F., 2011. Cast lipid implants for controlled drug delivery: importance of the tempering conditions. J. Pharm. Sci. 100, 3471–3481.

Kreye, F., Siepmann, F., Siepmann, J., 2008. Lipid implants as drug delivery systems. Expert Opin Drug Deliv 5, 291–308.

Kreye, F., Siepmann, F., Siepmann, J., 2011a. Drug release mechanisms of compressed lipid implants. Int. J. Pharm. 404, 27–35.

Kreye, F., Siepmann, F., Willart, J.F., Descamps, M., Siepmann, J., 2011b. Drug release mechanisms of cast lipid implants. Eur. J. Pharm. Biopharm. 78, 394–400.

Kreye, F., Siepmann, F., Zimmer, a, Willart, J.F., Descamps, M., Siepmann, J., 2011c. Controlled release implants based on cast lipid blends. Eur. J. Pharm. Sci. 43, 78–83.

Kulah, G., Kaya, O., 2011. Investigation and scale-up of hot-melt coating of pharmaceuticals in fluidized beds. Powder Technol. 208, 175–184.

Kumar, R., Palmieri, M.J., 2010. Points to consider when establishing drug product specifications for parenteral microspheres. AAPS J. 12, 27–32.

Kumar, T.R.S., Bai, M.V., Krishnan, L.K., 2004. A freeze-dried fibrin disc as a biodegradable

drug release matrix. Biologicals 32, 49–55.

Kumar, V., Kharb, R., Chaudhary, H., 2016. Optimization & Design of Isradipine Loaded Solid Lipid Nanobioparticles. Int. J. Biol. Macromol. 92, 338–346.

Kuntsche, J., Bunjes, H., 2007. Influence of preparation conditions and heat treatment on the properties of supercooled smectic cholesteryl myristate nanoparticles. Eur. J. Pharm. Biopharm. 67, 612–620.

Lang, B., McGinity, J.W., Williams, R.O., 2014. Hot-melt extrusion - basic principles and pharmaceutical applications. Drug Dev. Ind. Pharm. 9045, 1–23.

Langer, R., 1991. Polymer implants for drug delivery in the brain. J. Control. Release 16, 53–59.

Langer, R., Folkman, J., 1976. Polymers for the sustained release of proteins and other macromolecules. Nature 263, 797–800.

Langer, R., Moses, M., 1991. Biocompatible controlled release polymers for delivery of polypeptides and growth factors. J. Cell. Biochem. 45, 340–345.

Lee, L.L., Lee, J.C., 1987. Thermal Stability of Proteins in the Presence of Poly (ethylene glycols). Biochemistry 26, 7813–7819.

Lee, P.I., 1993. Swelling and Dissolution Kinetics During Peptide Release from Erodible Anionic Gel Beads. Pharm. Res. An Off. J. Am. Assoc. Pharm. Sci.

Lee, Y., Sah, H., 2016. Simple emulsion technique as an innovative template for preparation of porous, spongelike poly(lactide-co-glycolide) microspheres with pore-closing capability. J. Mater. Sci. 51, 6257–6274.

Limmatvapirat, S., Limmatvapirat, C., Puttipipatkhachorn, S., Nuntanid, J., Luangtana-anan, M., 2007. Enhanced enteric properties and stability of shellac films through composite salts formation. Eur. J. Pharm. Biopharm. 67, 690–698.

Liu, Y., Schwendeman, S.P., 2012. Mapping microclimate pH distribution inside protein-encapsulated PLGA microspheres using confocal laser scanning microscopy. Mol. Pharm. 9, 1342–50.

Lopac, S.K., Torres, M.P., Wilson-Welder, J.H., Wannemuehler, M.J., Narasimhan, B., 2009. Effect of polymer chemistry and fabrication method on protein release and stability from polyanhydride microspheres. J. Biomed. Mater. Res. B. Appl. Biomater. 91, 938–47.

Major, I., Mcconville, C., 2015. Hot Melt Extruded and Injection Moulded Dosage Forms : Recent Research and Patents. Recent Patents Drug Dlivery Formul. 9, 194–200.

Maniruzzaman, M., Boateng, J.S., Snowden, M.J., Douroumis, D., 2012. A review of hot-melt extrusion: process technology to pharmaceutical products. ISRN Pharm. 2012, 436763.

Manning, M., Patel, K., Borchardt, R., 1989. Stability of protein Pharmaceuticals. Pharm. Res. 6, 903–918.

Manning, M.C., Chou, D.K., Murphy, B.M., Payne, R.W., Katayama, D.S., 2010. Stability of protein pharmaceuticals: an update. Pharm. Res. 27, 544–75.

Maschke, A., Becker, C., Eyrich, D., Kiermaier, J., Blunk, T., Göpferich, A., 2007. Development of a spray congealing process for the preparation of insulin-loaded lipid microparticles and characterization thereof. Eur. J. Pharm. Biopharm. 65, 175–187.

Mitragotri, S., Burke, P.A., Langer, R., 2014. Overcoming the challenges in administering biopharmaceuticals: formulation and delivery strategies. Nat. Rev. Drug Discov. 13, 655–72.

Mohl, S., Winter, G., 2004. Continuous release of rh-interferon alpha-2a from triglyceride matrices. J. Control. Release 97, 67–78.

Mohl, S., Winter, G., 2006. Continuous release of Rh-interferon alpha-2a from triglyceride implants: storage stability of the dosage forms. Pharm. Dev. Technol. 11, 103–10.

Montanari, L., Cilurzo, F., Valvo, L., Faucitano, A., Buttafava, A., Groppo, A., 2001. Gamma irradiation effects on stability of poly(lactide-co-glycolide) microspheres containing clonazepam. J. Control. Release 75, 317–330.

Montanari, L., Costantini, M., Signoretti, E.C., Valvo, L., Santucci, M., Bartolomei, M., Fattibene, P., Onori, S., Faucitano, a, Conti, B., Genta, I., 1998. Gamma irradiation effects on poly(DL-lactictide-co-glycolide) microspheres. J. Control. Release 56, 219–29.

Moon, S., Song, K. Bin, 2001. Effect of γ-irradiation on the molecular properties of ovalbumin and ovomucoid and protection by ascorbic acid. Food Chem. 74, 479–483.

Negi, L.M., Jaggi, M., Talegaonkar, S., 2014. Development of protocol for screening the formulation components and the assessment of common quality problems of nano-structured lipid carriers. Int. J. Pharm. 461, 403–10.

Oh, C.M., Guo, Q., Wan, P., Heng, S., Chan, L.W., 2014. Spray-congealed microparticles for drug delivery - an overview of factors influencing their production and characteristics. Expert Opin. Drug Deliv. 11, 1047–1060.

Paillard-Giteau, a, Tran, V.T., Thomas, O., Garric, X., Coudane, J., Marchal, S., Chourpa, I., Benoît, J.P., Montero-Menei, C.N., Venier-Julienne, M.C., 2010. Effect of various additives and polymers on lysozyme release from PLGA microspheres prepared by an s/o/w emulsion technique. Eur. J. Pharm. Biopharm. 75, 128–36.

Park, J.S., Shim, J.Y., Truong, N.K.V., Park, J.S., Shin, S., Choi, Y.W., Lee, J., Yoon, J.H., Jeong, S.H., 2010. A pharma-robust design method to investigate the effect of PEG and PEO on matrix tablets. Int. J. Pharm. 393, 79–87.

Park, T.G., 1995. Degradation of poly(lactic-co-glycolic acid) microspheres: effect of copolymer composition. Biomaterials 16, 1123–30.

Park, T.G., Yong Lee, H., Sung Nam, Y., 1998. A new preparation method for protein loaded

poly(D, L-lactic-co-glycolic acid) microspheres and protein release mechanism study. J. Control. Release 55, 181–191.

Particle Sciences, 2009. Protein Structure [WWW Document]. Tech. Br. 2009 vol. 8. URL http://www.particlesciences.com/docs/technical_briefs/TB_8.pdf (accessed 1.30.17).

Particle Sciences, 2011. Hot Melt Extrusion [WWW Document]. Tech. Br. 2011 vol. 3. URL http://www.particlesciences.com/docs/technical_briefs/TB_2011_3.pdf (accessed 1.30.17).

Patil, Y.P., Jadhav, S., 2014. Novel methods for liposome preparation. Chem. Phys. Lipids 177, 8–18.

Pearnchob, N., Siepmann, J., Bodmeier, R., 2003. Pharmaceutical applications of shellac: moisture-protective and taste-masking coatings and extended-release matrix tablets. Drug Dev. Ind. Pharm. 29, 925–938.

Peters, K., Prinz, C., Salamon, A., Rychly, J., Neumann, H.G., 2012. In vitro evaluation of cytocompatibility of shellac as coating for intravascular devices. Trends Biomater. Artif. Organs 26, 110–113.

Pitt, C.G., 1990. The controlled parenteral delivery of polypeptides and proteins. Int. J. Pharm. 59, 173–196.

Pongjanyakul, T., Medlicott, N.J., Tucker, I.G., 2004. Melted glyceryl palmitostearate (GPS) pellets for protein delivery. Int. J. Pharm. 271, 53–62.

Privalov, P.L., 1990. Cold Denaturation of Protein. Crit. Rev. Biochem. Mol. Biol. 25, 281–306.

Qian, F., Saidel, G.M., Sutton, D.M., Exner, A., Gao, J., 2002. Combined modeling and experimental approach for the development of dual-release polymer millirods. J. Control. Release 83, 427–35.

Raiche, a T., Puleo, D. a, 2006. Modulated release of bioactive protein from multilayered blended PLGA coatings. Int. J. Pharm. 311, 40–9.

Rajagopal, K., Wood, J., 2013. Trehalose limits BSA aggregation in spray□dried formulations at high temperatures: Implications in preparing polymer implants for long□term protein delivery. J. Pharm. Sci. 102, 2655–2666.

Ramchandani, M., Pankaskie, M., Robinson, D., 1997. The influence of manufacturing procedure on the degradation of poly(lactide-co-glycolide) 85:15 and 50:50 implants. J. Control. release 43, 161–173.

Ranade, V., 1990. Drug Delivery Systems 4. Implants in Drug Delivery. J. Clin. Pharmacol. 30, 871–889.

Rather, G.M., Gupta, M.N., 2013. Refolding of urea denatured ovalbumin with three phase partitioning generates many conformational variants. Int. J. Biol. Macromol. 60, 301–8.

Reinhold, S.E., Desai, K.-G.H., Zhang, L., Olsen, K.F., Schwendeman, S.P., 2012. Self-

healing microencapsulation of biomacromolecules without organic solvents. Angew. Chem. Int. Ed. Engl. 51, 10800–10803.

Reitz, C., Kleinebudde, P., 2007. Solid lipid extrusion of sustained release dosage forms. Eur. J. Pharm. Biopharm. 67, 440–8.

Reitz, C., Strachan, C., Kleinebudde, P., 2008. Solid lipid extrudates as sustained-release matrices: the effect of surface structure on drug release properties. Eur. J. Pharm. Sci. 35, 335–43.

Repka, M. a, Battu, S.K., Upadhye, S.B., Thumma, S., Crowley, M.M., Zhang, F., Martin, C., McGinity, J.W., 2007. Pharmaceutical applications of hot-melt extrusion: Part II. Drug Dev. Ind. Pharm. 33, 1043–57.

Repka, M. a, Shah, S., Lu, J., Maddineni, S., Morott, J., Patwardhan, K., Mohammed, N.N., 2012. Melt extrusion: process to product. Expert Opin. Drug Deliv. 9, 105–125.

Repka, M., Majumdar, S., Battu, S.K., 2008. Applications of hot-melt extrusion for drug delivery. Expert Opin. Drug Deliv. 5, 1357–1376.

Reubsaet, J.L., Beijnen, J.H., Bult, A., van Maanen, R.J., Marchal, J. a, Underberg, W.J., 1998a. Analytical techniques used to study the degradation of proteins and peptides: physical instability. J. Pharm. Biomed. Anal. 17, 979–84.

Reubsaet, J.L., Beijnen, J.H., Bult, A., van Maanen, R.J., Marchal, J. a, Underberg, W.J., 1998b. Analytical techniques used to study the degradation of proteins and peptides: chemical instability. J. Pharm. Biomed. Anal. 17, 955–78.

Rhine, W.D., Hsieh, D.S.T., Langer, R., 1980. Polymers for sustained macromolecule release: Procedures to fabricate reproducible delivery systems and control release kinetics. J. Pharm. Sci. 69, 265–270.

Rothen-Weinhold, A., Besseghir, K., Gurny, R., 1997. Analysis of the influence of polymer characteristics and core loading on the in vivo release of a somatostatin analogue. Eur. J. Pharm. Sci. 5, 303–313.

Rothen-Weinhold, A., Besseghir, K., Vuaridel, E., Sublet, E., Oudry, N., Gurny, R., 1999a. Stability studies of a somatostatin analogue in biodegradable implants. Int. J. Pharm. 178, 213–21.

Rothen-Weinhold, A., Besseghir, K., Vuaridel, E., Sublet, E., Oudry, N., Kubel, F., Gurny, R., 1999b. Injection-molding versus extrusion as manufacturing technique for the preparation of biodegradable implants. Eur. J. Pharm. Biopharm. 48, 113–121.

Sahoo, S.K., Panda, A.K., Labhasetwar, V., 2005. Characterization of porous PLGA/PLA microparticles as a scaffold for three dimensional growth of breast cancer cells. Biomacromolecules 6, 1132–1139.

San Vicente, A., Hernández, R.M., Gascón, A.R., Calvo, M.B., Pedraz, J.L., 2000. Effect of aging on the release of salbutamol sulfate from lipid matrices. Int. J. Pharm. 208, 13–

21.

Sánchez, A., Villamayor, B., Guo, Y., McIver, J., Alonso, M.J., 1999. Formulation strategies for the stabilization of tetanus toxoid in poly(lactide-co-glycolide) microspheres. Int. J. Pharm. 185, 255–266.

Santoveña, A., García, J.T., Oliva, A., Llabrés, M., Fariña, J.B., 2006. A mathematical model for interpreting in vitro rhGH release from laminar implants. Int. J. Pharm. 309, 38–43.

Sato, K., 2001. Crystallization behaviour of fats and lipids — a review. Chem. Eng. Sci. 56, 2255–2265.

Sax, G., Feil, F., Schulze, S., Jung, C., Bräuchle, C., Winter, G., 2012. Release pathways of interferon α2a molecules from lipid twin screw extrudates revealed by single molecule fluorescence microscopy. J. Control. Release 162, 295–302.

Sax, G., Winter, G., 2012. Mechanistic studies on the release of lysozyme from twin-screw extruded lipid implants. J. Control. Release 163, 187–194.

Schulze, S., Winter, G., 2009. Lipid extrudates as novel sustained release systems for pharmaceutical proteins. J. Control. release 134, 177–185.

Schwab, M., Sax, G., Schulze, S., Winter, G., 2009. Studies on the lipase induced degradation of lipid based drug delivery systems. J. Control. Release 140, 27–33.

Schwartz, J.B., Simonelli, A.P., Higuchi, W.I., 1968. Drug release from wax matrices II. Application of a mixture theory to the sulfanilamide???wax system. J. Pharm. Sci. 57, 278–282.

Schwendeman, S.P., Shah, R.B., Bailey, B. a, Schwendeman, A.S., 2014. Injectable controlled release depots for large molecules. J. Control. Release.

Severino, P., Pinho, S.C., Souto, E.B., Santana, M.H.A., 2012. Crystallinity of Dynasan 114 and Dynasan 118 matrices for the production of stable Miglyol-loaded nanoparticles. J. Therm. Anal. Calorim. 108, 101–108.

Shin, S., Choi, D.H., Truong, N.K.V., Kim, N.A., Chu, K.R., Jeong, S.H., 2011. Time-oriented experimental design method to optimize hydrophilic matrix formulations with gelation kinetics and drug release profiles. Int. J. Pharm. 407, 53–62.

Siepmann, J., Siepmann, F., 2011. Mathematical modeling of drug release from lipid dosage forms. Int. J. Pharm. 418, 42–53.

Singhal, S., Lohar, V.K., Arora, V., 2011. Hot Melt Extrusion Technique. WebmedCentral Pharm. Sci. WMC001459 2, 1–20.

Sinha, V.R., Trehan, A., 2003. Biodegradable microspheres for protein delivery. J. Control. Release 90, 261–80.

Sonam, Chaudhary, H., Kumar, V., 2014. Taguchi design for optimization and development of antibacterial drug-loaded PLGA nanoparticles. Int. J. Biol. Macromol. 64, 99–105.

Sprengholz, M., 2014. Industrial Ram Extrusion as Innovative Tool for the Development of

Biodegradable Sustained Release Implants. Ludwig-Maximilians-Universität München.

Stanković, M., de Waard, H., Steendam, R., Hiemstra, C., Zuidema, J., Frijlink, H.W., Hinrichs, W.L.J., 2013. Low temperature extruded implants based on novel hydrophilic multiblock copolymer for long-term protein delivery. Eur. J. Pharm. Sci. 49, 578–587.

Stanković, M., Frijlink, H.W., Hinrichs, W.L.J., 2015a. Polymeric formulations for drug release prepared by hot melt extrusion: application and characterization. Drug Discov. Today 20, 812–823.

Stanković, M., Hiemstra, C., de Waard, H., Zuidema, J., Steendam, R., Frijlink, H.W., Hinrichs, W.L.J., 2015b. Protein release from water-swellable poly(D,L-lactide-PEG)-b-poly (e-caprolactone) implants. Int. J. Pharm. 480, 73–83.

Stanković, M., Tomar, J., Hiemstra, C., Steendam, R., Frijlink, H.W., Hinrichs, W.L.J., 2014. Tailored protein release from biodegradable poly(ε-caprolactone-PEG)-b-poly(ε-caprolactone) multiblock-copolymer implants. Eur. J. Pharm. Biopharm.

Strambini, G.B., Gabellieri, E., 1996. Proteins in frozen solutions: evidence of ice-induced partial unfolding. Biophys. J. 70, 971–976.

Sturesson, C., Carlfors, J., 2000. Incorporation of protein in PLG-microspheres with retention of bioactivity. J. Control. Release 67, 171–178.

Tan, M.L., Choong, P.F.M., Dass, C.R., 2010. Recent developments in liposomes, microparticles and nanoparticles for protein and peptide drug delivery. Peptides 31, 184–93.

Taylor, S.J., Sakiyama-Elbert, S.E., 2006. Effect of controlled delivery of neurotrophin-3 from fibrin on spinal cord injury in a long term model. J. Control. Release 116, 204–210.

Teekamp, N., Duque, L.F., Frijlink, H.W., Hinrichs, W.L., Olinga, P., 2015. Production methods and stabilization strategies for polymer-based nanoparticles and microparticles for parenteral delivery of peptides and proteins. Expert Opin. Drug Deliv. 12, 1–21.

Tracy, M. a, 1998. Development and scale-up of a microsphere protein delivery system. Biotechnol. Prog. 14, 108–15.

Vaishya, R., Khurana, V., Patel, S., Mitra, A.K., 2014. Long-term delivery of protein therapeutics. Expert Opin. Drug Deliv. 12, 415–440.

van de Weert, M., Hennink, W.E., Jiskoot, W., 2000. Protein instability in poly(lactic-co-glycolic acid) microparticles. Pharm. Res. 17, 1159–67.

Veerman, C., De Schiffart, G., Sagis, L.M.C., Van Der Linden, E., 2003. Irreversible self-assembly of ovalbumin into fibrils and the resulting network rheology. Int. J. Biol. Macromol. 33, 121–127.

Vesna Milacic, V.M., Schwendeman, S.P., 2014. Lysozyme release and polymer erosion behavior of injectable implants prepared from PLGA-PEG block copolymers and

PLGA/PLGA-PEG blends. Pharm. Res. 31, 436–48.

Vey, E., Roger, C., Meehan, L., Booth, J., Claybourn, M., Miller, A.F., Saiani, A., 2008. Degradation mechanism of poly(lactic-co-glycolic) acid block copolymer cast films in phosphate buffer solution. Polym. Degrad. Stab. 93, 1869–1876.

Vogelhuber, W., Magni, E., Gazzaniga, A., Göpferich, A., 2003a. Monolithic glyceryl trimyristate matrices for parenteral drug release applications. Eur. J. Pharm. Biopharm. 55, 133–138.

Vogelhuber, W., Magni, E., Mouro, M., Spruss, T., Guse, C., Gazzaniga, a, Göpferich, a, 2003b. Monolithic triglyceride matrices: a controlled-release system for proteins. Pharm. Dev. Technol. 8, 71–9.

Volland, C., Wolff, M., 1994. The influence of terminal gamma-sterilization on captopril containing poly(d,l-lactide-co-glycolide) microspheres. J. Control. Release 1, 293–305.

von Burkersroda, F., Schedl, L., Göpferich, A., 2002. Why degradable polymers undergo surface erosion or bulk erosion. Biomaterials 23, 4221–31.

Wang, C.K., Wang, W.Y., Meyer, R.F., Liang, Y., Winey, K.I., Siegel, S.J., 2010. A rapid method for creating drug implants: Translating laboratory-based methods into a scalable manufacturing process. J. Biomed. Mater. Res. - Part B Appl. Biomater. 93, 562–572.

Wang, N., Wu, X.S., Li, J.K., 1999. A heterogeneously structured composite based on poly(lactic-co-glycolic acid) microspheres and poly(vinyl alcohol) hydrogel nanoparticles for long- term protein drug delivery. Pharm. Res.

Wang, W., 1999. Instability, stabilization, and formulation of liquid protein pharmaceuticals. Int. J. Pharm. 185, 129–88.

Weijers, M., Barneveld, P.A., Cohen Stuart, M.A., Visschers, R.W., 2003. Heat-induced denaturation and aggregation of ovalbumin at neutral pH described by irreversible first-order kinetics. Protein Sci. 12, 2693–703.

Weijers, M., Sagis, L.M.C., Veerman, C., Sperber, B., Van Der Linden, E., 2002. Rheology and structure of ovalbumin gels at low pH and low ionic strength. Food Hydrocoll. 16, 269–276.

Windbergs, M., Strachan, C.J., Kleinebudde, P., 2009a. Investigating the principles of recrystallization from glyceride melts. AAPS PharmSciTech 10, 1224–1233.

Windbergs, M., Strachan, C.J., Kleinebudde, P., 2009b. Understanding the solid-state behaviour of triglyceride solid lipid extrudates and its influence on dissolution. Eur. J. Pharm. Biopharm. 71, 80–87.

Windbergs, M., Strachan, C.J., Kleinebudde, P., 2009c. Influence of structural variations on drug release from lipid/polyethylene glycol matrices. Eur. J. Pharm. Sci. 37, 555–62.

Witt, C., Mäder, K., Kissel, T., 2000. The degradation, swelling and erosion properties of

biodegradable implants prepared by extrusion or compression moulding of poly(lactide-co-glycolide) and ABA triblock copolymers. Biomaterials 21, 931–938.

Wong, J., Brugger, A., Khare, A., Chaubal, M., Papadopoulos, P., Rabinow, B., Kipp, J., Ning, J., 2008. Suspensions for intravenous (IV) injection: A review of development, preclinical and clinical aspects. Adv. Drug Deliv. Rev. 60, 939–954.

Wright, J.C., Tao Leonard, S., Stevenson, C.L., Beck, J.C., Chen, G., Jao, R.M., Johnson, P.A., Leonard, J., Skowronski, R.J., 2001. An in vivo/in vitro comparison with a leuprolide osmotic implant for the treatment of prostate cancer. J. Control. Release 75, 1–10.

Yoshida, R., Sakai, K., Okano, T., Sakurai, Y., 1993. Pulsatile drug delivery systems using hydrogels. Adv. Drug Deliv. Rev. 11, 85–108.

Yu, L.X., Amidon, G., Khan, M.A., Hoag, S.W., Polli, J., Raju, G.K., Woodcock, J., 2014. Understanding pharmaceutical quality by design. AAPS J. 16, 771–83.

Zaky, A., Elbakry, A., Ehmer, A., Breunig, M., Goepferich, A., 2010. The mechanism of protein release from triglyceride microspheres. J. Control. Release 147, 202–210.

Zema, L., Loreti, G., Melocchi, A., Maroni, A., Gazzaniga, A., 2012. Injection Molding and its application to drug delivery. J. Control. Release 159, 324–31.

Zhu, G., Mallery, S.R., Schwendeman, S.P., 2000. Stabilization of proteins encapsulated in injectable poly (lactide- co-glycolide). Nat. Biotechnol. 18, 52–57.

Zhu, G., Schwendeman, S.P., 2000. Stabilization of proteins encapsulated in cylindrical poly(lactide-co-glycolide) implants: mechanism of stabilization by basic additives. Pharm. Res. 17, 351–357.

8. Publications and presentations resulting from this work

- **Duque, L.** Körber, M., Bodmeier, R. Improving release completeness from PLGA-based implants for the acid labile model protein ovalbumin. Under preparation
- **Duque, L.** Körber, M., Bodmeier, R. Impact of change on matrix crystallinity and polymorphism on ovalbumin release from lipid-based implants. Under preparation
- **Duque, L.**, Bodmeier, R. 2016. Improving release completeness of Ovalbumin from PLGA-based implants. Short oral presentation. 10th World meeting on Pharmaceutics, Biopharmaceutics and Pharmaceutical technology, Glasgow, United Kingdom**.**
- **Duque, L.** Körber, M., Bodmeier, R. 2016. Accelerated dissolution testing of goserelin PLGA-based implants and its relation to polymer erosion. Poster # 99. 10th World meeting on Pharmaceutics, Biopharmaceutics and Pharmaceutical technology, Glasgow, United Kingdom**.**
- **Duque, L.**, Bodmeier, R. 2015. Understanding the incomplete release of Ovalbumin from PLGA-based implants. Poster # T2283. 2015 AAPS Annual Meeting and Exposition; Orlando, Florida, USA.
- Körber. M., **Duque, L.**, Bodmeier, R. 2015. Goserelin Release from PLGA Implants Prepared by Hot Melt Extrusion and Its Relation to Polymer Erosion. Poster # M1049. 2015 AAPS Annual Meeting and Exposition; Orlando, Florida, USA.
- Teekamp, N., **Duque, L.F.**, Frijlink, H.W., Hinrichs, W.L.J., Olinga, P., 2015. Production methods and stabilization strategies for polymer-based nanoparticles and microparticles for parenteral delivery of peptides and proteins. Expert Opin. Drug Deliv. 1–21

9. Curriculum vitae

For reasons of data protection, the Curriculum vitae is not published in the online version

Der Lebenslauf ist in der Online-Version aus Gründen des Datenschutzes nicht enthalten

For reasons of data protection, the Curriculum vitae is not published in the online version

Der Lebenslauf ist in der Online-Version aus Gründen des Datenschutzes nicht enthalten